universität wien

DIPLOMARBEIT / DIPLOMA THESIS

Titel der Diplomarbeit / Title of the Diploma Thesis

„Synthese neuer interkalierender Pyridocarbazole“

verfasst von / submitted by

Jelena Kalinovic

angestrebter akademischer Grad / in partial fulfilment of the requirements for the degree of

Magistra der Pharmazie (Mag.pharm.)

Wien, 2018 / Vienna, 2018

Studienkennzahl lt. Studienblatt:	A 449
Studienrichtung lt. Studienblatt:	Diplomstudium Pharmazie
Betreut von / Supervisor:	Ao. Univ.-Prof. Mag. Dr. Helmut Spreitzer

Acknowledgements

The practical part of this work was performed at the Department for drug and natural product synthesis of University of Vienna in the period from March 2017 to November 2017 under the supervision of ao. Univ.-prof. Mag, Helmut Spreitzer. There are so many people to thank for helping me during the last months.

First of all, I want to thank my supervisor ao. Univ.-prof. Mag, Helmut Spreitzer with sincere gratitude for the interesting topic as well as for his help and support.

My sincere appreciation goes to ao. Univ. - Prof. Dr. Wolfgang Holzer for performing NMR experiments and interpreting NMR spectra of my compounds.

My gratitude goes out to ao. Univ. - Prof. Dr. Norbert Haider for solving all my computer problems.

I am also grateful to Mag. Regina Schoba for her endless amount of patience and countless help that made my diploma thesis a pleasure.

To my colleagues and friends at the University Albana, Sarala and Kimi: Thank you for your moral support in everything over the years. I am extremely lucky that we have met each other and share some great memories.

Finally, my biggest esteem goes to my parents and my boyfriend Stipo, for providing me with unfailing support and continuous encouragement throughout my years of study and through the process of research and writing this diploma thesis.

Abstract

Cancer is one of the leading causes of death in the world. In 2012, there were 14.1 million new cancer cases and 8.2 cancer deaths worldwide and by the year 2030, the incidence of cancer and cancer-related deaths is expected to grow to 21.4 million and 13.2 million. Interestingly, many of these cancers could be prevented by lifestyle changes. The cancer treatment options depend, inter alia, on the type and stage of the cancer and new methods of treatment which respond to this disease are of great interest for research and development. In this work, it was attempted to open a route to new anti-tumour compounds, deriving from 5H,6H,11H-pyrido[4,3-b]carbazole-5,11-dione **(21)** which was made accessible from the MOM-protected precursor **(20).**

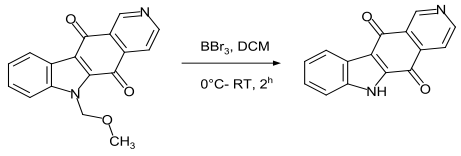

20 **21**

Figure 1: Deprotection of the methoxymethyl (MOM) group for the synthesis of **21.**

In addition, various side chains such as trans-alkenes 6-[(3E)-6-[(tert-butyldiphenylsilyl) oxy]hex-3-en-1-yl]-5H,6H, 11H-pyrido[4,3-b]carbazole-5,11-dione **(6),** [(3E)-6-chloro-hex-3-en-1-yl]di-methyl amine **(9),** (3E)-6-(dimethylamino)- hex-3-en-1-ylmethane sulfonate **(10)** and chains with S-insertion compounds, such as the sulfoxides: tert-Butyl- ({2-[(2-chloroethyl)sulfanyl]ethoxy})diphenylsilane **(13)** and 2-{2-[(tert-butyl-diphenylsilyl) oxy] ethanesulfinyl}-ethylmethanesulfonate **(17)** were synthesized with the aim of attach them to the core structure.

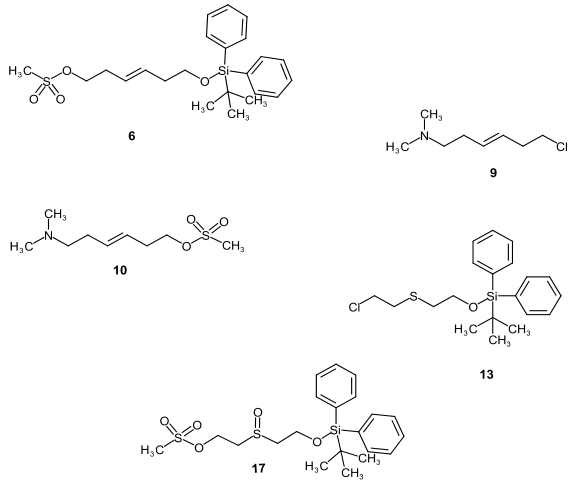

6 **9** **10** **13** **17**

Figure 2: Side chains

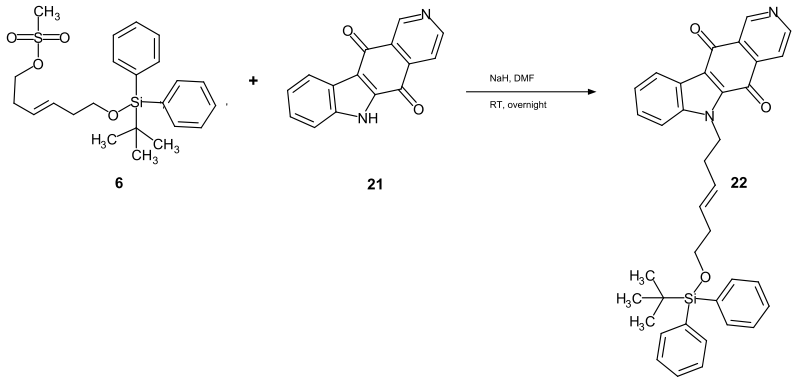

Figure 3: Side-chain alkylation of the core structure

Finally in this diploma thesis only the aliphatic chain **(6)** was used for alkylation of compound **(21)**, thus furnishing the target-compound 6-(methoxymethyl)-5H,6H,11H-pyrido[4,3-b]carbazole-5,11-dione **(22).**

Krebs gilt als eine der häufigsten Todesursachen weltweit. Im Jahr 2012 gab es 14,1 Millionen neue Krebsfälle und 8,2 Krebstodesfälle und bis zum Jahr 2030 wird die Häufigkeit von Krebs- und krebsbedingten Todesfällen auf 21,4 Millionen und 13,2 Millionen steigen. Interessanterweise könnten viele dieser Krebsarten durch Veränderungen des Lebensstils verhindert werden. Die Wahl der Behandlung ist unter anderem abhängig von Art und vom Stadium des Krebses und neue Behandlungsmethoden, die auf diese Krankheit ansprechen, sind für Forschung und Entwicklung von großem Interesse. In dieser Arbeit wurde versucht, einen Weg zu neuen Antitumorverbindungen zu eröffnen, die von 5H, 6H, 11H-Pyrido [4,3-b] carbazol-5,11-dion **(21)** abstammen, die wiederum aus dem MOM-geschützten Vorläufer zugänglich gemacht **(20).**

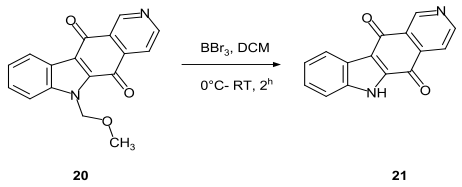

Abbildung 1: Entschützung der Methoxymethylgruppe (MOM) für die Synthese von **(21)**

Zusätzlich wurden verschiedene Seitenketten wie trans-alkenes 6-[(3E)-6-[(tert-Butyldiphenylsilyl)oxy]hex-3-en-1-yl]-5H,6H, 11H-pyrido[4,3-b]carbazol-5,11-dion **(6),** [(3E)-6-chlor-hex-3-en-1-yl]di-methylamin **(9),** (3E)-6-(dimethyl¬amino)-hex-3-en-1-ylmethansulfonat **(10)** und Ketten mit S-Insertionsverbindungen, wie den Sulfoxiden: tert-Butyl- ({2-[(2-Chlorethyl)sulfanyl]ethoxy}) diphenyl silan**(13)** und 2-{2-[(tert-Butyl-diphenylsilyl)oxy] ethan sulfinyl}-ethyl-methansulfonat **(17)** mit dem Ziel synthetisiert, diese an die Kernstruktur zu binden.

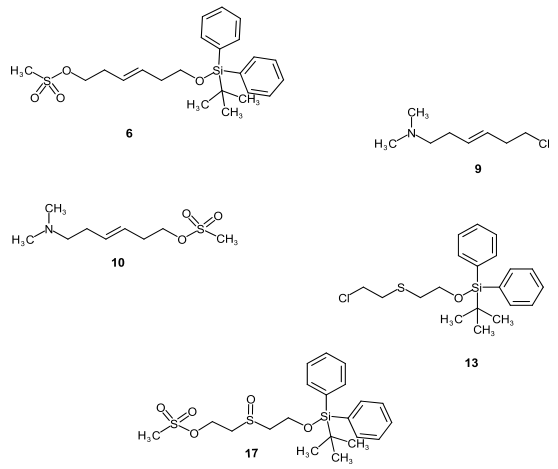

Abbildung 2: Seitenketten

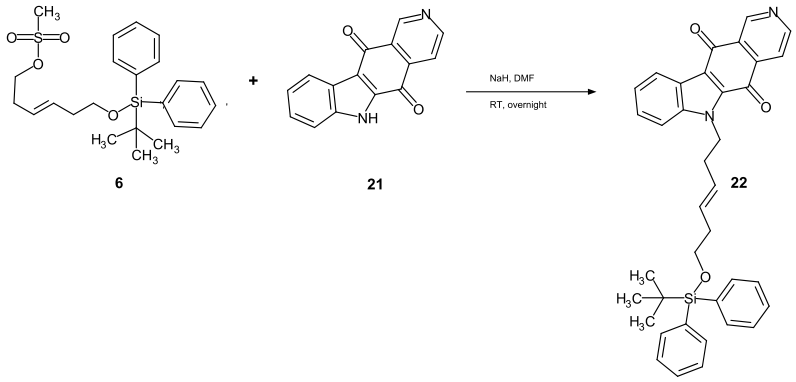

Abbildung 3: Alkylierung der Seitenkette mit dem Grundkörper

Letztendlich wurde in dieser Diplomarbeit nur die aliphatische Kette **(6)** zur Alkylierung des Grundkörpers **(21)** verwendet, wodurch die Zielverbindung 6-(Methoxymethyl)-5H,6H,11H-pyrido-[4,3-b]carbazol-5,11-dion **(22)** synthetisiert wurde.

Table of Contents

1.Introduction

1.1 Definition of Cancer And Its History

Cancer is a term for a group of more than 100 diseases, involving abnormalities in cell divison[1]. The word ‘cancer’ stems from the words carcinos and carcinoma, which is the Greek word for ‘crab’ , due to the appearance of a tumour and it’s spreading projections that are reminiscent of a crab, and is credited to the Greek physician Hippocrates (460-370BC)[2,3].The so-called ’Father of Medicine‘ used the terms ‘carkinos’ to describe non ulcera- forming tumours as well as ‘carkinoma’ for ulcera-forming tumours. Later, the roman physician Celsus (28-50 BC) translated the Greek term into the Latin ‘cancer’, also a crab analogy, and the Greek physician Galen (130-200 AD) coined the word ‘oncos’ (means swelling in Greek) for the description of tumours. His term is now used as a part of the oncologists, the name for cancer specialists whilst Hippocrates and Celsus terms are still used for the description of malignant tumours[3].

Generally considered as the earliest known description of cancer appearance (although the term ‘cancer’ was not used) are found in the Edwin Smith Papyrus, an Egyptian medical text that dates back to about 3000 BC. This fragmentary copy of an ancient Egyptian textbook on trauma surgery describes eight cases of tumours, occurring on the breasts, that were removed by cauterization with an instrument called ‘the fire drill’[3], and according to the information recorded on this writing, at that time, Egyptians were able to distinguish between benign and malignant tumours[4] , even though their less knowledge in human body, compared to the level of knowledge today.

1.2 Epidemiology - Global Cancer Statistics

The term cancer involves abnormalities in cell division[1] and represents a major burden worldwide. Tens of millions of cancer cases are diagnosed annually and more than half of these patients eventually are overtaken by death[5]. When countries are put on a continuum based on the level of economic development, cancer is the leading cause of death in developed countries and ranks the second leading cause of death in developing countries following cardiovascular diseases.[6] In consequence of observations, the conclusion has been drawn that by the year 2030, the incidence of cancer and cancer-related deaths worldwide is expected to grow to 21.4 million and 13.2 million, respectively, due to the increasing population size and age[7] alongside an increasing adoption of western lifestyles,

especially smoking, poor diet and physical inactivity, in economically developing countries. [8] In 2012, there were 14.1 million new cancer cases, 8.2 million cancer deaths and 32.6 million people living with cancer (within five years of diagnosis) worldwide. 57 % (8 million) of new cancer cases, 65% (5.3 million) of the cancer -related deaths and 48% (15.6 million) of the 5-year prevalent cancer cases occurred in less developed countries.[9]

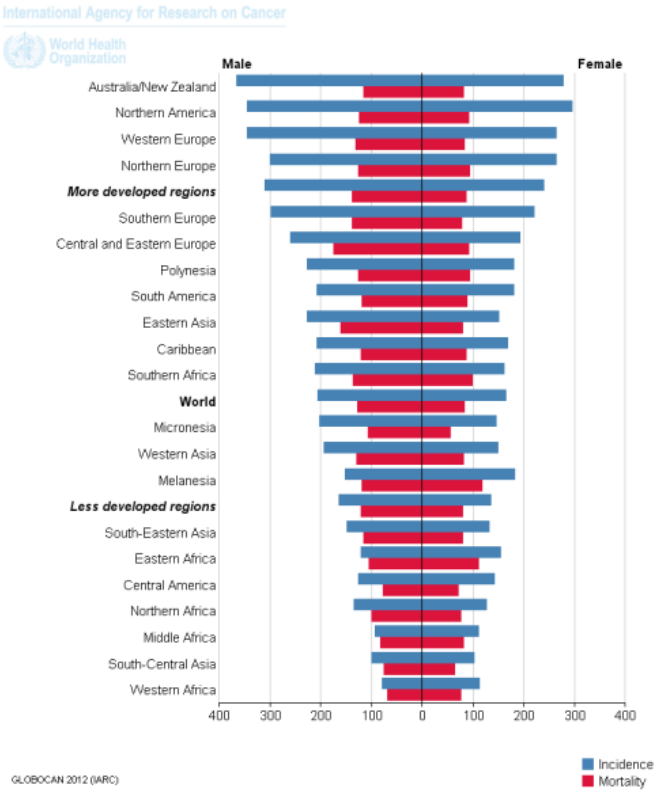

Figure 4: Estimated Incidence, Mortality and Prevalence Worldwide in 2012 (Globocan 2012) [9]

The incidence rate of cancer is almost 25% higher in men than in women. There is a great variation in men cancer incidence rates, almost five-fold, across the different regions of the world, with rates ranging from 79 per 100.000 in Western Africa to 365 per 100.000 in Australia/New Zealand (particularly high incidence rates of prostate). By contrast, cancer incidence rate in women has a less variation, almost three-fold, with rated ranging from 103 per 100.000 in South-Central Asia to 295 per 100.000 in Northern America. Comparing with it, the regional disparities in cancer mortality are lower, with higher rates of 15% in more developed than in less developed countries in men, and 8% higher in women. The highest mortality rate in men is observed in Central and Eastern Europe with rates of 173 per 100.000, whereas the lowest rate with the total number of 69 per 100.000

in Western Africa. By contrast, the highest mortality rate in women represents Melanesia with 119 per 100.000 and Eastern Africa with 111 per 100.000, whereas the lowest rates apply to Central America, the rate being 72 per 100.000 and South-Central Asia 65 per 100.000. [7] In the year 2012, regarding incidence and mortality in both sexes, the most frequent cancer type in the world is lung cancer. Among women, breath cancer is the most commonly diagnosed cancer and the second prevalent disease overall with 1.68 million cases, 119% of the total number, but the breast cancer mortality rates are ranked 5th, with a number of 0.52 million deaths, 6.4% of the total number.[9] Although the most common cancer site worldwide among men is lung, it is exceeded by prostate cancer in developed countries[10].

1.3 Classification of Cancer

Cancer in general is a group of diseases, resulting from an unregulated proliferation of cancer cells, originated from one single cell. Even though there are many types of cancer, due to the fact that cancer can develop in virtually any of the human tissues and has its unique features[11], but the fundamental processes that are responsible for the production of cancer are similar in all forms of the disease[12]. First of all, tumours can be classified in two ways, by their benignity or malignity or by the type of tissue in which the cancer originates and cell that is initially affected[11,13]. A benign tumour, for instance the common skin wart, does not invade nearby tissue or spread in the body through the lymphatic or blood system and most of them can be removed by surgery and are not life threatening, in contrast to the cancerous type, that has both capabilities and causes significant mortality[12]. According to the latter classification, based on histological type, it provides it's tissue of origin or the cell that has been modified, adding the suffix '–oma', if the tumour is benign and the suffix´-carcinoma´ or´ – sarcoma´ in a case of a malignant tumour. For instance, a benign tumour of fibrous connective tissue is called a 'fibrom', whilst the term 'fibrosarcoma' is used as the malignant counterpart [14]. In general, the different types of cancer are grouped into five major categories, including carcinoma, sarcoma, myeloma, leukemia and lymphoma. For instance, carcinoma that account about 90% of all human cancer cases refers to a cancerous tumour of epithelial origin[11, 13]. The second one, sarcoma, generally occurring rare in humans often develops in connective tissues, such as muscle, bone, cartilage and fibrous tissue. Myeloma refers to a malignancy of plasma cells of bone marrow that produce some of the proteins found in

blood. Leukemia and lymphoma include approximately 8% of all cancer cases, are cancers of the cells of the blood and immune system[11]. The internationally accepted standard for cancer staging system is the anatomically based tumour – node – metastases system, TNM, developed by Pierre Denoix in the 1940s in France[15]. TNM classification has been published by the UICC for over 50 years[16] and it is updated every six to eight years[17]. In this TNM classification system, T refers to the size and extent of the primary tumour, N is assigned to nodes, or more precisely to the nearby lymph nodes that may be affected, and M standing for the appearance of distant metastases[18,19]. Cancer staging can be separated into a clinical and pathologic stage. The first-mentioned is based on all information received from physical examination, laboratory findings and imaging tests (X-rays, CT-scans, etc.) and is determined before treatment. The pathologic staging, also called the surgical stage, is established after surgery, based on the results of the tests mentioned before, as well as on the additional information gained during the treatment and histological examination of tissue[17,18]. Due to the using of different criteria, the clinical stage may differ from the pathologic rating, for instance, if the surgery examination reveals that the cancer has spread more than it was assumed, and thus, the second rating is considered to be more accurate[17]. Staging stage provides a glimpse into the severity of cancer based on it's magnitude and if it has spread, serving the purpose for helping doctors to plan the appropriate treatment and prognosis[19].

1.4 Cell Cycle and Cancer

The most of the cells in the human body don't undergo the cycling and remain in 'out-of-cycle' states. Only a tiny subset of cells, also called transit amplifying cells, located mainly in the compartments of self–renewing tissues and involves epithelia and bone marrow[20]. The cell cycle is a process encompassing four sequential phases including the S Phase, in which DNA is replicated, the two gap phases G1- and G2-phase, all three known as the interphase and M Phase, the part when cell are separated into two daughter cells, the so called mitotic phase. During the first gap between M-phase and S-phase, G1-phase, the cell cycle progression can be regulated by positive and negative cues from growth signalling networks, with the aim of preparing the cell for DNA synthesis[20,21]. The second gap after S phase, the G2-phase, is the timeframe within the cell is prepared for the entry to mitosis, the M-phase[21]. G0-phase is a non-dividing period when the cell leave the cell cycle either reversibly under conditions of high cell density or lack of mitogenic

activity [20], thus may remain quiescent for some time, or irreversibly in response to DNA damage, which means these senescent cells are not capable of further cell division[22,23]. An altered cell cycle machinery and uncontrolled cell division due to aberrant patterns of gene expression lead to acquisition of genetic instability and contribute to development of malignant tumours[20,24, 25].

1.5 Tumourigenesis and the "Hallmarks of Cancer"

Tumourigenesis takes place in a multi-step process, in which normal cells gradually become malignant through an ongoing process of modifications[11 26]. The hallmarks of cancer are recognizes organizing principles, and define a distinct set of acquired traits 'hallmarks' for understanding the transformation of normal cells to 'cancerous cells'[27, 28] This framework include six biological principles for distinction between cancer and normal cells, including self-sufficiency in growth signals, resistance to signals to stop cell division, evasion of apoptosis, limitless potential of replication, promotion of their own blood supply (angiogenesis), and progression of invasion and spreading beyond its original point of development (metastatis)[26, 27]. Each capability will be described in turn below.

1.5.1 Self-Sufficiency In Growth Signals

Usually, normal cells show an absolute requirement for mitogenic growth signals (GS) before they entry and develop through the cell and division cycle, by moving from a quiescent state into an active proliferative stage. These signals are conveyed by growth factors (GF), extracellular matrix components and cell-to cell adhesion/interaction molecules, that are able to bind transmembrane receptors and typically contain intracellular tyrosine kinase domains[26, 27]. This leads to emitting signals through intracellular signalling pathways to regulate both the progression through the cell cycle and the cell growth. Frequently, these signals have an impact on other cell- biological properties, such as cell survival and energy metabolism[26,27]. Transmembrane receptors are able to bind distinctive classes of signalling molecules, for instance, diffusible growth factors, extracellular matrix components, and cell-to-cell adhesion/interaction molecules. This behaviour differs hugely from that of tumour cells, as they not proliferate only in the absence of stimulatory signals. This arguably indicates that cancer cells are endowed with the capability to generate many of their own growth signals. Usually, the most soluble

mitogenic growth factors are produced by one type of cell and stimulate proliferation of another (the process of heterotypic signalling), whereas many tumour cells acquire the ability to produce GF to which they are responsive and stimulate their own proliferation, creating a positive feedback signalling loop and thus to a continuous auto-stimulation (autocrine stimulation). Obviously, the production of a GF by a cancerous cell avoids dependence on GFs from other cells within the tissue. Two illustrative examples are the manufacture of PDGF (platelet-derived growth factor) and TGFα (tumour growth factor α) by glioblastomas and sarcomas, respectively[26].

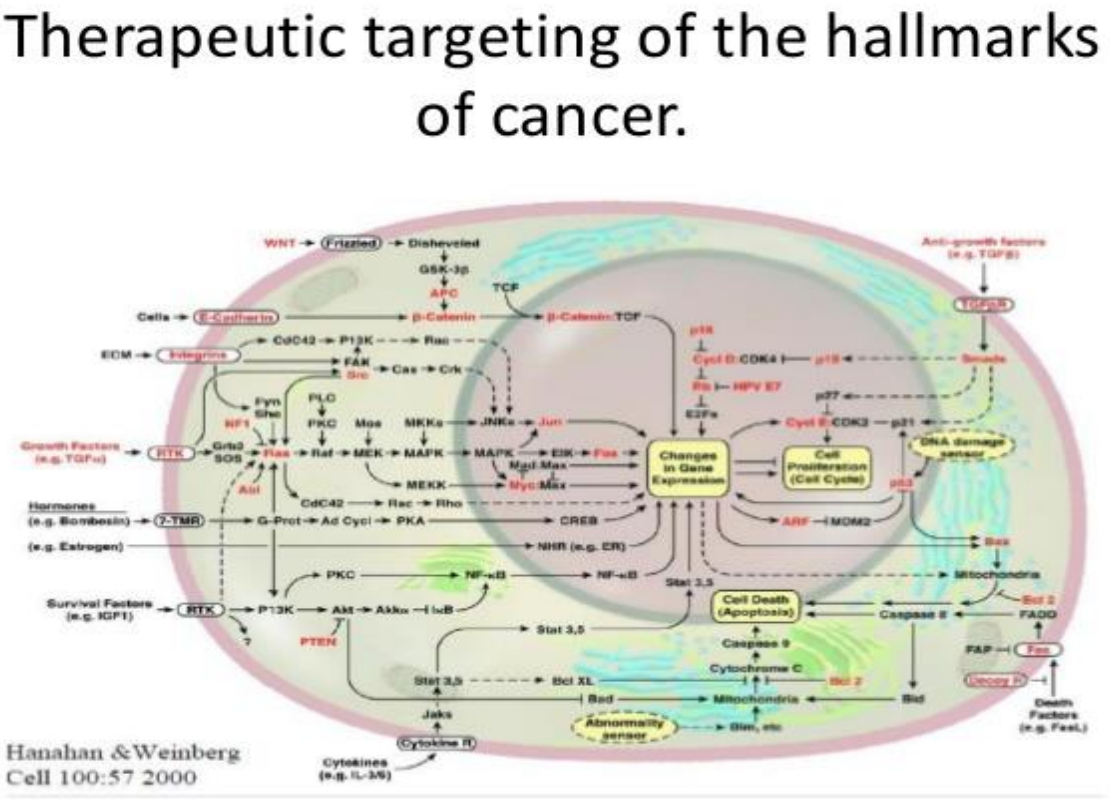

Figure 5: Therapeutic targeting of the hallmarks of cancer *Hanahan et al, 2000* [26]

1.5.2 Insensitivity to Antigrowth Signals

In addition to being capable of inducing and sustaining positively acting growth-stimulatory signals, cancer cells must also evade powerful programs that provide negative control of cell proliferation, depending on the actions of tumour suppressor genes in many cases[27]. To tightly control cellular quiescence and tissue homeostasis, normal cells have processes that negatively regulate cell proliferation. The cell cycle is the determinant for the response of normal cells to these antigrowth signals, notably the components

governing the transit of the cell through the G1 phase. During the cell cycle the genome maintenance teams aim at ensuring that DNA sequence remains intact. The assurance of karyotypic order is provided by yet other watchmen, the so-called checkpoints, that operate at critical times in the cell's life, especially mitosis. All these systems acting in concert ensure that mutations rarely occur. Anti-proliferative signals can be either soluble growth inhibitors or immobilized inhibitors that are incorporated into the extracellular matrix and on the surfaces of nearby cells. In the same way as their positively acting counterparts, growth-inhibitory signals are received by transmembrane cell surface receptors coupled to intracellular signalling pathways. There are two distinct mechanisms for blocking cell proliferation. Either cells may be forced out of the active proliferative cycle into the quiescent state(G0), which is a reversible arrest. Alternatively, cells may be forced to permanently relinquish their ability to proliferation, by being induced to enter into postmitotic states. Cancer cells must circumvent these antiproliferative signals[26]. Great amounts of tumour suppressors that operate in many ways to limit cell growth and proliferation have been revealed. The two crucial tumour suppressors within the cellular regulatory circuits are the pRB (retinoblastoma protein) and the TP53 (tumour–suppressor protein), operating as central control nodes within two key complementary cellular regulatory circuits that control decisions of cell either to proliferative or, alternatively, activate senescence and apoptosis programs[27]. Abnormalities of these proteins play a crucial role in the development of most human cancers[29].

1.5.3 Evading Apoptosis

The capability of tumour cells to increase in number is defined by the rate of cell proliferation as well as by the rate of cell attrition. Apoptosis constitutes a major source of this attrition. Generally, studies in mouse models, cultured cells, as well as on descriptive analyses of biopsied stages in human carcinogenesis provide mounting evidence that acquired resistance towards apoptosis is a hallmark of most and even perhaps of all types of cancer. Observations collected over the last decade show that the apoptotic program is present in latent form in almost all cell types. Once triggered by a variety of physiological signals, during this process the cell membranes are disrupted, the cytoplasmic and nuclear skeletons collapse, the cytosol is extruded, the chromosomes are degraded and the cell nucleus breaks up into fragments, all in a span of 30-120 minutes. Finally, the shrunken cell corpse is engulfed by adjacent cells in a tissue and disappears, typically within 24

hours[26]. There are upstream regulators as well as downstream effector components involved in the apoptotic signalling machinery. On the other hand, these regulators can be divided into two major apoptotic pathways: The first one, being termed "extrinsic apoptotic program", sensing and processing extracellular death-inducing signals and the second one, receiving and integrating a variety of signals of intracellular origin, known as "the intrinsic program"[27]. Both are responsible for the assessment of risks from the extracellular and intracellular environment and thus, influence whether a cell should live or die. Each culminates in the activation of intracellular proteases termed caspases, including the two "gatekeeper" caspases, −8 and −9. They, in turn, are induced by interfering with death receptors such as FAS or by cytochrome C release (from mitochondria). These caspases induce the activation of a dozen or even more effector caspases that execute the death program by selective destruction of subcellular structures and organelles and the genome cell[26].

1.5.4 Limitless Replicative Potential

All three capabilities, namely growth signal autonomy, insensitivity to antigrowth signals, and resistance to apoptosis decouple the growth program a cell from signals in its environment. However, studies that have been performed over the past 30 years show that this acquired disruption of cell-to-cell signalling, on its own, does not ensure extensive tumour growth. Many and perhaps all types of mammalian cells carry a program that limits their proliferation. This intrinsic, cell-autonomous program appears to work independently of the cell-cell signalling pathways described above. Early work showed that the cells in culture have a limited replicative potential. Once such cell populations have gone through a certain number of duplications, they stop growing(senescence). The senescence of cultured human fibroblasts can be circumvented by deactivating their pRb and p53 tumour suppressor proteins, enabling these cells to continue extending for additional generations until they enter into the crisis state. This second state is characterized by massive cell death, karyotypic disorder and the occasional appearance of a variant (1 in 107) that has gained the ability to proliferate without limit, manning so-called immortalization. Normal human cells have the capacity for 60-70 doublings[26]. According to multiple investigations, a protection facility of the ends of chromosomes, called telomeres that comprise the termini of eukaryotic linear chromosomes, has increasingly been determined to play a central role in the neoplastic state, the concept of

replication-induced senescence as a protective barrier requires refinement and reformulation[26,27]. Approximately 50–100 base pairs of telomeric repeat sequences are lost each time a cell divides. This progressive telomere shortening results from a combination of a failure to completely replicate the 3'ends chromosomal DNA during each S-phase. The progressive degradation of telomeres through successive cycles of replication has been attributed to the loss of their ability to protect the ends of the chromosomal DNA. The unprotected ends of chromosomes are involved in end-to-end chromosomal fusion, which in turn, may cause cell death.[26] Therefore, the length of telomeric DNA in a cell determines how many consecutive generations of cells can pass through their progeny before the telomeres end become uncapped, and thus lost their protective functions, leading to crisis[27]. The maintenance of telomeres is evident in almost all types of malignant cells, upregulating expression of the telomerase enzyme is a feature in 85%–90% of cancers.

1.5.5 Sustained Angiogenesis

Like normal tissues, tumours require for its survival nutrition in the form of nutrients, such as glucose and oxygen as well as the capability to evacuate metabolic wastes and carbon dioxide[27,30] from their blood supply. This is necessary to cell function and survival, forcing nearly all cells in a tissue to move within 100μM of a capillary blood vessel. This proximity is ensured during organogenesis by coordinated growth of vessels and parenchyma. Once a tissue is formed, the growth of new blood vessels (the process of angiogenesis) is transiently and carefully regulated. Because of this dependence on nearby capillaries, it seems plausible that proliferating cells in a tissue have an intrinsic ability to promote blood vessel growth. But the evidence is proved to be different. The cells in abnormal proliferative lesions initially have no angiogenic ability, which limits their ability to expand. In order to become larger, incipient neoplasms must develop an angiogenic ability[26]. The tumour-associated neovasculature addresses these needs. During embryogenesis, the development of the vasculature comprises the birth of new endothelial cells as well as their assembly in tubes (vasculogenesis) in addition to angiogenesis (new vessels sprout of from existing ones). After this morphogenesis, the normal vascular system is largely quiescent. In the adult, angiogenesis is activated as part of physiological processes such as wound healing and female reproductive cycling, but only temporarily. In contrast, during the development of tumours, an "angiogenic switch" is turned on and

remains in most cases, enabling normally quiescent vasculature to continuous sprouting of new vessels[27]. Angiogenesis is controlled by counterbalancing positive and negative signals, that are able to induce or block this process[26]. Signalling proteins are one of the groups of these angiogenic regulators that bind to activating or inhibitory receptors on the surface of endothelial cells. One well-described prototype of angiogenesis activator is VEGF-A (vascular endothelial growth factor-A), a secreted protein whose expression may be triggered by hypoxia or oncogenic signals[27]. The VEGF-A gene encodes those ligands are involved in the regulation of the growth of new blood vessels during embryonic and postnatal development, as well as in homeostatic survival of endothelial cells, and in addition in physiological and pathological situations in adults[26].

1.5.6 Tissue Invasion and Metastasis

During the development of most types of human cancer, pioneer cells are spawned out of the primary tumour masses that move out, invade nearby tissues, and thence migrate and put down roots in distant locations. These newly settlements-'metastases'- are responsible for about 90% of cancer deaths[26]. Metastatic cascade can be parsed into distinct steps, including the first process, called invasion, the second one intravasation into adjacent blood and lymphatic vessels, passage of cancer cells through the lymphatic and hematogenous systems, followed by the extravasation, the process when the cells exit the lumina of vessels and enter the parenchyma of distant tissues, formation of micrometastases as the penultimate step and finally the last one, called 'colonization', where the micrometastatic lesions outgrow into macroscopic tumours[27]. The associated cancer cells typically develop changes in their shape as well as an altered cell-cell and cell-extracellular matrix (ECM) interactions. The best documented alteration involves by carcinoma cells the loss of E-cadherin that is an important cell-to-cell adhesion molecule. By forming adherens junctions with nearby epithelial cells, E-cadherin is associated with the assembly of epithelial cell sheets and maintenance of quiescence of the cells within these sheets. Increased expression of E-cadherin was well-known as an antagonist of metastasis as well as of invasion, whereas it's decreased expression was established to potentiate these phenotypes.

1.5.7 Enabling Characteristics and Emerging Hallmarks

These acquired functional capabilities that are defined as the hallmarks of cancer include those that allow cancer cells to survive, proliferative as well as to disseminate, acquired in distinct tumour types through the series of steps in the process of tumourigenesis. The acquisition of these hallmarks of cancer cells can be enhanced by two enabling characteristics, including the most common one, the development of genomic instability in cancer cells. This instability is responsible for generating random mutations, for instance, chromosomal rearrangements, including rare genetic changes that may play a major role in orchestrating these capabilities. The second one is the inflammatory state excited by premalignant and frankly malignant lesions through the activation of the cells of the immune system that may promote tumour growth and spread via various means. Furthermore, other distinct capabilities of cancer cells have been considered to be of importance for the tumourigenesis might be added to the list of these framework, including reprogramming of cellular metabolism for satisfaction the demands of growth and proliferation, by causing metabolic alterations of normal tissues. The second that has emerged as a critical capability of cancer cells is evasion of immune destruction from the destruction by the immune system and simultaneously indicates the importance of immune system alteration to cancer survival[27].

1.6 Contributing Factors

Craig Venter, who is known for sequencing his own genome, noticed that certain risk factors may increase the chance of developing cancer and that our genes have a very little impact on life[31]. More particularly, only 5 to 10 % of all cancer cases can be attributed to inherited genetic mutations, whereas the remaining 90% to 95% are attributable to various lifestyle and environmental factors. Studies have shown that the concordance for developing cancer among monozygotic twins account for 20%, in contrast to 90%, where the environmental risk factors are an important issue. These observation indicates that cancer is a preventable disease. These modifiable lifestyle factors include tobacco use, alcohol consumption, eating habits, especially heavy consumption of fried foods and red meat, sun exposure, environmental contaminants, obesity, stress, infections and physical inactivity. The exposure to the at least 50 carcinogens in tobacco smoke causes at least 14 types of cancer. Furthermore, compared with non smokers, female smokers are 17 times and male smokers even 23 times more likely to develop lung cancer. It is not completely

clear how the tobacco use relates to the development of cancer. However, it's a fact that a variety of signal paths are modified and the cigarette smoke is a trigger for NF κB activation, an inflammatory marker, and therefore also for the inflammatory response. Further contributing factor is the consumption of alcohol and since the year 1910, it is known that there is an concordance between alcohol and an increased risk of esophageal cancer. Whereupon follow several studies that reported an association between alcohol and increased risk for for cancers of the upper aerodigestive tract, oral cavity, pharynx, larynx, hypopharynx, esophagus as well as of the liver-, pancreas-, mouth-, and breast cancer. How alcohol intake contributes to cancer is not completely understood, the same as the dietary habits. It is suggested, that ethanol, a cocarcinogen, and carcinogens in food and food additives, like nitrates, nitrosamine, pesticides and dioxins may induce activation of inflammatory pathways and are thus important issues related to cancer. Research has gained insights into the association between obesity and the increased mortality of some types of cancers, especially of the colon, breast (in postmenopausal women), kidneys (renal cell), endometrium, pancreas, gastric cardia, prostate, gallbladder, liver and the adenocarcinoma – cancer of esophagus. According to studies there is a a consistent evidence that the common denominators between obesity and cancer are neurochemicals, hormones, for instance IGF – 1 (Insulinlike Growth Factor 1), insulin, leptin, sex steroids, adiposity,insulin resistance and inflammation, including all their associated pathways.Worldwide, an estimated percentage of 17,8 of diagnosed cancer may be attributable to infections, varying between 10% in high-income countries and 25% in African countries[31]. Infectious agents such as hepatitis B (HBV) and C viruses (HCV) , Epstein-Bass virus (EBV), human papillomavirus (HPV), human immunodeficiency virus type 1 (HIV -1), herpes virus associated with Kaposi's sarcoma, Human T-Lymphotropic virus 1, Helicobacter pylori (H.pylori) and Streptococcus bovis (S. bovis) play an increasingly important role in developing cancer, especially of cervical-, anogenital-, skin-, nasopharyngeal-, gastric-, and liver cancer, as well as Burkitt's lymphoma, Hodgkin's lymphoma, B-cell lymphoma Kaposi's sarcoma and adult T-cell leukemia[31,32]. The causal role of these agents is their ability to activate the inflammatory marker NF-κB. Environmental contaminants has also been linked to a large number of cancer, including outdoor air pollutants like carbon particles related with polycyclic aromatic hydrocarbons (PAHs), indoor air ones like tobacoo smoke, formaldehyde, and volatile organics compounds, for instance, benzene and 1,3–butadiene, food additives, carcinogenic metals and metalloids, pharmaceutical medicines and cosmetics. Up to 10%

of the total number of cancer cases are related to radiation exposure, including ionizing as well as non-ionizing radiation, the pulsed electromagnetic fields produced by radioactive substances and ultraviolet (UV), caused mainly by the depletion of the ozone layer in the stratosphere[31].

1.7 Cancer–Treatment

There are many possibilites to treat cancer and the choice of treatment depends on the type of the tumour, it's stage, side effects that may occur as well as the overall health of the patient. Moreover, personal preferences may also affect the therapeutic options[33]. All of these methods cause vast side effects due to their lack of specificity and selectivity[34]. The most effective treatment of localized primary tumor and associated regional lymph nodes is surgery[35]. Although it is the oldest type of cancer therapy, it stil forms a mainstay of treatment in solid tumors[36]. In the case, it is used as a single treatment, surgery cures more patients than any other individual treatment option due to the fact that surgery operates by zero-order kinetics ensuring that 100% of excised cells are killed. In contrast, chemotherapy and radiation therapy operate by first-order kinetics and are only capable of killing a fraction of tumor cells by each treatment. Because of the fact that both processes are complementary, they were often used in combination. In the 1920s radiation therapy began to be used, following by the advent of chemotherapy after the 1940s and thus, lead that cancer surgery has become conservative. Approximately 45% of all incident cases of cancer radiotherapy (RT) is used, with an increasing tendency. Furthermore, RT is responsible for 40% of cancer cure presenting a cost-effective treatment. RT as a single treatment (external beam and/or brachytherapy) is used as curative therapy in a number of types of cancer, for instance, in early stage head and neck tumors as well as in the case of prostate cancer or early stage Hodgkin’s disease. Nowadays, preoperative RT is used in a limited number of tumour locations such as rectal and oesophagueal carcinomas whereas postoperative RT is used in many tumor sites including breast and central nervous system tumors among others. In occasional cases, intraoperative RT is used, a technology that delivers a large dose during surgery with either electrons or low energy photons in a single treatment session. Combination of radiation with surgery and/or chemotherapy is more commonly used as a treatment[35]:

Adjuvant therapy: The administration of additional cancer treatment as after the primary treatment such as surgery and/or radiation to lower the relapse rate. Examples of

adjuvant therapy may include chemotherapy, radiotherapy, hormone therapy, targeted therapy, or biological therapy.

Neoadjuvant therapy: An anti-cancer treatment given as a first step to shrink a tumor before the main streatment is given, which is usuallly surgery. It is regarded as a type of induction therapy and may include chemotherapy radiation therapy, and hormone therapy[34]. Over the past years, a new generation of cancer treatment has become of paramount importance in cancer research, i.e. targeted cancer therapy. These therapies use pharmacological agents that inhibit growth, increase the occurrence of cell death and limit the spread of cancer. As the name suggests, they function by interfering with specific proteins, related to tumourigenesis[37]. Research on the treatment of cancer is essential to improve outcomes for patients that combat this disease. These fundamental requirements include the development of treatments with less toxicity and better efficacy, such as targeted therapies, immunotherapies, and cancer vaccines, as well as the improvement of therapies that have been used for decades, like for instance chemotherapy, radiation therapy, and surgery[38].

1.7.1 Chemotherapy

The era of chemotherapy began in the 1940s with the first uses of nitrogen mustard and antifolate drugs to treat cancer. Since then, the development of cancer drugs has transformed from a low-budget, government-sponsored research effort to a high-stakes, multi- billion dollar industry. Although the targeted-therapy revolution has arrived, the principles and disadvantages of chemotherapy still remain valid[39]. The entirety of anti-cancer drugs (chemotherapeutic agents) function by fighting rapidly dividing tissue and due to the inability to distinguish malignant cells from normal cells, both are affected in the same toxic way[40,41]. The normal cells most commonly affected by chemotherapy are those with fast proliferation rates, for instance, the hair follicles, bone marrow and gastrointestinal tract cells, causing the characteristic side effects of this treatment, for instance, alopecia, bone marrow aplasia and mucositis[34]. Some side effects are short-lived include those toxic effects occurring during chemotherapy, while long-term side effects include later complications that become apparent after treatment has been concluded.[42] For instance, some types of chemotherapeutics may cause permanent damage to the heart, lung, reproductive system as well as to eliminating organs such as liver and kidneys[43]. As in the case of surgery and RTadiotherapy, chemotherapy is also commonly categorized as

being either curative or palliatively[34]. Curative chemotherapy has the goal of achieving a complete remission whereas the goal of palliative care is to alleviate symptoms or postponing future symptoms of the disease and thus maintain or enhance the best possible quality of life[34,44]. Despite occasional successes the treatment for most cancers turns out to be difficult . This occur due to the development of resistance and and result in loss of effectiveness of therapy[45].

Although many cancerous cells are initially susceptible to chemotherapy, over time they may develop different mechanism of resistance to the treatment, as followed[46] :

- Inactivation of absorption into the cell, e.g. of methotrexate
- Inactivation of cytostatic function of the drugs, e.g. as a result of an increased aldehyde-dehydrogenase, inactivating cyclophosphamides
- Lower level of inactive prodrugs, which happens very often by antimetabolites
- Increase of drugs like alkylating agents, cisplatin or topoisomerase II inhibitors, that occur in DNA damage repair mechanism
- The target molecule is altered, where drug binding is prevented
- Altered Substrate Specificity
- Overexpression of Glycoprotein P-170 and other ABC transporters

To combat resistance to chemotherapy several strategies have been developed with some success, including the combination of chemotherapeutics with RT and surgery, local application of high dose agents and combination of therapeutics with different targets. Nevertheless, the drug resistance remains a major obstacle in oncology[34].

1.7.1.1 Anti- Cancer Agents

The next chapter will provide a small insight into the present agents for tumour treatment, classifying and summarizing single compunds by their point of action.

1.7.1.1.1 Molecular Pathway Targeted Therapy

The introduction of mechanism-based targeted therapies to combat human cancers has been heralded as one of the fruits of three decades of remarkable advances in research into the mechanisms of cancer pathogenesis[27]. Targeted anti-cancer therapy(TAT) refers to the systemic administration of drugs with certain mechanisms that act specifically to well-defined targets or biological pathways that, in case of activation or deactivation, can lead to regression or destruction of the malignant process. while at the same time harmful effects on healthy tissues are minimized[47]. By comparison to surgery, RT and chemotherapy, TATs based on cutting-edge translational, obtained either from the unique characteristics of molecules, antibodies, proteins, and peptides or from structures, metabolism, and other phenotypic properties of cancer, in order to destroy cancerous cells more effectively and thus, improve the treatability[35]. The fast-growing number of targeted therapeutics can be classified by their respective effects on one or more hallmarks capabilities[27]**.** Over the past 10 years, the treatment of cancer have considerably changed. With the advent of TAT, including monoclonal antibodies and small molecule inhibitors, distinct mechanism of action were developed and toxicities were generated from those of the traditional chemotherapy[48].

1.7.1.1.2Intervention of Cell Metabolism and DNA-Synthesis

1.7.1.1.2.1 Antimetabolites

Antimetabolites are chemicals that ‘inhibits’ the synthesis of DNA and RNA by competitively inhibiting and self-binding natural metabolic components(metabolites). Non-functional molecules are formed or blocked by the antimetabolites enzymes, disturbing cell division and metabolism. The group of antimetabolites includes folic acid antagonists such as Methotrexate and Pemetrexed, and purine- and pymiridine- base analogs such as Mercaptopurine and Fluorouracil.

1.7.1.1.2.2 Alkylating Agents

Agents of this type comprise reactive, mostly bifunctional cytostatic drugs that have in common their phase-unspecific effect primarily based on alkylation of nuclei acids[34] Their therapeutic cytotoxicity is based on the formation of strong bonds with covalent characteristics on both strands of DNA, leading to multiple DNA alterations, including

cross-linking of bases, abnormalities in base pairing and DNA strand breakage[49,50]. Thus, these subgroup of medications inhibit DNA reduplication and cell division. There are several different types of alkylating agent, including nitrogen mustard derivatives (e.g. Cyclophosphamide) aziridine compounds (e.g. Thiotepa), alkyl Sulfonates (e.g. busulfan), N-nitroso-carbamide derivatives (e.g. Carmustine) and platinum complexes (e.g. Cisplatin).

1.7.1.1.2.3 Topoisomerase Inhibitors

DNA can be packaged by forming coils in order to fit into the nucleus. The enzymes that are able to control the topology of DNA are called topoisomerase[34]. Topoisomerase is able to cut DNA at a particular point and untangle the twist in order to relieve the supercoil and thus, allow the space for another DNA synthesis, followed by rejoining them again after the replication. There are two forms of the topoisomerase inhibitors: topoisomerase I and topoisomerase II. Topoisomerase I inhibitors form a complex with the enzyme and the DNA, which in turn results either in uncontrolled single strand breaks, whereas topoisomerase II is able to separate both of the duplexes. Examples of topoisomerase inhibitors are: Topotecan, Irinotecan or Etoposide.

1.7.1.1.2.4 Microtubule Inhibitors

Inhibition of cell cycle is possible through a mitotic block. This class of pharmaceuticals, derived from natural sources, comprises drugs, like colchicine, and vinca alkaloids including their derivatives, that interact with tubulin and inhibit its polymerization to microtubules and thus the mitotic spindle formation, and drugs, like taxanes, that stabilize tubulin in the microtubules, thereby inhibiting the process of cell division due to the fact that depolymerization is prevented[34].

1.7.1.1.2.5 Intercalating Agents

The molecular mechanism of the intercalation process remains still discussed controversially, According to research findings, this class of agents have several mechanism of action[51]. Further types of anti-cancer drugs include hormones, enzymes, immunotoxines, cytokines and histone-deacylase inhibitors, without going into details within this thesis.

The typical intercalating substances bear some common characteristics in order to be used in cancer therapy:

- • Polyaromatic (3-4 rings) and coplanar
- • 3-4 Å wide and 6-8Å long
- • Surface 28Å^2
- •Charge-transfer complexes, dipole-dipole-interactions, electrostatic potential
- •Para-conjugated quinone ring and nitrogen in the system show positive effects on intercalation[52,53]

In most cases, intercalating substances consist of three or four fused rings that have the ability to absorb light in the UV-visible region of the electromagnetic spectrum, and thus usually known as chromophores. Generally, it can be distinguished between two types of intercalating agents, namely: monofunctional and bifunctional intercalators. The first mentioned group consists of one intercalating unit and the so-called bis-intercalators contain two intercalating units, usually cationic, separated by a spacer chain with a sufficient length to allow double intercalation, including the most general rule for intercalative binding, the neighbour-exclusion principle. In order to insert an intercalator between DNA base pairs, the DNA has to undergo a conformational change involving an increased vertical separation between base pairs to open a space for the incoming ligand. This partial unwinding induces distortions of the sugar-phosphate backbone and changes in the twist angle between adjacent base-pairs [54].

1.7.1.1.2.5.1 Anthracyclines

Anthracycline and related compounds are originally derived from bacteria Streptomyces and thus, also grouped under a larger class of anti-tumor antibiotics, even if they are not used to treat infections[55]. The best known representative of this group is doxorubicin. Doxorubicin and related anthracyclines (Daunorubicin, Epirubicin, Idarubicin, etc.) have the advantage of a broad spectrum of activity. Nevertheless, this class of drugs has a massive disadvantage on many cancer cells, namely the cardiotoxicity. [56] Thus, in long-term therapy is the dose-dependent myocardial damage to take into account. The mechanism of action by which this class of anti-cancer drugs inhibit cancer is still not

completely clear and multiple mechanism have been proposed to explain the cytotoxicity of anthracyclines, including the most prominent mechanism including the inhibition of topoisomerase II and the intercalation. This is triggered by placing a planar drug between base pairs of the strand. This intercalation leads subsequently to the disruption of the replication and transcription processes massively[57].

1.7.1.1.2.5.2 Mitoxantrone

This synthetic anthraquinone class with structural similarities to anthracycline lacks the sugar moiety, but interacts by intercalation due to their planar polycyclic aromatic ring structure, Mitoxantrone has been reported to have lower propensity for production of quinone-type free radicals and cardiotoxicity relative to the anthracyclines. Two mechanism of action can be distinguished. The highest-affinity interaction by intercalation, with the preference occurring at G-C base pairs, and the lower-affinity bindings by electrostatic interactions, which may explain the compaction of the chromatin structure, induced by Mitoxantrone what has been observed in cells. As discussed for the anthracyclines, Mitoxantrone intercalate into DNA and interferes with the strand-reunion reaction of topoisomerase II, resulting in DNA cleavage. This anti-cancer drug also causes some non-protein-linked single strand breakage, but they provide a minor contribution to the cytotoxicity. By contrast with the anthracyclines, this type of DNA damage is apparently due to oxidative activity of Mitoxantrone itself, reacting with DNA and not due to the generation of active species of oxygen[58]. A randomized trial compared side effects of Mitoxantrone and Doxorubicine, and even though they share similarities in their modes of toxicant action, Mitoxantrone shows a significant reduction of side effects, such as nausea, vomiting, stomatitis and alopecia[59]. Mitoxantrone was approved for the treatment of symptomatic hormone-refractory prostate cancer, leukemia, lymphoma and breast cancer[34].

2. Results and Discussion

2. Results and Discussion

2.1. Aim of The Work

The aim of the thesis was to modify as well as to expand the core structure which was already synthesized at the Department of Drug and Natural Product Synthesis to exhibit it's cytotoxic effects. Moreover, this work has the aim to extend the substance library by N-alkylated ellipticin derivatives, with side chains of complex nature.

The reason for the synthesis of new anti-tumour compounds was on the basis of the works of *Krapcho and Menta* [60], who have developed a variety of aza-bioisosteric chemotypes structurally related to Mitoxantrone that has been replaced by a pyridine ring in the 5,8-dihydroxyphenyl ring, which is believed to be responsible for its cardiotoxicity. This modification led to the development of topoisomerase II inhibitor Pixantrone, an aza-anthracenedione heterocyclic compound, initially known under the code name BBR 2778, that was revealed to have anti-tumour activity without cardiotoxicity. This cytostatic agent received in the year 2012 conditional marketing authorisiation in the European Union under the name Pixuvri® for the monotherapy of adult patients with multiply relapsed or refractory aggressive B cell lymphomas (NHL). The purpose to synthesize a potent anticancer agent with exhibiting cytotoxic effects, but retaining the broad therapeutic spectrum of mitoxantrone could not be achieved[61].

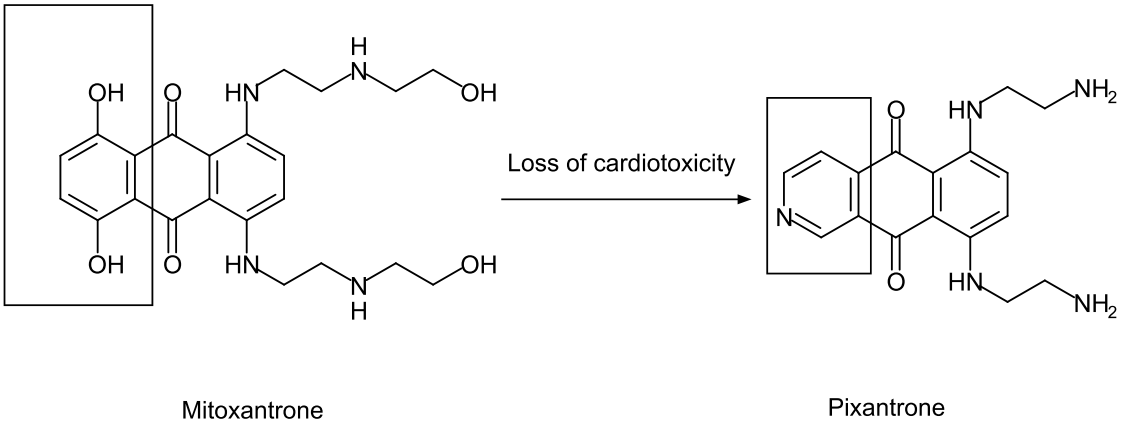

Figure 6: Aza-bioisosteric chemotype related to Mitoxantrone [61]

In the following thesis an indolo-annelated pyridoquinone was chosen for further structure-activity relationships. It exhibits an indolo-moiety instead of the diaminosubstituted benezene.

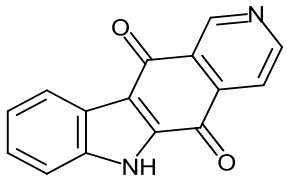

21

Figure 7: Target compound

Side chains have been synthesised, such as trans-alkenes and chains with S-inserted compounds, such as sulfoxides. The end of each side chain should consist of a hydroxyl function or an amino function in order to be able to test an increasing activity by interactions via hydrogen bonding or reversible binding to the DNA phosphate backbone.

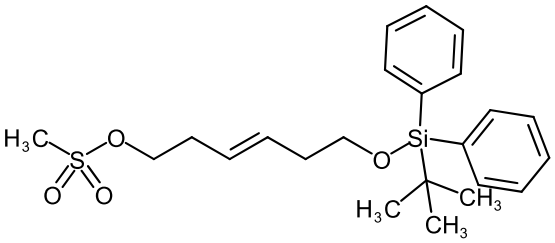

6

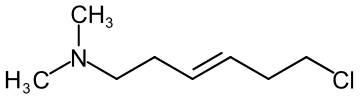

9

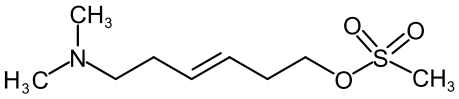

10

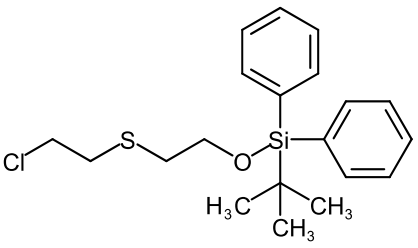

13

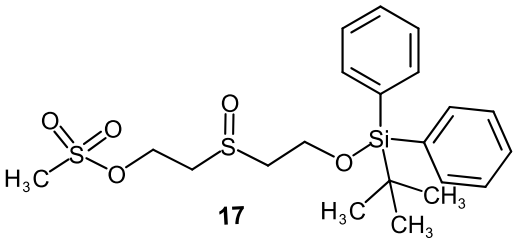

17

Figure 8: Side chains for alkylation

2.2 Synthesis of Aliphatic Side Chains

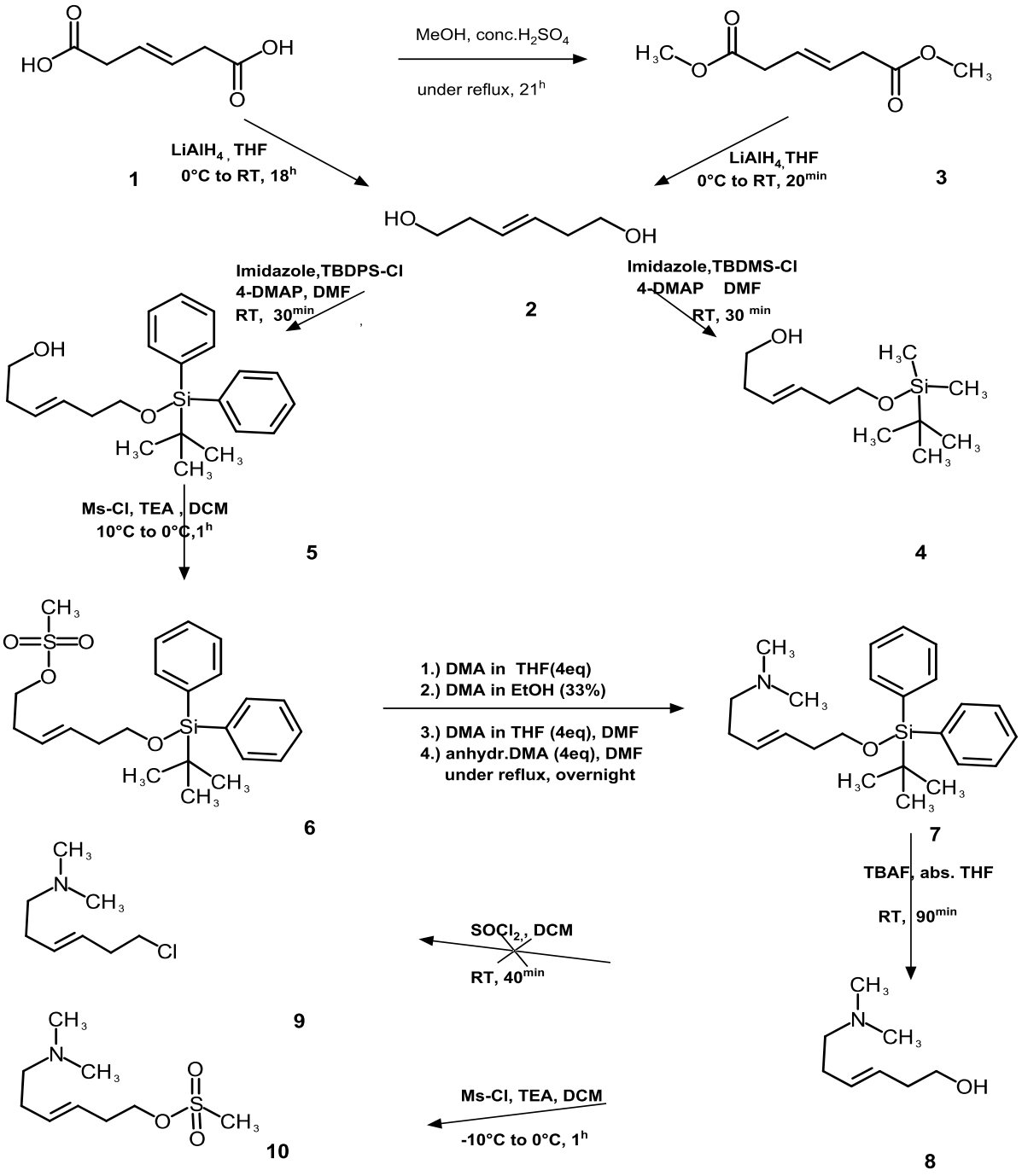

Figure 9: Reaction scheme of aliphatic side chains

2.2.1. Synthesis of (3E)-hex-3-ene-1,6-diol

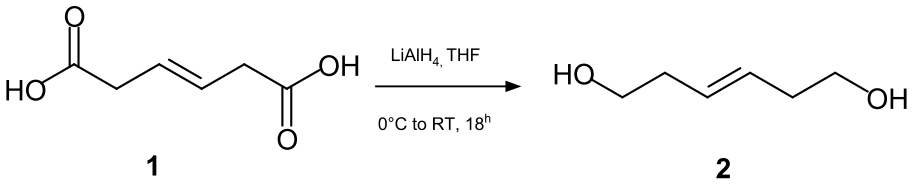

The conversion of trans hydromuconic acid **(1)** to the alcohol (E)-3-hexene-1,6-diol **(2)** was carried out using the strong reducing agent $LiAlH_4$ according to *Shahabi Mohammad Shahi 2016* [62] could not be successfully realized. Due to the unsatisfactory outcome of the reaction, combined with a great deal of effort involved in this synthesis, especially the separation of the small amounts of the compounds with high boiling point of 110°C via Kugelrohr Distillation, no further reactions were performed. According to NMR analysis, starting material was left as well as unwanted side products were formed. An alternative, suitable method to overcome these problems is the Fischer Esterification, according to *Triantafyllakis et al. 2014* [63], where a reduction the carboxylic acid **(1)** leads to the formation of diester **(3).**

2.2.2 Synthesis of 1, 6-dimethyl (3E)-hex-3-enedioate

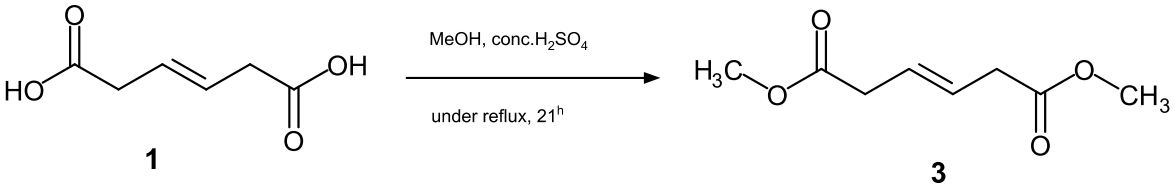

Fischer esterification is an equilibrium reaction by heating a carboxylic acid **(1**) and an alcohol (MeOH), using an acid catalyst (H_2SO_4) to form an ester. Thus, this reversible reaction must be driven and shifted to the product either by continuously removing one of the products in the system or by using excess reagent[64]. While stirring the acid **(1**) in the alcohol vigorously, the conc. sulfuric acid was added dropwise from a dropping funnel to make sure that the reagent is being mixed properly. After refluxing overnight, the flask was cooled down to RT and the solvent was removed without any problems, followed by the workup to remove impurities. NH_4Cl and $NaHCO_3$ were used to stop the reaction and to remove unwanted acids and the last wash with brine removes residual water from the layer. $NaHCO_3$ was used to eliminate last traces of acid. ^{1}H-NMR spectra showed that the resulting diester **(3**) was formed without observing any by-products (yield 94 %).

2.2.3 Synthesis of (3E)-hex-3-ene-1,6-diol

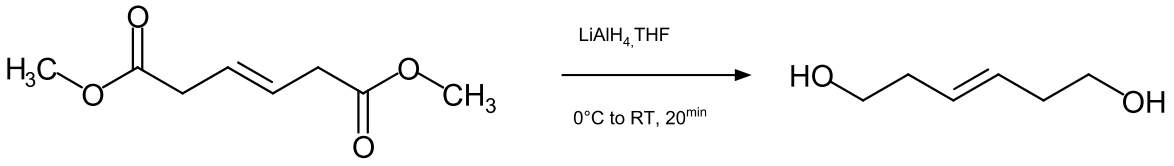

3 **2**

Based on the fact that $LiAlH_4$ is a high reactive solid toward water, by releasing H_2, the reaction has to be performed in inert atmosphere and with dry solvents. Moreover, $LiAlH_4$ charge should be new and clear without any precipitations. Following the protocol of *Triantafyllakis et al. 2014* [63], it is very important is to put $LiAlH_4$ in the flask first, followed by adding the diester **(3**) in anhydrous THF dropwise to the reactive solid, thereby paying attention to the temperature that should not be higher than 10°C. After 20 min, the finished reduction should be cooled down to 0°C and a saturated aqueous solution of Rochelle's salt which functions as an excellent ligand for aluminum, should be added dropwise under vigorous stirring. After the reaction is quenched, precipitates from the solution can be easily filtered off. After removing the solvent *in vacuo*, the NMR spectroscopy determined that the resulting clear oil was isolated in good yields and good purity as the product **(2).** The diol can be used for the next reaction without any further purification.

2.2.4 Synthesis of (3E)-6-{[tert-butyl(chloro)methylsilyl]oxy}hex-3-en-1-ol

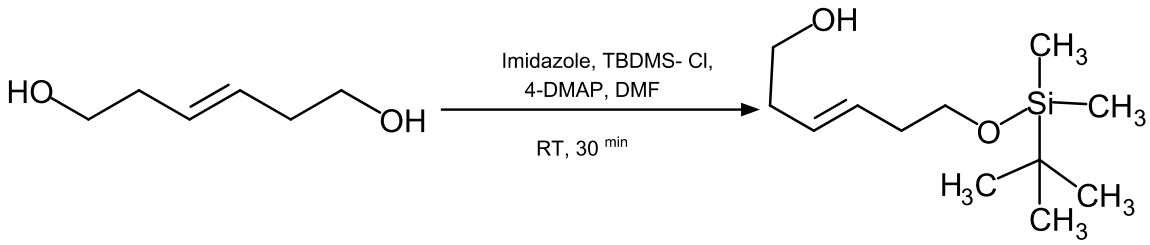

2 **4**

1.Attempt:

In the next step, the protocol of *Triantafyllakis et al. 2014*[63] was followed, where one of the two hydroxy groups of the diol **(2)** was protected with TBDMS-Cl (t-Butyldimethylsilyl-chloride) that was expected to succeed according to the TLCs, but after purification it was revealed that the product **(4)** was unstable in silica gel.

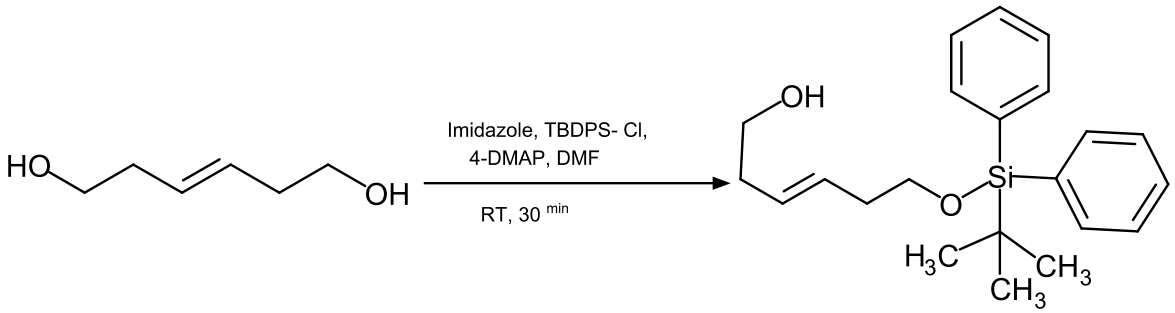

2 **5**

2.Attempt:

After searching the literature for better conditions, the second attempt protecting one of the two hydroxy groups of the diol **(2)** according to *Triantafyllakis et al. 2014* [63], was performed by using tert.-Butyldiphenylsilyl chloride (TBDPS-Cl) instead of TBDMS-Cl that afforded better yields and the purification of the crude product caused no problems.

2.2.5 Synthesis of (3E)-6-[(tert-butyldiphenylsilyl)oxy] hex-3-en-1-yl-methane-sulfonate

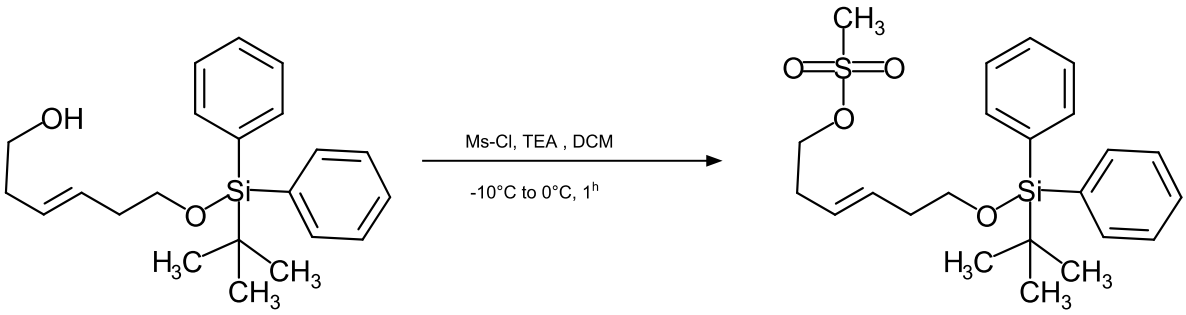

5 **6**

Using the protocol by *Shahabi Mohammad Shahi 2016* [62], alcohol **(5)** was mesylated with methanesulfonyl (Ms-Cl) chloride in anhydrous CH_2Cl_2, under basic condition, for preparing a mesylate **(6).** The reaction was observed *via* TLC. According to the work-up of *Whelton and Huitric 1970*[65], the basic aqueous solution should be quenched with ice-water, neutralized by washing with ice-cold 10%HCl, $NaHCO_3$, and finally with brine. According to the TLC monitoring the conversion to the product **(6)** was successful and gave a yield of 98%, moreover NMR spectroscopy did not determine any by-products.

2.2.6 Synthesis of [(3E)-6-[(tert-butyldiphenyl silyl)oxy] hex-3-en-1-yl]dimethyl-amine

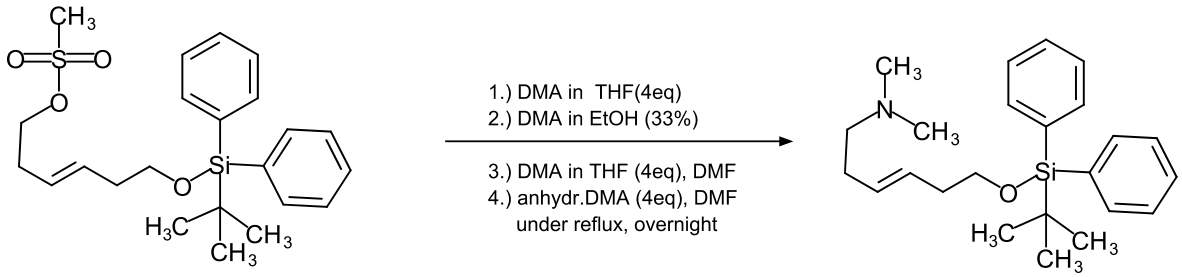

6 **7**

The desired amine **7** was prepared in four different ways under different reaction conditions in order to maximize the yields.

1. Attempt:

The first attempt to synthesize the amine **(7)** was made by *Shahabi Mohammad Shahi 2016* [62], using a slightly modified procedure by using 4 equiv. of THF instead of 1 equiv.

2.Attempt

The second try was made by using a different solution of 33% dimethylamine in EtOH, increased the yield.

3.Attempt:

In the third attempt DMF was used as the second solvent. These conditions, led to a satisfactory outcome.

4.Attempt:

According to the NMR analysis, the reaction carried out in anhydrous DMA (4eq) and DMF as the only solvent under oxygen free conditions obtained the most satisfactory yield (94%).

2.2.7 Synthesis of (3E)-6-(Dimethylamino)hex-3-en-1-ol

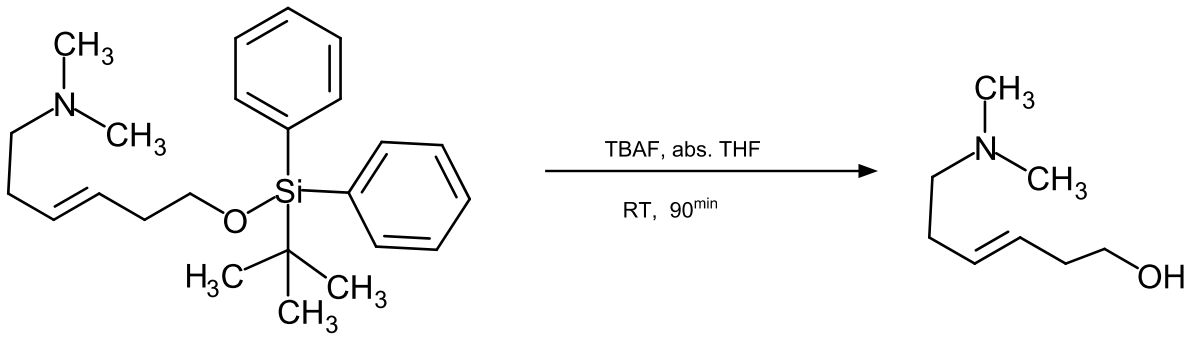

7 **8**

Tetra-n-butylammonium fluoride (TBAF) is a commonly used desilylation reagent to remove

the protection group. This rapid cleavage has the advantage that the synthesis can be performed at RT. The reaction, according to *Shahabi Mohammad Shahi 2016* [62], was observed via TLC and after 90^{min}, the spot of the protection group vanished. Upon the purification of the crude residue by column chromatography (Alumina II, Hexan/MeOH/EtOAc, 6/1/3), the product could not be isolated according to the NMR spectrum, since a by-product was formed with the same R_f value as the desired compound **(8)**.

2.2.8 Synthesis of [(3E)-6-chlorohex-3-en-1-yl]dimethyl amine

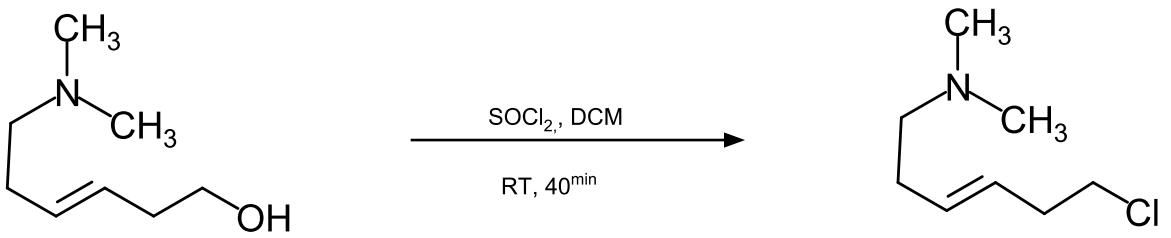

8 **9**

Contrary to expectations, the transformation of the alcohol to the corresponding chloride **(9)** in abs. DMF, according to *Shahabi Mohammad Shahi 2016* [62], was not successful according to the NMR analysis.

2.2.9 Synthesis of (3E)-6-(dimethylamino)hex-3-en-1-ylmethanesulfonate

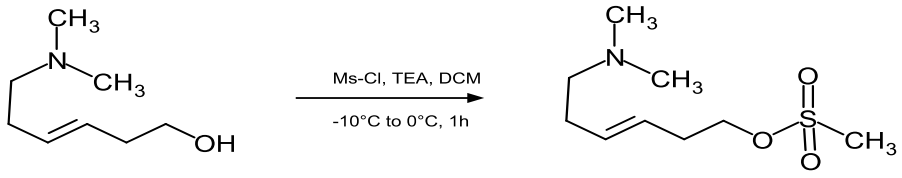

8 **10**

The alternative route, namely the transformation of the alcohol to the corresponding mesylate **(10)** in abs. DCM, according to *Shahabi Mohammad Shahi 2016*[62], was confirmed by the spectroscopy to be successful, but the product **(10)** was unstable during the purification in silica gel (0%).

As a conclusion follows to sum up that, neither the substitution of the hydroxy group with chlorine using thionyl chloride nor mesylation was successful. The chloride **(9)** was not formed at all and the mesylate **(10)** could not be isolated.

2.3 Synthesis of Sulfur Containing Side Chains

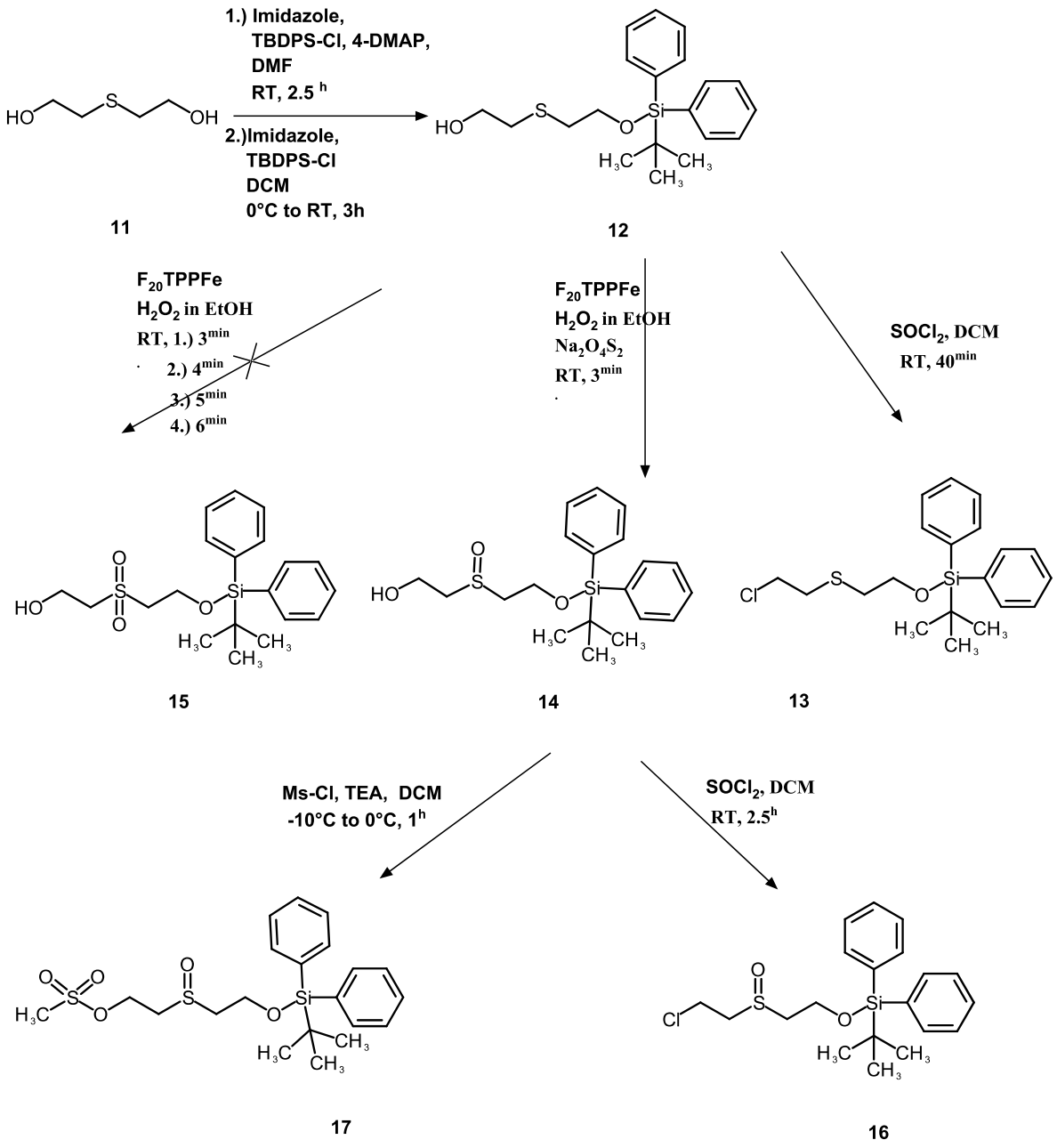

Figure 10: Reaction scheme of sulfur containing side chains

2.3.1 Synthesis of 2-({2-[(tert-butyldiphenylsilyl)oxy]ethyl}sulfanyl)ethan-1-ol

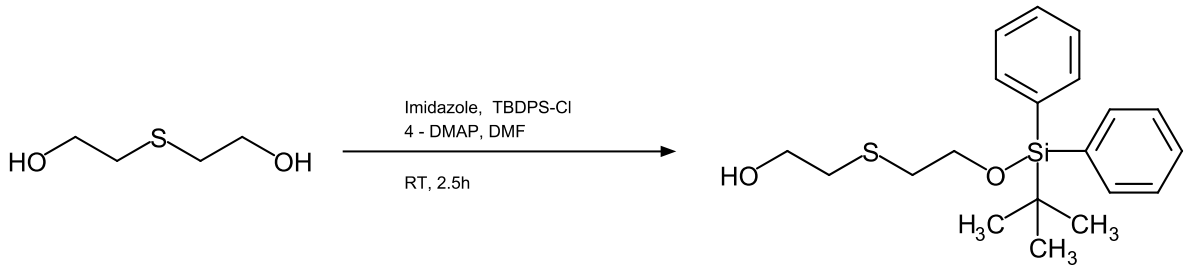

11 **12**

1.Attempt:

This step includes the protection of one of the two hydroxy groups with TBDPS-Cl in DMF, using 4-DMAP as an nucleophilic catalyst like in the synthesis of **(4)**, according to *Triantafyllakis et al. 2014*[63], which was expected to succeed. Upon work-up isolation of the residue by flash column chromatography (silica gel, Petroleum ether/EtOAc, 7/3) the desired product **(12)** was afforded in moderate yields (54%).

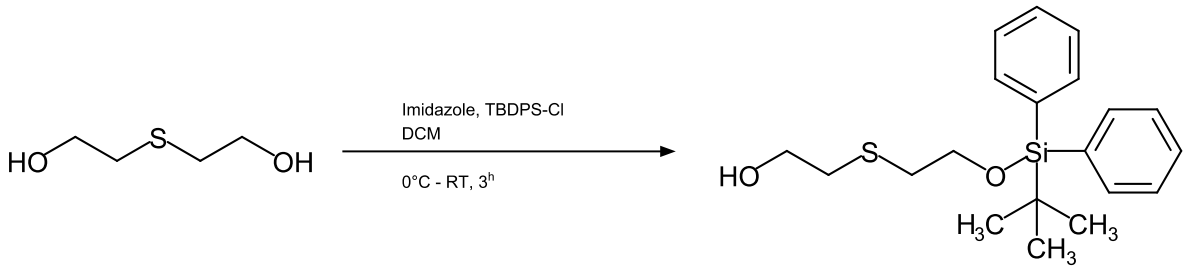

11 **12**

2.Attempt:

The protection of one of the two hydroxy groups with TBDPS-Cl in DCM, following a protocol published by *Shahabi Mohammad Shahi 2016* [62], without 4-DMAP gave only 25% of the desired product **(12)**. It was concluded that it is important to add the catalyst to obtain a satisfactory yield.

2.3.2 Synthesis of tert-butyl({2-[(2-chloroethyl)sulfanyl]ethoxy})diphenylsilane

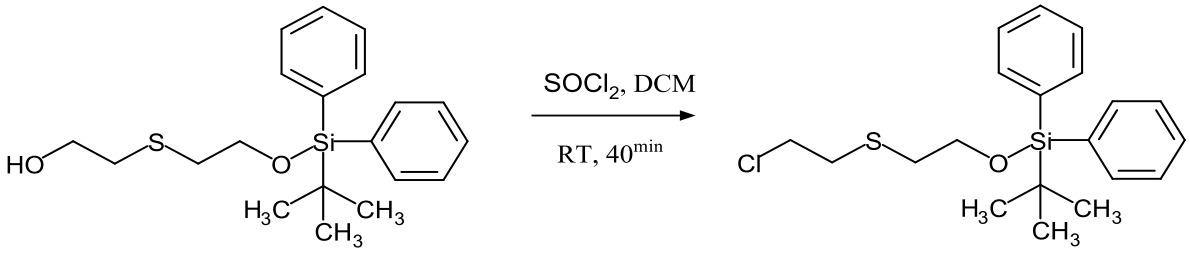

12 **13**

The preparation of the desired product **(13)**, followed a protocol published by *Shahabi Mohammad Shahi 2016* [62] that was also used for the synthesis of **(9)**, was successful and gave a yield of 95%, without any further purification needed.

2.3.3 Synthesis of {2-[(tert-butyldiphenylsilyl)oxy]ethanesulfinyl}ethan-1-ol

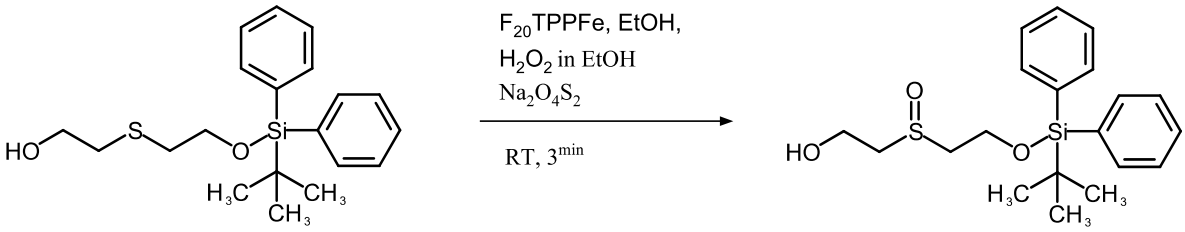

12 **14**

For the formation of sulfoxide **(14)**, a solution of sulfide **(12)** in EtOH and F_{20}TPPFe an equimolar solution of ethanolic hydrogen peroxide to the substrate was added and stirred for 1^{min}, followed by 3^{min} stirring (until the colours of the solution changed from darkgreen to orangebrown), following the protocol of *Shahabi Mohammad Shahi 2016* [62]. The isolated white-yellow crystals of **(14)** could be characterized based on NMR analysis as the desired product, but also a small amount of the sulfone **(15)**. It was concluded that the purification by flash chromatography is important, as the formed inorganic salt disturbed the following mesylation.

2.3.4 Synthesis of tert-butyl[2-(2-chloroethanesulfinyl)ethoxy]diphenylsilane

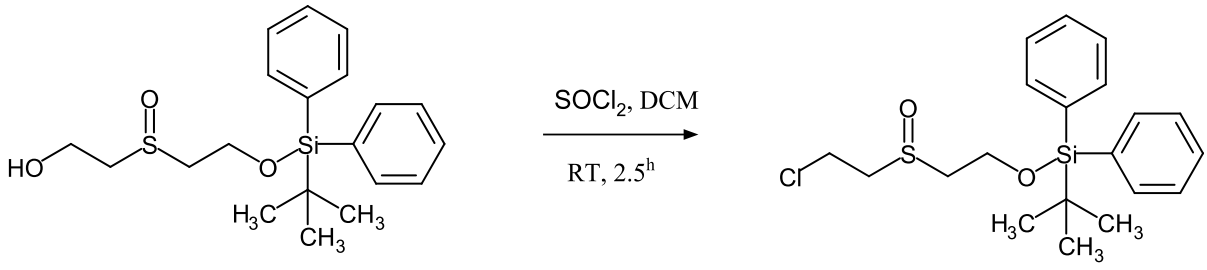

14 **16**

The preparation of the desired product **(16)**, followed a protocol published by *Shahabi Mohammad Shahi 2016* [62], was performed at RT and the reaction was controlled by TLC. According to NMR analysis, the reaction led to the product **(16)**, but it was unstable under chromatographic conditions and decomposed on silica gel.

2.3.5 Synthesis of 2-{2-[(tert-butyldiphenylsilyl)oxy]ethanesulfinyl}ethyl methane-sulfonate

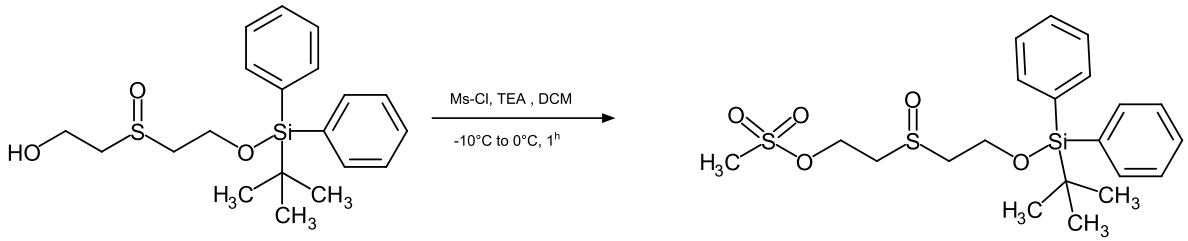

14 **17**

Due to the instability of **16**, it was tried to transform the alcohol to the corresponding mesylate **(17)** in abs. DCM, according to *Shahabi Mohammad Shahi 2016* [62]. The mesylation was successful and the crude product was stable under chromatographic conditions.

2.3.7 Synthesis of 2-{2-[(tert-butyldiphenylsilyl)oxy]ethanesulfonyl}ethan-1-ol

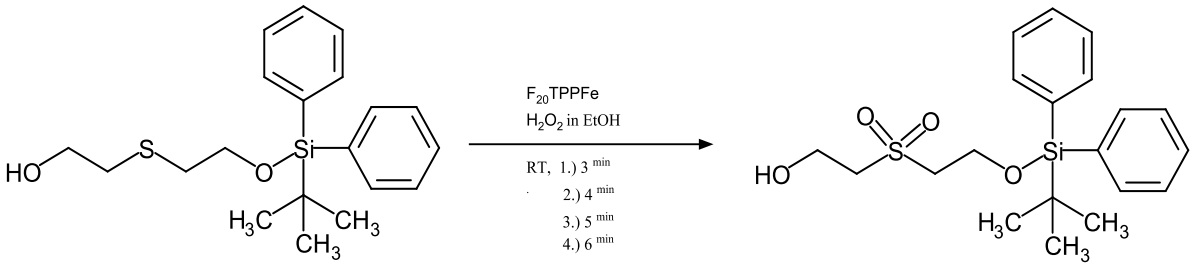

12 **15**

Because of the successful conversion of sulfide **(12)** to sulfoxide **(14)** and a small amount of the by-product sulfone **(15),** it was tried to selectively synthesize the sulfone **(15)** under the same conditions as described in the protocol of *Shahabi Mohammad Shahi 2016* [62], except using the reducing agent sodium dithionite. Carrying out synthesis with different reaction times had the purpose of figuring out if it has an influence on the structural variations.

	30% of H_20_2 in EtOH solution	Reaction time
Reaction 1	1.0 EQ	3 min
Reaction 2	1.0 EQ	4 min
Reaction 4	1.0 EQ	5 min
Reaction 5	1.0 EQ	6 min

According to NMR analysis of the crude product, the oxidation did not lead to the sulfone **(15)**, but to the sulfoxide again **(17).** No further reactions were performed.

2.4 Synthesis of the Core Structure

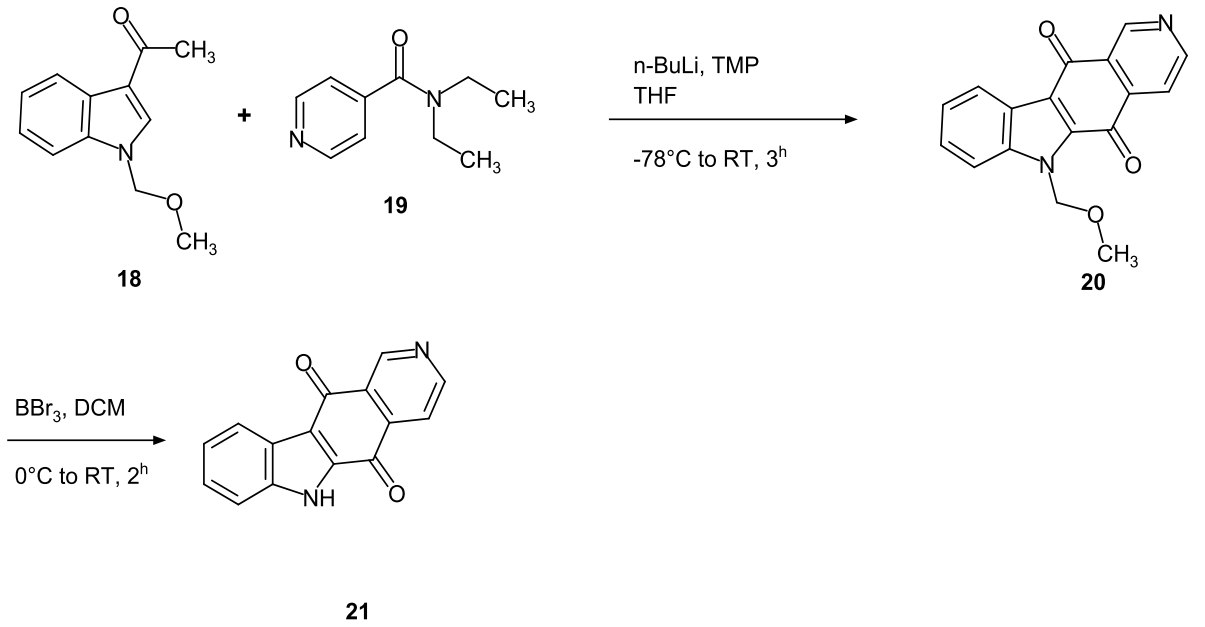

Figure 11: Reaction scheme of the synthesis of the core structure

2.4.1 Synthesis of 6-(methoxymethyl)-5H,6H,11H-pyrido[4,3-b]carbazole-5,11-dione

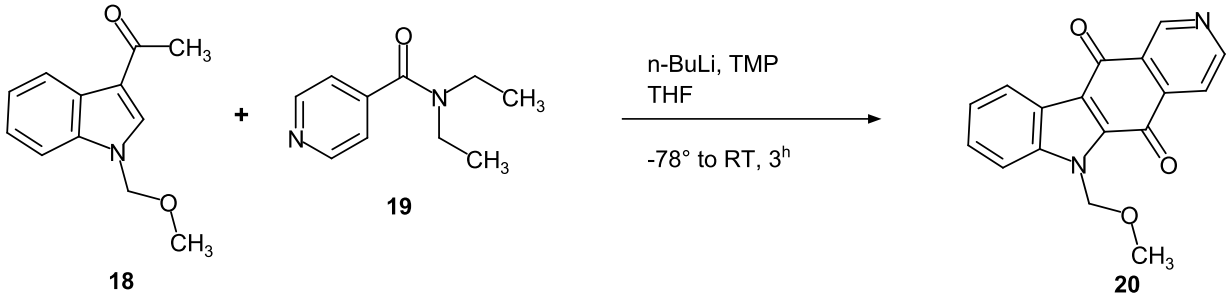

The synthesis of the intermediary MOM-protected pyridocarbazole-dione **(20)** by the protocol of *Nagel 2005* [61], was performed by adding TMP dropwise to a solution of n-BuLi (4 equiv.) in abs. THF under an argon atmosphere at -70°C. The lithium TMP solution was allowed to warm up to -5°C to 0°C within 30^{min} and was stirred at the same temperature for further 30 min, followed by cooling down the reaction mixture to -78° C. At this temperature, a solution of **(19)** (1 equiv.) and **(19)** (1 equiv.) in abs. THF was added dropwise in order to keep the internal temperature not higher than -65° C. After reaching RT within 2^{h}, the mixture was quenched with water and the aqueous layer was extracted with EtOAc, dried with Na_2SO_4 and concentrated *in vacuo*. The dark orange residue was purified by flash column chromatography (silica gel, petroleum ether/EtOAc, 5/5), and recrystallized from EtOAc, giving the desired product **(20)** (0.754 g, 22 %) as orange needles.

2.4.2 Synthesis of 5H,6H,11H-pyrido[4,3-b]carbazole-5,11-dione

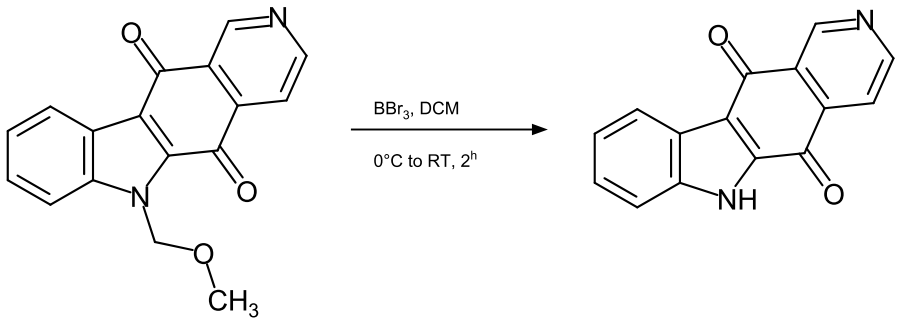

20 **21**

The cleavage of the MOM protection group was followed by the protocol of *Nagel 2005* [61], reacting the educt **(20)** with 1.2 equiv. of BBr_3 in anhyd. DCM at 0°C and stirring for 1^h at RT. BBr_3 is highly Lewis acidic and has been widely used, because the cleavage proceeds completely under mild conditions. The reaction was quenched with a saturated $NaHCO_3$ solution, followed by the collection of the product by suction filtration. The filter cake was washed with cold water and DCM, because the starting material can be removed in contrast to the product by washing with DCM. The recrystallization of the filter cake from EtOAc, gave the desired product **(21)** as orange crystals in 85% yield. This deprotection was verified by NMR analysis and HRMS.

2.4.3Synthesis of 6-[(3E)-6-[(tert-butyldiphenylsilyl)oxy]hex-3-en-1-yl]-5H,6H,11H-pyrido[4,3-b]carbazole-5,11-dione

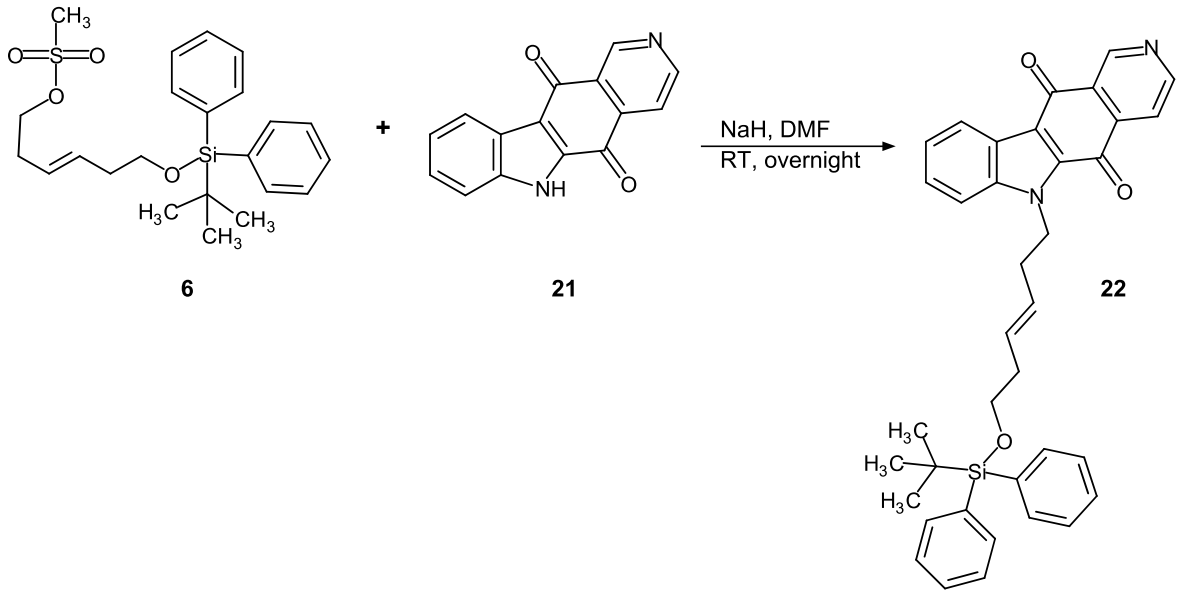

6 **21** **22**

The alkylation of the core structure **(21)** with the aliphatic side chain **(6)** was followed by the

protocol of *Nagel 2005* [61], by adding the solution of **(21)** in dry DMF to the cold suspension (-10°C) of NaH in dry DMF. The mixture was running at 75°C, controlling the reaction with TLC and the spot of the side chain completely disappeared overnight. After cooling down the flask, the reaction was quenched with water and extracted with EtoAc. The combined organic layers were dried with Na_2SO_4 and concentrated *in vacuo.* The crude product was purified by flash chromatography (silica gel, petroleum ether/EtOAc, 7/3) and gave a yield of 70 %.

3.Experimental Part

3. Experimental Part

3.1 Instrumentation and Chemicals

^{1}H- and ^{13}C-NMR spectra:

^{1}H-NMR spectra were recorded using a Bruker Avance DPX-200 at 200 MHz and ^{13}C-NMR spectra using the same spectrometer at 50 MHz. Chemical shifts (δ) are noted in parts per million (ppm) and the signal of the solvent is used as internal standard, which was related to TMS (Tetramethylsilane) with δ=7.26 ppm (^{1}H in $CDCl_3$), δ=2.49 ppm (^{1}H in DMSO-d_6), δ=77.0ppm (^{13}C in $CDCl_3$), δ=39.5ppm (^{13}C in DMSO-d_6).

Chromatographic analysis:

TLC (Thin Layer Chromatography) was carried out on Merck Millipore aluminium sheets pre-coated with Silica gel 60 F_{254}, Silica gel 60 RP-18 F_{254} and Acros Alumina (basic activated 50-200 Micron, Nr. 189990010) that were developed under UV light. For preparative chromatography, Merck Silica gel 60 F_{254} and Alumina F_{254} (neutral activated) were used. Column chromatography was carried out using Merck Silica gel 60 (230-400 mesh ASTM, Nr. 107734) and Acros Alumina (basic activated, 50-200 Micron, Nr. 189990010) as the stationary phase.

Chemicals:

All chemicals were purchased from Sigma Aldrich (https://www.sigmaaldrich.com) or TCI (http://www.tcichemicals.com/de/eu/)

3.2 Synthesis of Aliphatic Side Chains

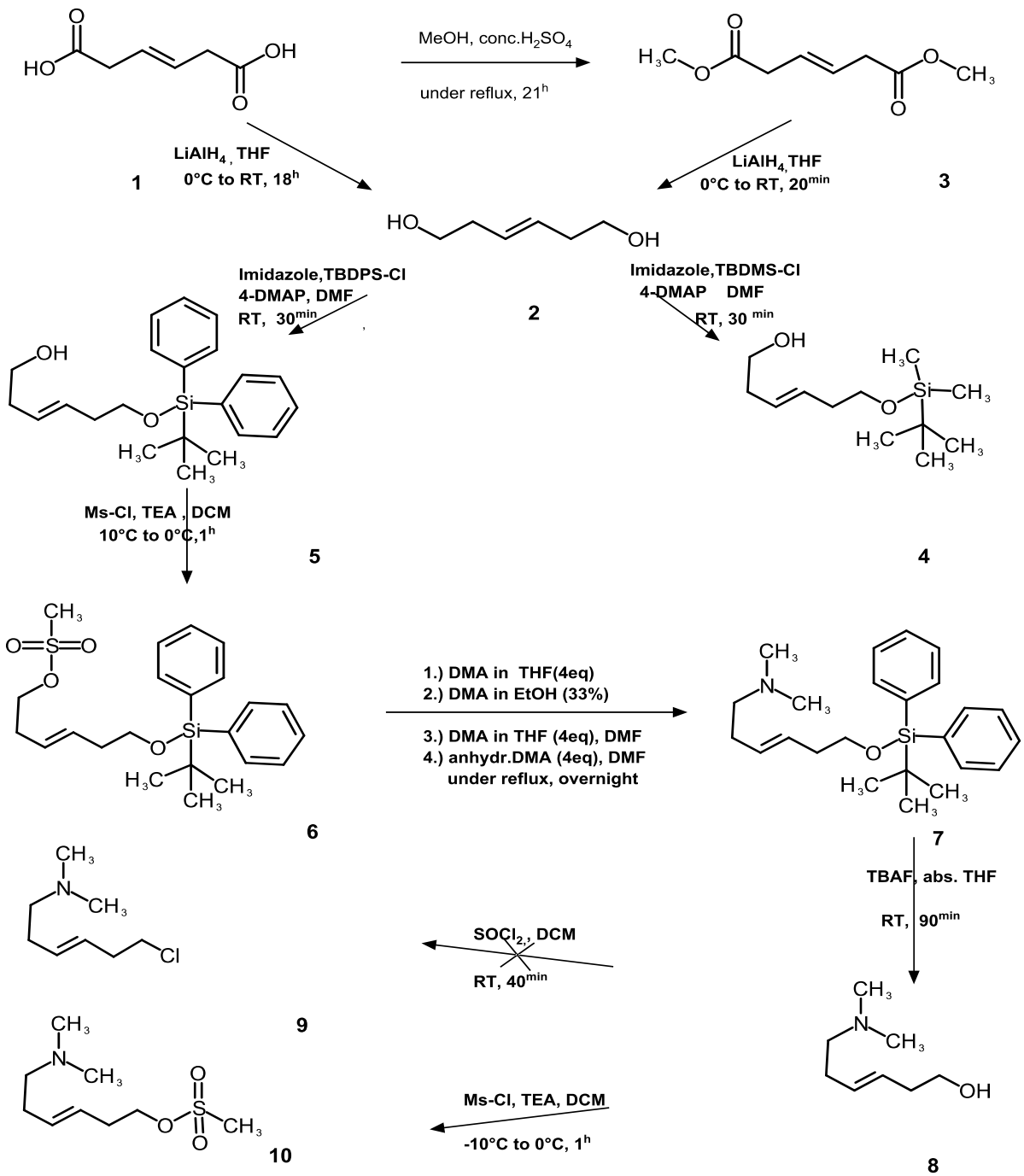

Figure 9: Reaction scheme of aliphatic side chains

3.2.1 Synthesis of (3E)-hex-3-ene-1,6-diol [62]

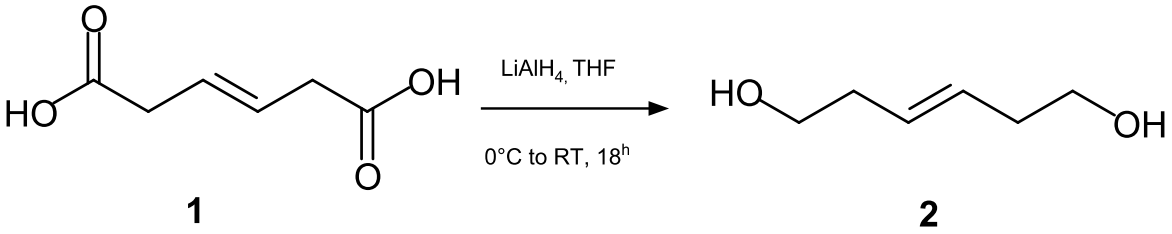

1 **2**

To a solution of trans hydromuconic acid **(1)** (69.38 mmol, 10.0 g) in abs. THF (220ml), 49ml of a suspension of $LiAlH_4$ (1M) in THF (0.049 mol, 1.85 g) was added dropwise at 0°C stirred at RT for 18^h. Upon completion, the reaction mixture was cooled to 0°C, subsequently quenched into ice water and should be neutralized with dil. H_2SO_4. Then, a continuous liquid-liquid extraction with ether was performed and after removing the solvent, the residue was purified with the Kugelrohr short path distillation apparatus (bp. 100-110° C; 0.9 mm Hg), giving a white-yellow oil (0.081 g, 1%)

HRMS: m/z calc. for $C_6H_{12}NaO_2$([M+Na]$^+$): 139.0730; found: 139.0739.

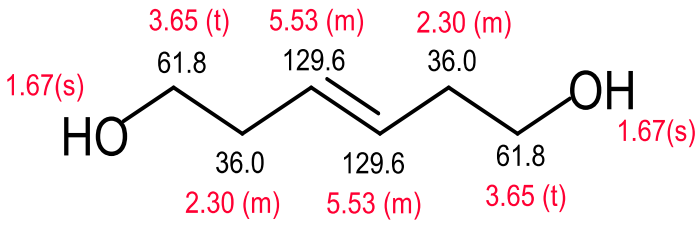

^{1}H-NMR (500 MHz, $CDCl_3$): 1.67 (s, 2H, -O-H), 2.30 (m, 4H, $(-CH_2)_2$, 3.65 (t, 4H, (6.1Hz), $(-O-CH_2)_2$, 5.53 (m, 2H,$-(CH)_2$).

^{13}C-NMR (125 MHz, $CDCl_3$): 36.0 (C^2, C^5), 61.8 (C^1, C^6), 129.6 (C^3, C^4).

3.2.2 Synthesis of 1,6-dimethyl-(3E)-hex-3-enedioate [63]

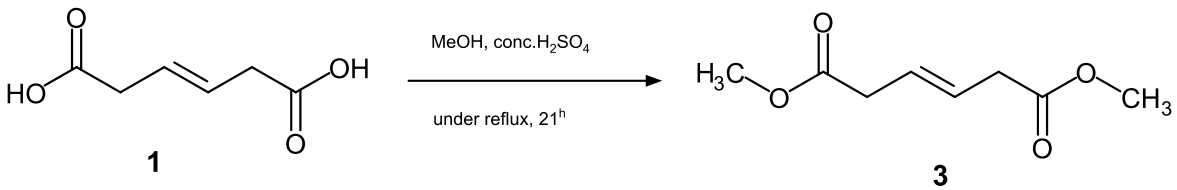

1 **3**

To a stirred solution of trans hydromuconic acid **(1)** (68.5 mmol, 9.88 g) in MeOH, (49 ml), conc. H_2SO_4 (1.7 ml) was slowly added and the resulting solution was heated to achieve a gently boiling of the reaction mixture for 21^h. Then, the mixture was allowed to cool down and the solvent was removed *in vacuo*. The residue was diluted with Et_2O and washed with a

saturated aqu. solution of NH_4Cl (2 x 13 ml), a saturated aqueous solution of $NaHCO_3$ (2 x 13 ml) and brine (13 ml). The combined aqueous washings were re-extracted with Et_2O and all organic extracts were dried with Na_2SO_4, the solvent was removed *in vacuo* and the residue **(3)** was used in the next step without any purification (10.7 g, 91%).

HRMS: m/z calc. for $C_8H_{12}NaO_4$ ($[M+Na]^+$): 195.0628; found: 195.0628.

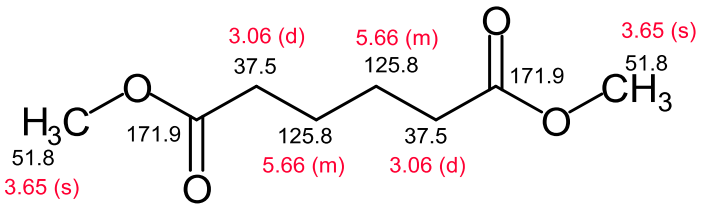

^{1}H-NMR (500 MHz, $CDCl_3$): 3.06 (d, 4H, (5.5Hz), $(-CH_2)_2$), 3.65 (s, 6H, $(-O-CH_3)_2$), 5.66 (m, 2H, $-(CH)_2$).

^{13}C-NMR (125 MHz, $CDCl_3$): 37.5(C^3,C^6), 51.8(C^1,C^8), 125.8 (C^4,C^5), 171.9 (C^2,C^7).

3.2.3. Synthesis of (3E)-hex-3-ene-1,6-diol [63]

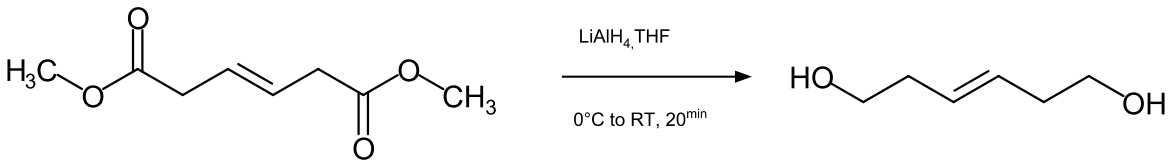

3 **2**

Under an argon atmosphere a solution of the diester **(3)** (54.01mmol, 9.30 g) in abs. THF (40 ml) was added to a suspension of $LiAlH_4$ in anhydrous THF (1M, 81 ml) between 0°C to -5°C. Then, the mixture was allowed to warm to RT and was stirred for further 2^{min}. After the slow addition of a saturated aqueous solution of Rochelle salt (27 ml) stirring was continued for a further 1^h at room temperature, until the organic phase became completely clear. The layers were separated and the aqueous phase was extracted with Et_2O. The combined organics were dried with Na_2SO_4 and concentrated *in vacuo* to give the diol **(2)**, without any special purification needed (5.29 g, 84 %).

HRMS: m/z calc. for $C_6H_{12}NaO_2$ ($[M+Na]^+$): 139.0730; found: 139.0732.

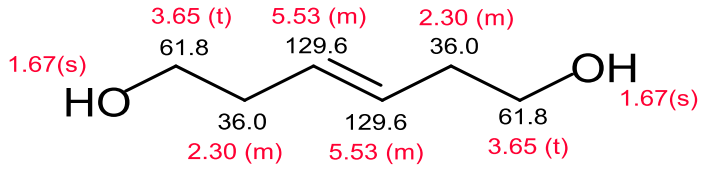

^{1}H-NMR (500 MHz, $CDCl_3$): 1.67 (s, 2H, -O-H), 2.30 (m, 4H, $(-CH_2)_2$, 3.65 (t, 4H, (6.1Hz), $(-O-CH_2)_2$, 5.53 (m, 2H, $-(CH)_2$).

^{13}C-NMR (125 MHz, CDCl3): 36.0 (C^2 C^5), 61.8 (C^1, C^6), 129.6 (C^3, C^4).

3.2.4. Synthesis of (3E)-6-{[tert-butyl(chloro)methylsilyl]oxy}hex-3-en-1-ol [63]

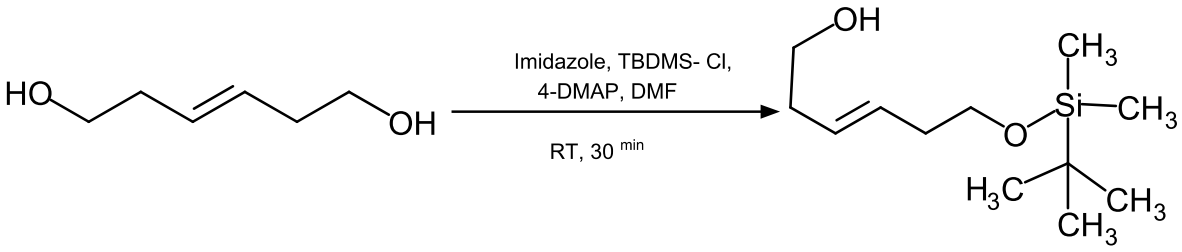

2 **4**

At RT, imidazole (11.91mmol, 0.811g), tert. butyldimethylsilyl chloride (10.92mmol, 1.65g) and 4-DMAP (0.39mmol, 48.17mg) were added to a solution of the 1,2-diol **(2)** (9.935mmol, 1.15g) prepared above in abs. DMF (11.20ml). The mixture was stirred for 30$^{min.}$ Then, MeOH (0.56ml) was added to the reaction and continued stirring for a further 1^{h} at the same temperature. The phases were partitioned between Et_2O and H_2O and separated. The organic layer was dried with Na_2SO_4 and concentrated *in vacuo*. The residue was purified by flash column chromatography (silica gel, petroleum ether/EtOAc = 9/1). The compound **(4)** was unstable in the presence of silica gel.

3.2.5. Synthesis of (3E)-6-[(tert-butyldiphenylsilyl) oxy]hex-3-en-1-ol [63]

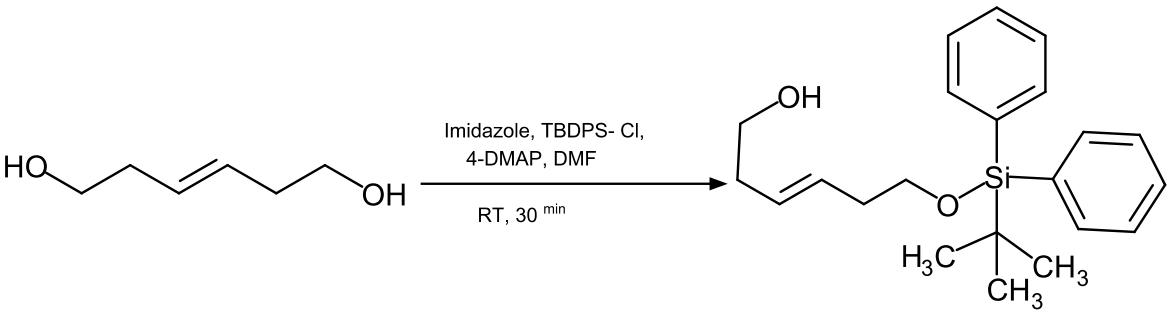

2 **5**

At RT imidazole (27.4 mmol, 1.87g), tert. butyldimethylsilyl chloride (25.14 mmol, 6.91 g) and 4-DMAP (0.52 mmol, 63.64 mg) were added to a solution of the 1,2-diol **(2)** (22.90

mmol, 2.66 g) in abs. DMF (26 ml). The mixture was stirred for 30[min]. After MeOH (1.3 ml) was added to the reaction, the mixture continued stirring for a further 1[h] at the same temperature. The phases were partitioned between Et_2O and H_2O (4 x 15 ml) and separated. The organic layer was dried with Na_2SO_4 and concentrated *in vacuo*. The residue was purified by flash columns chromatography (silica gel, petroleum ether/EtOAc, 9/1) and the successful purification gave the desired product **(5)** (3.15 g, 39%).

HRMS: m/z calc. for $C_{22}H_{30}NaO_2Si$ ($[M+Na]^+$): 377.1907; found: 377.1908.

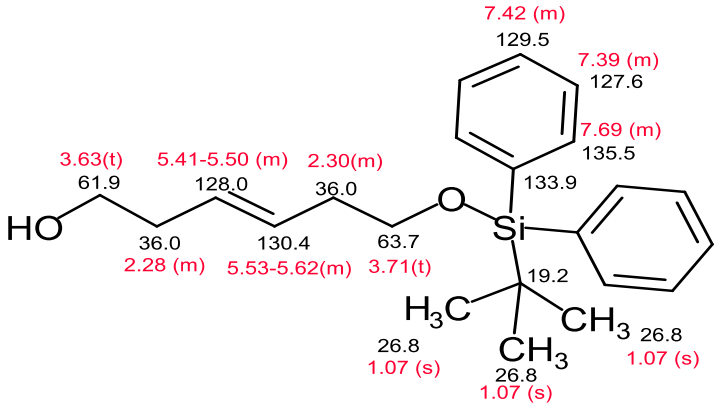

[1]H-NMR (500 MHz, $CDCl_3$): 1.07 (s, 9H, -$(CH_3)_3$,1.51(s. 1H. –OH), 2.30 (m, 2H, -C^5H_2), 3.63 (t, 2H (6.3Hz), -HO-$(CH_2)_2$), 5.41-5.50 (m, 1H, -(CH), 5.53-5.62 (m, 1H, -(CH)), 7.39 (m, 4H, 2x ($C^{3'}$H, $C^{5'}$ H), 7.42 (m, 2H, 2x($C^{4'}$H)), 7.69 (m, 4H, 2x ($C^{2'}$H, $C^{6'}$H)

[13]C-NMR (125 MHz, $CDCl_3$): 19.2 (-C(CH_3)$_3$), 26.8 (-C(CH_3)$_3$), 36.0 (C^2, C^5), 61.9 (C^1), 63.7 (C^6), 127.6 ($C^{3'}$, $C^{5'}$), 128.0 (C^3), 129.5 ($C^{4'}$), 130.4 (C^4), 133.9 ($C^{1'}$), 135.5 ($C^{2'}$, $C^{6'}$).

3.2.6. Synthesis of (3E)-6-[(tert-butyldiphenylsilyl)oxy]hex-3-en-1-ylmethane-sulfonate [62]

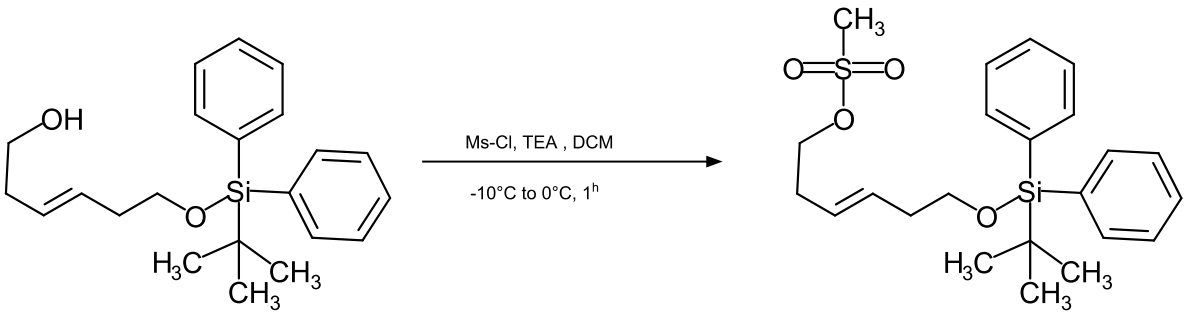

5 **6**

To a solution of the starting material **(5)** (7.56 mmol, 2.68 g), and TEA (15.12 mmol, 1.53 g) in anhydrous CH_2Cl_2 (52ml) under an argon atmosphere between 0° C to -10° C slowly add methanesulfonic acid chloride (13.09 mmol, 1.50 g) and was stirred for 1[h]. The formation of the product was observed by TLC and showed that no starting material was left. After the

dilution with CH_2Cl_2 the reaction mixture was transferred to a separatory funnel and first extracted with ice water, followed by cold 10% Hydrochloric acid, saturated sodium bicarbonate solution, and brine. The combined aqueous phases were re-extracted with CH_2Cl_2 and all organics were dried with Na_2SO_4 and concentrated *in vacuo*. According to the TLC and NMR analysis, the conversion of the desired compound **(6)** was successful without any by-products (3.20 g, 98 %).

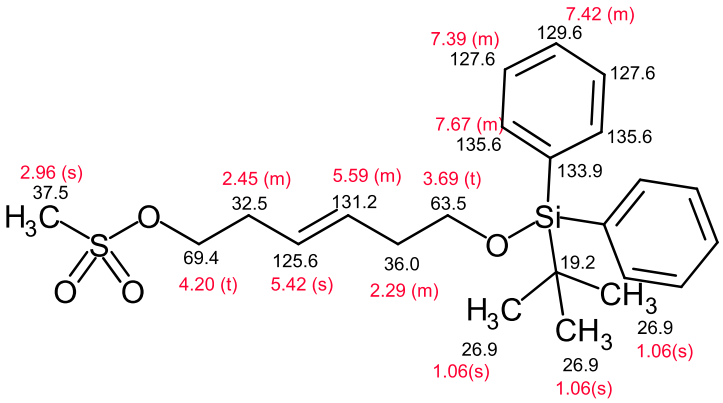

^{1}H-NMR (500 MHz, $CDCl_3$): 1.06 (s, 9H, -$(CH_3)_3$, 2.29 (m, 2H, -C^5H_2), 2.45 (m, 2H, -C^2H_2), 2.96 (s, 3H, -S-CH_3), 4.20 (t, 2H, (6.9Hz) -C^1H_2), 5.59 (m, 1H, (15.4Hz)-C^4H), 7.39 (m, 4H, 2x ($C^{3'}H$, $C^{5'}H$), 7.42 (m, 2H, 2x($C^{4'}H$)), 7.67 (m, 4H, 2x ($C^{2'}H$, $C^{6'}H$)).

^{13}C-NMR (125 MHz, $CDCl_3$): 19.2 (-C(CH_3)$_3$), 26.9 (-C(CH_3)$_3$), 32.5 (C^2), 36.0 (C^5), 37.5 (-S(CH_3), 63.5 (C^6), 69.4 (C^1), 125.6 (C^3), 127.6 ($C^{3'}$, $C^{5'}$), 129.6 ($C^{4'}$), 131.2 (C^4), 133.9 ($C^{1'}$), 135.6 ($C^{2'}$, $C^{6'}$).

3.2.7. Synthesis of [(3E)-6-[(tert-butyldiphenylsilyl) oxy]hex-3-en-1-yl] dimethylamine [62]

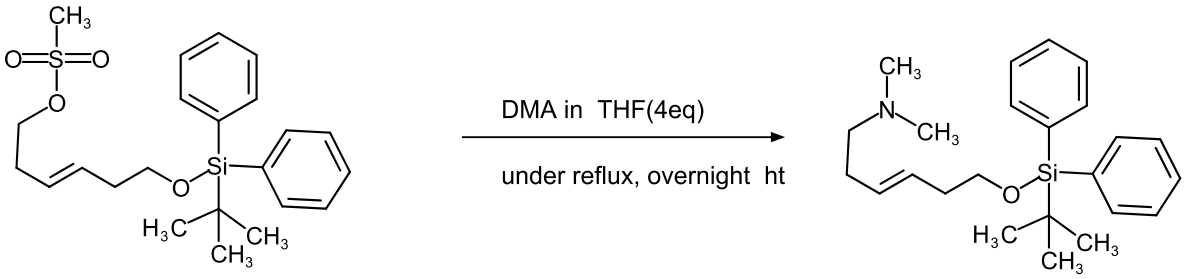

6 **7**

The mesylate **(6)** (7.21 mmol, 3.12 g) was stirred in the presence of a 2M solution of dimethylamine in THF (4 equiv. 28.85 mmol, 14.4 ml) under reflux overnight. The solid was removed through a pad of celite and washed with CH_2Cl_2. The filtrate was washed with water and brine and the washings were re-extracted with CH_2Cl_2. The organics were dried with Na_2SO_4, followed by evaporation of the solvent and purification by column chromatography

(silica gel, petroleum ether/EtOAc$^{1\%\ TEA}$, 8/2), to afford the corresponding amine **(7)** (0.790 g, 29 %).

HRMS: m/z calc. for $C_{24}H_{36}NOSi$ ($[M+H]^+$): 382.2561; found: 382.2564.

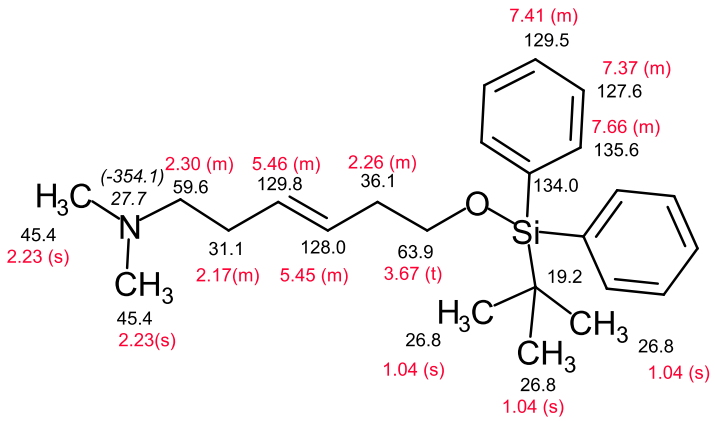

^{1}H-NMR (500 MHz, $CDCl_3$): 1.04 (s, 9H, -C(CH_3)$_3$, 2.17 (m, 2H, -CH_2), 2.23 (2.26, 9H, (2x (-N-(CH_3), 2.26 (m, 2H, -CH_2) 2.30 (m,2H, -N-(CH_2)), 3.67 (t, 2H, (3.7 Hz), -O-(CH_2)), 5.45 (m, 1H, -CH), 5.46 (m, 1H, -CH), 7.37 (m, 4H, 2x ($C^{3'}$H, $C^{5'}$H)), 7.41 (m, 2H, 2x ($C^{4'}$H)), 7.66 (m, 4H, 2x ($C^{2'}$H, $C^{6'}$H))

^{13}C-NMR (125 MHz, $CDCl_3$):19.2 (-C(CH$_3$)$_3$), 26.8 (-C(CH$_3$)$_3$, 31.1 (C^2), 36.1 (C^5), 45. 4 (2x (N-(CH$_3$)$_2$, 59.6 (C^1), 63.9 (C^6), 127.6 ($C^{3'}$, C5'), 128.0 ($C^{4'}$), 129.5 ($C^{4'}$), 129.8 (C^3), 134.0 ($C^{1'}$), 135.6 ($C^{2'}$, $C^{6'}$).

3.2.8. Synthesis of [(3E)-6-[(tert-butyldiphenylsilyl) oxy]hex-3-en-1-yl] dimethylamine [62]

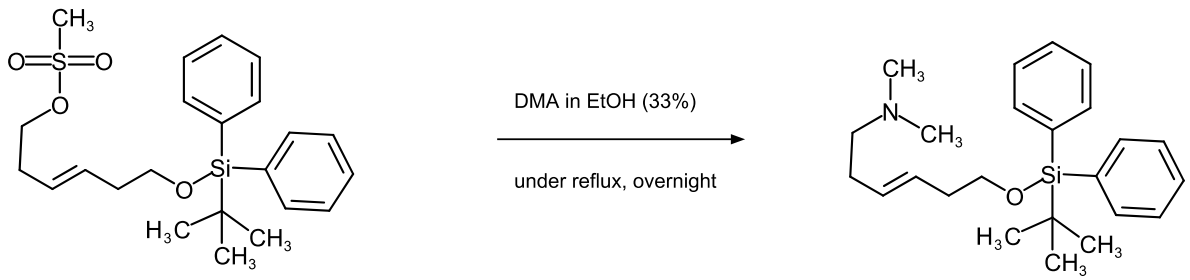

6 **7**

The mesylate **(6)** (0.49 mmol, 0.21 g) was stirred with 33 % Dimethylamine in EtOH (4.7 equiv. 2.30 mmol, 0.31 g of the solution) under reflux overnight. The solid was removed through a pad of celite and washed with CH_2Cl_2. The filtrate was washed with water and brine and the washings were re extracted with CH_2Cl_2. The organics were dried with Na_2SO_4, followed by evaporation of the solvent and purification by column chromatography (silica gel, petroleum ether/EtOAc $^{1\%TEA}$, 8/2), to afford the corresponding amine **(7)** (0.102 g, 56 %).

HRMS: m/z calc. for $C_{24}H_{36}NOSi$ ($[M+H]^+$): 382.2561; found: 382.2564.

^{1}H-NMR (500 MHz, $CDCl_3$): 1.04(s, 9H,-$(CH_3)_3$, 2.17(m, 2H, -CH_2), 2.23 (2.26, 9H, (2x(-N-(CH_3), (m, 2H, -CH_2) 2.30 (m, 2H, -N-(CH_2)), 3.67(t, 2H, (3.7 Hz), -O-(CH_2)), 5.45 (m, 1H, -CH), 5.46 (m, 1H, -CH), 7.37 (m, 4H, 2x ($C^{3'}$H, $C^{5'}$ H)), 7.41 (m, 2H, 2x ($C^{4'}$H)), 7.66 (m, 4H, 2x ($C^{2'}$H, $C^{6'}$H)).

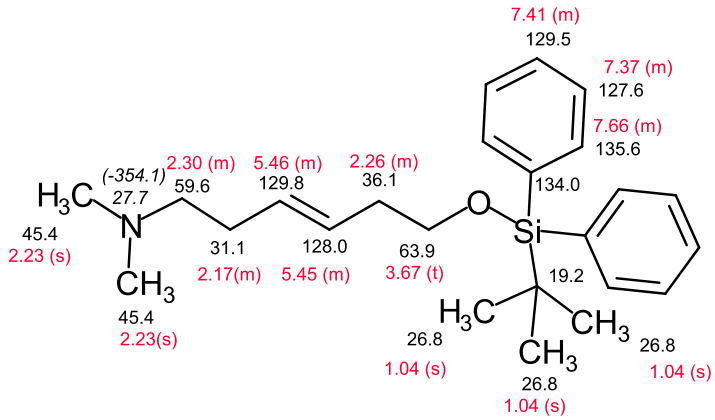

^{13}C-NMR (125 MHz, $CDCl_3$):19.2(-C$(CH_3)_3$), 26.8(-C$(CH_3)_3$, 31.1 (C^2), 36.1 (C^5), 45.4 (2x (-N-$(CH_3)_2$, 59.6 (C^1), 63.9 (C^6), 127.6 ($C^{3'}$, C5'), 128.0 ($C^{4'}$), 129.5 ($C^{4'}$), 129.8 (C^3), 134.0 ($C^{1'}$, 135.6($C^{2'}$, $C^{6'}$).

3.2.9. Synthesis of [(3E)-6-[(tert-butyldiphenylsilyl)oxy]hex-3-en-1-yl]dimethyl-amine [62]

6 **7**

The mesylate **(6)** (5.39, 2.33 g) was stirred with 2M Dimethylamine in THF (4 equiv., 21.54 mmol, 10.8 ml of this solution) and DMF under reflux overnight. The solid was removed through a pad of celite and washed with CH_2Cl. The filtrate was washed with water and brine and the washings were re extracted with CH_2Cl_2. The organics were dried with Na_2SO_4, followed by evaporation of the solvent and purification by column chromatography (silica gel, petroleum ether/EtOAc$^{1\%TEA}$ = 8/2), to afford the corresponding amine **(7)** (0.940 g, 46 %).

HRMS: m/z calc. for $C_{24}H_{36}NOSi$ ($[M+H]^+$): 382.2561; found: 382.2564.

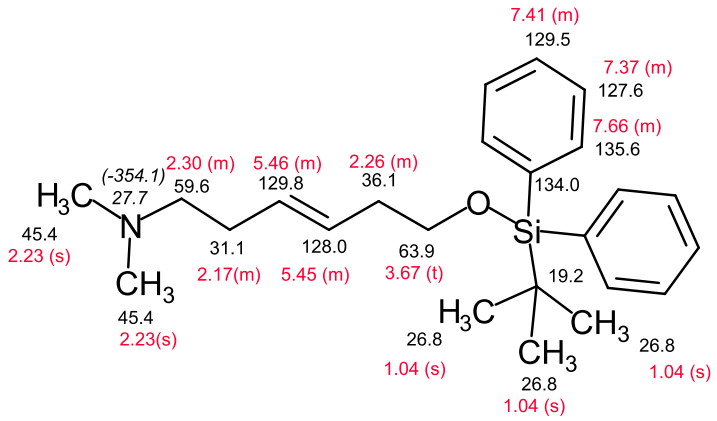

^{1}H-NMR (500 MHz, $CDCl_3$): 1.04 (s, 9H, -$(CH_3)_3$, 2.17 (m, 2H, -CH_2), 2.23 (2.26, 9H, (2x (-N-(CH_3)), 2.26 (m, 2H, -CH_2) 2.30 (m,2H, -N-(CH_2)), 3.67 (t, 2H, 3.7 Hz, -O-(CH_2)), 5.45 (m, 1H, -CH), 5.46 (m, 1H, -CH), 7.37 (m, 4H, 2x ($C^{3'}$H, $C^{5'}$H)), 7.41 (m, 2H, 2x ($C^{4'}$H)), 7.66 (m, 4H, 2x ($C^{2'}$H, $C^{6'}$H)).

^{13}C-NMR (125 MHz, $CDCl_3$) :19.2 (-C(CH_3)$_3$), 26.8 (-C(CH_3)$_3$, 31.1 (C^2), 36.1 (C^5), 45. 4 (2x N-(CH_3)$_2$, 59.6 (C^1), 63.9 (C^6), 127.6 ($C^{3'}$, C5'), 128.0 ($C^{4'}$), 129.5 ($C^{4'}$), 129.8 (C^3), 134.0 ($C^{1'}$), 135.6 ($C^{2'}$, $C^{6'}$).

3.2.10. Synthesis of [(3E)-6-[(tert-butyldiphenylsilyl)oxy]hex-3-en-1-yl]dimethyl-amine [62]

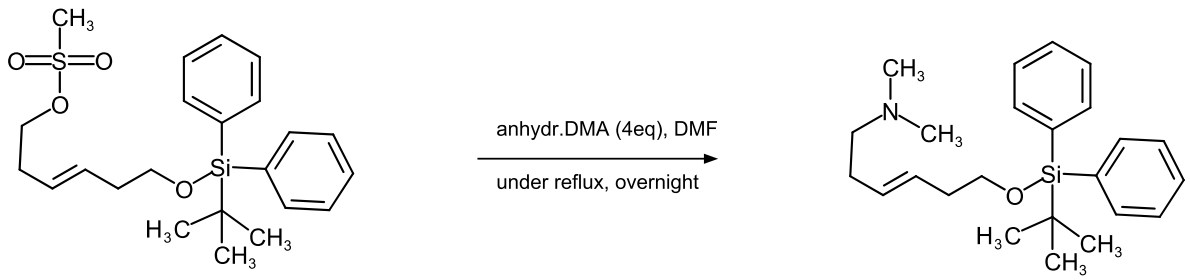

6 **7**

To the mesylate **(6)** (1.25 mmol, 0.54 g) the reactant - 2M Dimethylamine in DMF (16 equiv. 19.97 mmol, 10.0 ml of this solution) was added under oxygen free conditions and stirred under reflux overnight. The solid was removed through a pad of celite and washed with CH_2Cl_2. The filtrate was washed with water and brine and the washings were re extracted with CH_2Cl_2. The organics were dried with Na_2SO_4, followed by evaporation of the solvent and purification by column chromatography (silica gel, petroleum ether/EtOAc$^{1\%TEA}$, 8/2), to afford the corresponding amine **(7)**. According to the TLC and NMR analysis, the conversion was successful without any by-products (0.455 g, 96 %).

HRMS: m/z calc. for $C_{24}H_{36}NOSi$ ($[M+H]^+$): 382.2561; found: 382.2564.

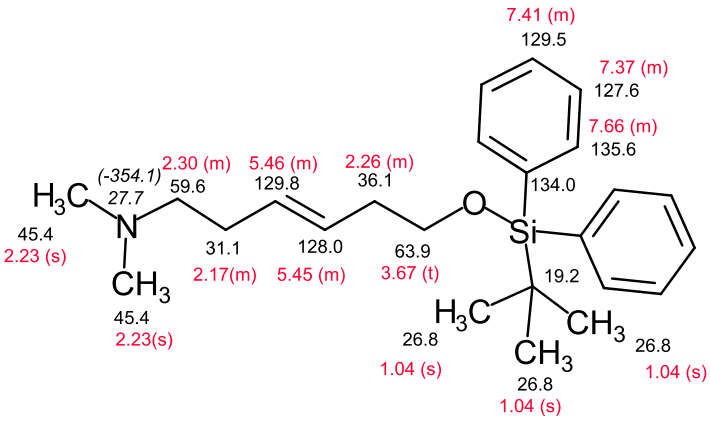

^{1}H-NMR (500 MHz, $CDCl_3$): 1.04 (s, 9H,-$(CH_3)_3$, 2.17(m, 2H, -CH_2), 2.23 (2.26, 9H, (2x (-N-(CH_3), 2.26(m, 2H, -CH_2), 2.30 (m, 2H, -N-(CH_2)), 3.67 (t, 2H, (3.7 Hz), -O-(CH_2)), 5.45 (m, 1H, -CH), 5.46 (m, 1H, -CH), 7.37 (m, 4H, 2x ($C^{3'}$H, $C^{5'}$ H)), 7.41 (m, 2H, 2x ($C^{4'}$H)), 7.66 (m, 4H, 2x ($C^{2'}$H, $C^{6'}$H)).

^{13}C-NMR (125 MHz, $CDCl_3$):19.2 (-$\underline{C}(CH_3)_3$), 26.8 (-C($\underline{C}H_3)_3$, 31.1(C^2), 36.1(C^5), 45. 4 (2x (-N-($\underline{C}H_3)_2$, 59.6(C^1), 63.9 (C^6), 127.6 ($C^{3'}$, C5'), 128.0 ($C^{4'}$), 129.5 ($C^{4'}$), 129.8 (C^3), 134.0 ($C^{1'}$, 135.6($C^{2'}$, $C^{6'}$).

3.2.11. Synthesis of (3E)-6-(dimethylamino)hex-3-en-1-ol[62]

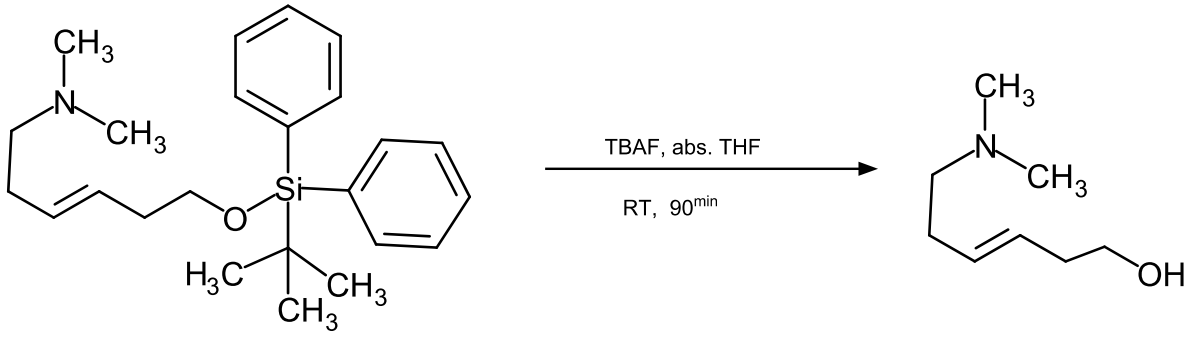

7 **8**

The solution of amine **(7)** (2.07 mmol, 0.789 g) in anhydrous THF (18.3 ml), 1M TBAF in THF (4.13 mmol, 1.08 g) was slowly added and stirred for 90^{min} at RT. The reaction was controlled by TLC (Alumina, EtOAc/MeOH/hexane, 6/1/3) detection with iodine test. After finishing the reaction, the solution was diluted with water and extracted 3 times with EtOAc. The organic layers were combined and dried with Na_2SO_4. After evaporation of the solvent, the residue was purified by flash chromatography Alumina, EtOAc/MeOH/Hexan 6/1/3). The isolation faces difficulties due the similar R_f-values of the product **(8)** and by-product so the purification had to be performed several times (0.210 g, 71 %).

HRMS: m/z calc. for $C_8H_{18}NO$ ($[M+Na]^+$): 144.1383; found: 144.1385.

3.2.12. Synthesis of [(3E)-6-chlorohex-3-en-1-yl]dimethylamine [62]

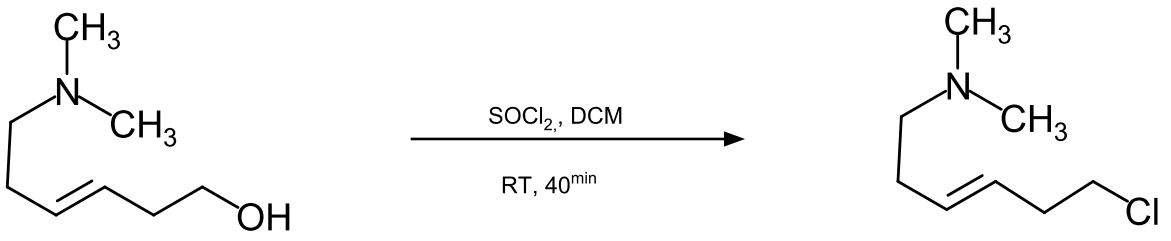

8 **9**

To a solution of thionyl chloride (5.77 mmol, 0.69 g) in abs. DMF (2.0 ml), the mixture of the amine **(8)** (1.43 mmol, 0.205 g) in abs. CH_2Cl_2 (1.5 ml) was slowly added and stirred for 40^{min} at RT. Then, the reaction mixture was slowly diluted with saturated $NaHCO_3$ (14.4 ml) solution and stirred for further 10^{min}, followed by extraction with CH_2Cl_2 and drying. According to the NMR analysis, the desired product **(9)** was not formed at all.

3.2.13 Synthesis of (3E)-6-(dimethylamino)hex-3-en-1-yl methanesulfonate [62]

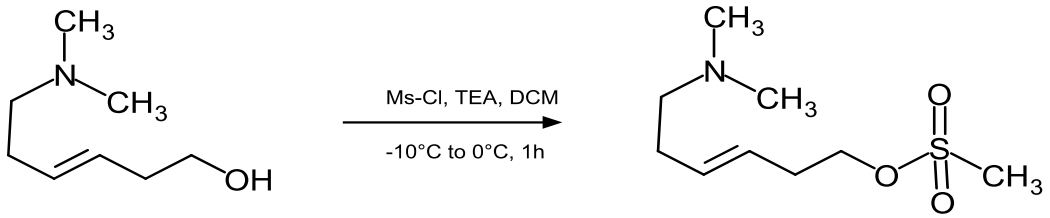

8 **10**

To a solution of the amine **(8)** (3.76 mmol, 0.539 g) prepared above and TEA (7.53 mmol, 0.762 g) in abs. CH_2Cl_2 (10.4 ml) under an argon atmosphere between 0° C and -10° C methanesulfonic acid chloride (6.59 mmol, 0.754 g) was slowly added and stirred for 1^{h}. After the dilution with CH_2Cl_2 the reaction mixture was transferred to a separatory funnel and first extracted with ice water, followed by cold 10% hydrochloric acid, saturated sodium bicarbonate solution, and brine. The combined aqueous phases were re-extracted with CH_2Cl_2 and all organics were dried with Na_2SO_4 and concetrated in vacuo. The residue was purified by flash column chromatography (silica gel, petroleum ether/EtOAc$^{1\%TEA}$, 8/2), but the product **(10)** was unstable and decomposed during the purification procedure.

HRMS: m/z calc. for $C_9H_{20}NOS$ ($[M+Na]^+$): 222.1158; found: 222.1159.

3.3 Synthesis of Sulfur-Containing Side Chains

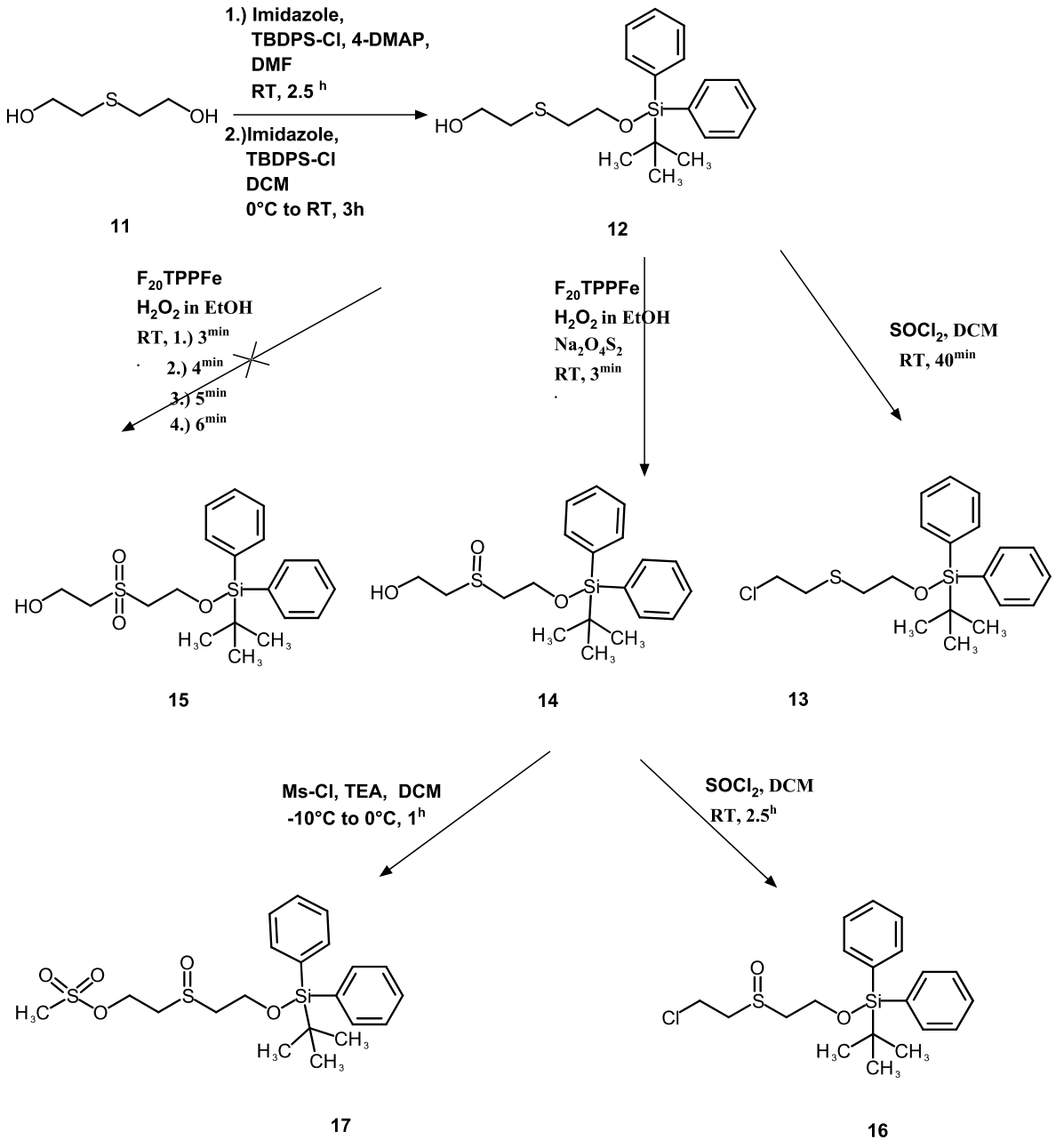

Figure 10: Reaction scheme of sulfur containing side chains

3.3.1 Synthesis of 2-({2-[(tert-butyldiphenylsilyl)oxy]ethyl}sulfanyl)ethan-1-ol [63]

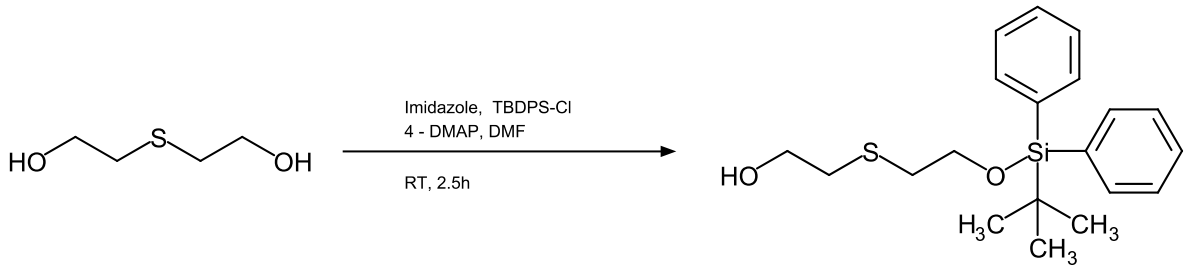

11 **12**

To a solution of thiodiglycole **(1)** (39 mmol, 4.76 g) in DMF (45 ml), imidazole (39 mmol, 2.653 g), 4-DMAP (1.55 mmol, 189 mg) and tert. butyldiphenylsilyl chloride (39 mmol, 10.71 g) were added and stirred for 1^h, followed by stirring at 1.5^h at RT. Then, the mixture was diluted with water and extracted with CH_2Cl_2. The organic layer was dried with Na_2SO_4 and purified by flash column chromatography (silica gel, Petroleum ether/EtOAc, 7/3) to afford the desired product **(12)** (7,012 g; 54 %) as yellow oil.

HRMS: m/z calc. for $C_{20}H_{28}NaO_2SSi$ ($[M+Na]^+$): 383.1471; found: 383.1466

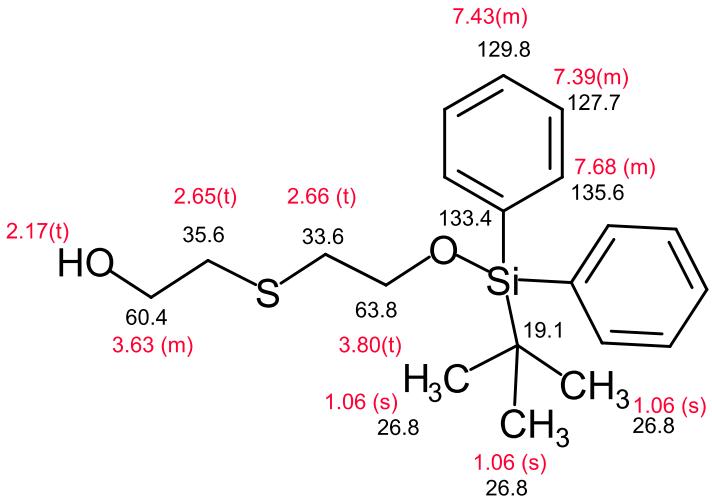

^{1}H-NMR (500 MHz, $CDCl_3$): 1.06(s, 9H, -C(CH_3)$_3$,), 2.17(t, 1H, -0H), 2.65 (t, 2H, (5.8Hz), -CH_2), 2.66 (t, 2H, (6.8Hz), -CH_2), 3.63 (m, 2H, (5.9Hz), 0-CH_2), 3.80 (t, 2H, (6.8Hz), -O-(CH_2)), 4.71 (m, 2H, -N-(CH_2)), 5.47 (m, 2H, -(CH)$_2$), 7.39 (m, 4H, 2x ($C^{3'}$H, $C^{5'}$ H), 7.43 (m, 2H, 2x($C^{4'}$H)), 7.68 (m, 4H, 2x ($C^{2'}$H, $C^{6'}$H)).

^{13}C-NMR (125 MHz, $CDCl_3$): 19.1 (-C(CH_3)$_3$), 26.8 (-C(CH_3)$_3$), 33.6 (C^3), 35.6 (C^2), 60.4 (C^1), 63.8 (C^4), 127.7 ($C^{3'}$, $C^{5'}$), 129.8 ($C^{4'}$), 133.4 ($C^{1'}$), 135.6 ($C^{2'}$, $C^{6'}$).

3.3.2. Synthesis of 2-({2-[(tert-butyldiphenylsilyl)oxy]ethyl}sulfanyl)ethan-1-ol [62]

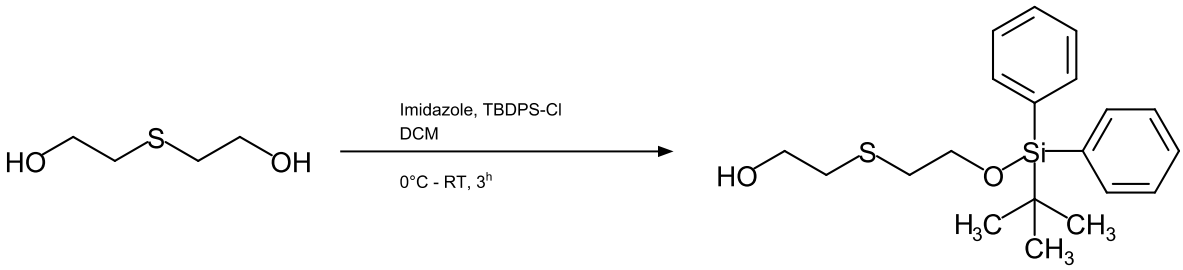

11 **12**

To a solution of thiodiglycole **(11)** (134 mmol, 16.32 g) in CH_2Cl_2 (155 ml) at 0° C, imidazole (134 mmol, 9.09 g) and tert. butyldiphenylsilyl chloride (134 mmol, 36.94 g) were added and stirred for 1^h, followed by stirring 2^h at RT. Then, the mixture was diluted with water and extracted with CH_2Cl_2. The organic layer was dried with Na_2SO_4 and purified by flash column chromatography (silica gel, petroleum ether/EtOAc, 7/3) to afford the desired product **(12)** (11.249 g, 25 %) as yellow oil.

HRMS: m/z calc. for $C_{20}H_{28}NaO_2SSi$ ($[M+Na]^+$): 383.1471; found: 383.1466.

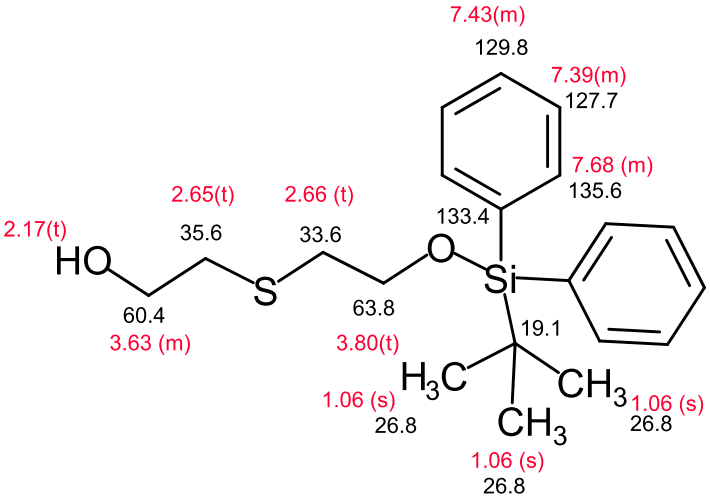

^{1}H-NMR (500 MHz, $CDCl_3$): 1.06 (s, 9H, -C(CH_3)$_3$,), 2.17 (t, 1H, -OH), 2.65 (t, 2H, (5.8Hz), -CH_2), 2.66 (t, 2H, (6.8Hz), -CH_2), 3.63 (m, 2H, (5.9Hz), 0-CH_2), 3.80(t, 2H, (6.8Hz), -O-(CH_2)), 4.71(m, 2H, -N-(CH_2)), 5.47 (m, 2H, -$(CH)_2$), 7.39 (m, 4H, 2x ($C^{3'}$H, $C^{5'}$H), 7.43 (m, 2H, 2x ($C^{4'}$H)), 7.68 (m, 4H, 2x ($C^{2'}$H, $C^{6'}$H)).

^{13}C-NMR (125 MHz, $CDCl_3$):19.1 (-C(CH_3)$_3$), 26.8 (-C(CH_3)$_3$), 33.6 (C^3), 35.6 (C^2), 60.4 (C^1), 63.8 (C^4), 127.7 ($C^{3'}$, $C^{5'}$), 129.8 ($C^{4'}$), 133.4 ($C^{1'}$), 135.6 ($C^{2'}$, $C^{6'}$).

3.3.3.Synthesis of tert-butyl({2-[(2-chloroethyl)sulfanyl]ethoxy})diphenylsilane [62]

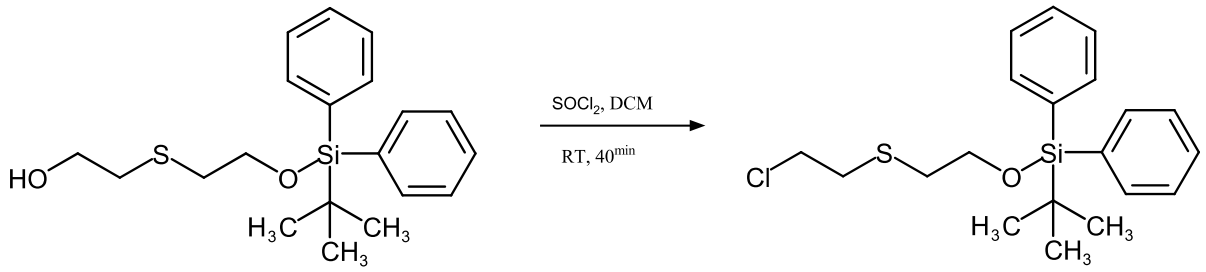

12 **13**

To a solution of thionyl chloride (40.47 mmol, 4,815 g) in anhydrous CH_2Cl_2 (9.70 ml), the mixture of the alcohol prepared above **(12)** (10.06 mmol, 3.364 g) in anhydrous CH_2Cl_2 (7.50 ml) was slowly added and stirred for 40^{min} at RT. Then, the reaction mixture was slowly diluted with saturated $NaHCO_3$ solution (220 ml) and stirred for further 10^{min}, followed by extraction with CH_2Cl_2 and drying with Na_2SO_4. Concentration *in vacuo* gave the desired product**(13)**, a yellow oil (3,605 g, 95 %), without any further purification.

HRMS: m/z calc. for $C_{20}H_{27}ClNaOSSi$ ($[M+Na]^+$): 401.1133; found: 401.1134

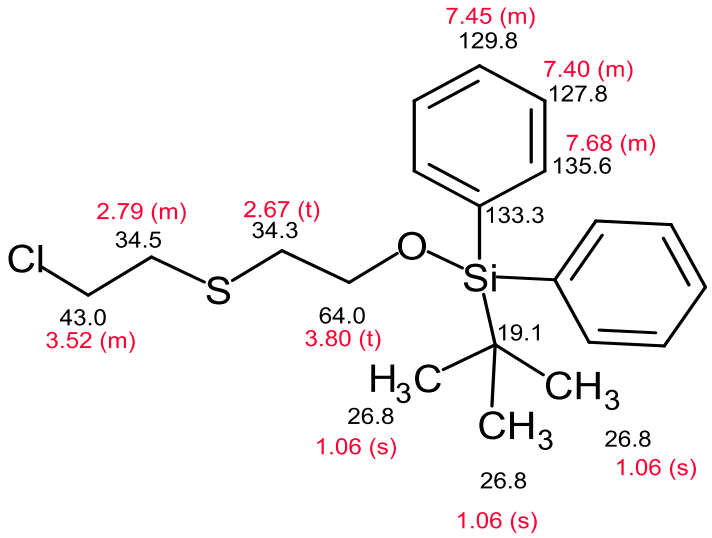

^{1}H-NMR (500 MHz, $CDCl_3$): 1.06 (s, 9H,-$(CH_3)_3$,), 2.67(t, 2H, (6.8 Hz), -S-CH_2), 2.79 (m, 2H, -S-CH_2), 3.80 (t, 2H, (6.8Hz), -O-CH_2), 3.52 (m, 2H, -Cl-CH_2), 7.40 (m, 2H, 2x ($C^{3'}$H, $C^{5'}$ H)), 7.45 (m, 2H, 2x (($C^{4'}$H)), 7.68 (m, 2H, 2x ($C^{2'}$H, $C^{6'}$H)).

^{13}C-NMR (125 MHz, $CDCl_3$): 19.1 (-C($CH_3)_3$), 26.8 (-C($CH_3)_3$), 34.3 (C^3), 34.5 (C^2), 43.0 (C^1), 64.0 (C^4), 127.8 ($C^{3'}$, $C^{5'}$), 129.8 ($C^{4'}$), 133.3 ($C^{1'}$), 135.6 ($C^{2'}$, $C^{6'}$).

3.3.4 Synthesis of {2-[(tert-butyldiphenylsilyl)oxy]ethanesulfinyl}ethan-1-ol [62]

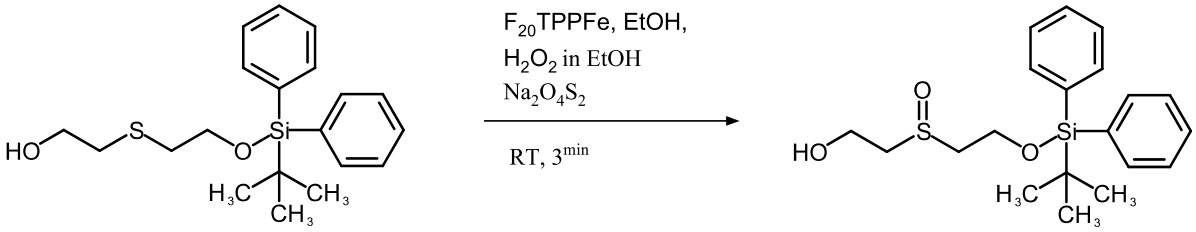

12 **14**

To a solution of the alcohol **(12)** (21.12 mmol, 7.615 g) and F_{20}TPPFe (0.012 mmol, 13.88 mg) in EtOH (77 ml) a mixture of H_2O_2 (21.12 mmol, 717.70 mg, 2.39 ml of a 30 % H_2O_2 solution) in EtOH (19 ml) was slowly added within 1^{min} , followed by 3^{min} stirring (until the colours of the solution changed from darkgreen to orange-brown). Then, a tip of a spatula of the strong reducing agent, sodium dithionite, was added, diluted with water and extracted with CH_2Cl_2. The organic layer was dried with Na_2SO_4 and concentrated *in vacuo*. The residue was purified by flash column chromatography (silica gel, Petroleum ether/EtOAc, 7/3) and obtained a satisfactory yield of white-yellow crystals **(14)** (6.846 g, 86 %) and a small amount of the by-product sulfone **(15)** (0.953g, 11%).

HRMS: m/z calc. for $C_{20}H_{28}NaO_3SSi$ ($[M+Na]^+$): 399.1421; found: 399.1422.

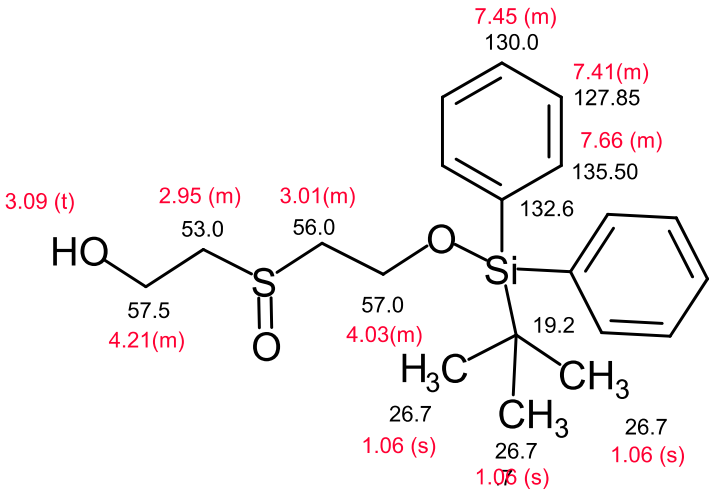

^{1}H-NMR (500 MHz, $CDCl_3$): 1.06 (s, 9H,-C(CH_3)$_3$,), 2.95(m, 2H, -CH_2), 3.01 (m, 2H,-CH_2), 3.09 (t, 1H, (5.7 Hz), -OH), 4.03 (m, 2H, O-CH_2), 4.21(m, 2H, HO-CH_2), 7.41 (m, 4H, 2x($C^{3'}$H, $C^{5'}$ H), 7.45 (m, 2H, 2x($C^{4'}$H)), 7.66 (m, 4H, 2x ($C^{2'}$H, $C^{6'}$H)).

^{13}C-NMR (125 MHz, $CDCl_3$): 19.2 (-C(CH_3)$_3$), 26.7 (-C(CH_3)$_3$), 53.0 (C^2), 56.0 (C^3), 57.0 (C^4), 57.5 (C^1) , 127.85 ($C^{3'}$, $C^{5'}$), 130.0 ($C^{4'}$), 132.6 ($C^{1'}$), 135.50 ($C^{2'}$, $C^{6'}$).

HRMS: m/z calc. for $C_{20}H_{28}NaO_4SSi$ ($[M+Na]^+$): 415.1370; found: 415.1381.

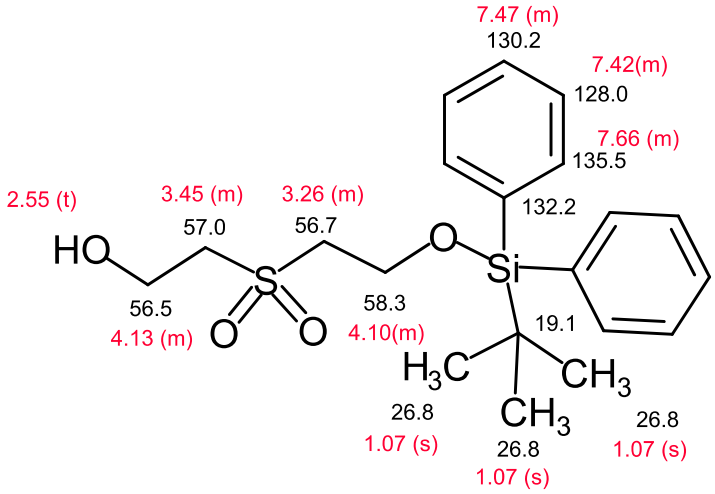

^{1}H-NMR (500 MHz, $CDCl_3$): 1.07 (s, 9H, -C(CH_3)$_3$,), 2.55 (t, 1H, (6.2 Hz), -OH), 3.26 (m, 2H, -CH_2), 3.45 (m, 2H,-CH_2), 4.10 (m, 2H, O-CH_2), 4.13 (m, 2H, HO-CH_2), 7.42 (m, 4H, 2x ($C^{3'}$H, $C^{5'}$ H), 7. 47 (m, 2H, 2x ($C^{4'}$H)), 7.66 (m, 4H, 2x ($C^{2'}$H, $C^{6'}$H)).

^{13}C-NMR (125 MHz, $CDCl_3$): 19.1 (-C-CH_3)$_3$), 26.8 (-C(CH_3)$_3$), 56.5 (C^1), 56.7 (C^3), 57.0 (C^2), 58.3 (C^4), 128.0 ($C^{3'}$, $C^{5'}$), 130.2 ($C^{4'}$), 132.2 ($C^{1'}$), 135.5 ($C^{2'}$, $C^{6'}$).

3.3.5 Synthesis of tert-butyl[2-(2-chloroethanesulfinyl)ethoxy]diphenylsilane [62]

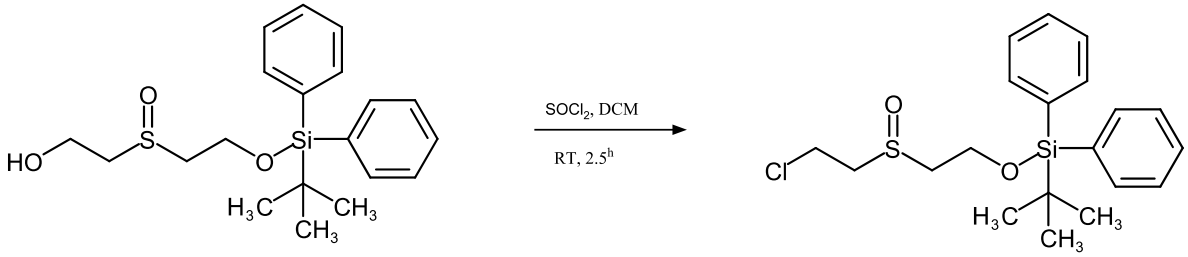

14 **16**

To a solution of thionyl chloride (2.10 mmol, 0.25 g) in abs. CH_2Cl_2 (0,56 ml), the mixture of the alcohol prepared above **(14)** (0.512 mmol, 0.193 g) in abs. CH_2Cl_2. (0.71 ml) was slowly added and stirred for 2.5^h at RT, the reaction was controlled by TLC. Then, the reaction mixture was slowly diluted with saturated $NaHCO_3$ solution (16 ml) and stirred for further 10^{min}, followed by extraction with CH_2Cl_2 and drying with Na_2SO_4. The residue was purified by flash chromatography (silica gel, petroleum ether/EtOAc, 9:1), but the product **(16)** was unstable.

3.3.6 Synthesis of 2-{2-[(tert-butyldiphenylsilyl)oxy] ethanesulfinyl}ethylmethane-sulfonate [62]

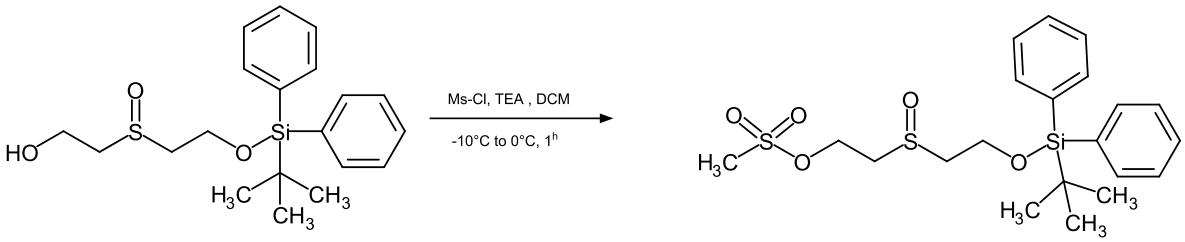

14 **17**

To a solution of the alcohol **(14)** (18.97 mmol, 6.846 g) and TEA (37.94 mmol, 3.840g) in anhydrous CH_2Cl_2 (36 ml) under an argon atmosphere between 0°C and -10°C methanesulfonic acid chloride (33.20 mmol, 3.80 g) was slowly added and stirred for 1^h at 0°C. After the residue was concetrated *in vacuo*, it was purified by flash column chromatography (silica gel, petroleum ether/EtOAc, 5/5), giving the desired product **(17)** (3.0 g, 35 %).

HRMS: m/z calc. for $C_{21}H_{30}NaO_5S_2Si$ ($[M+Na]^+$): 477.1196; found: 477.1198

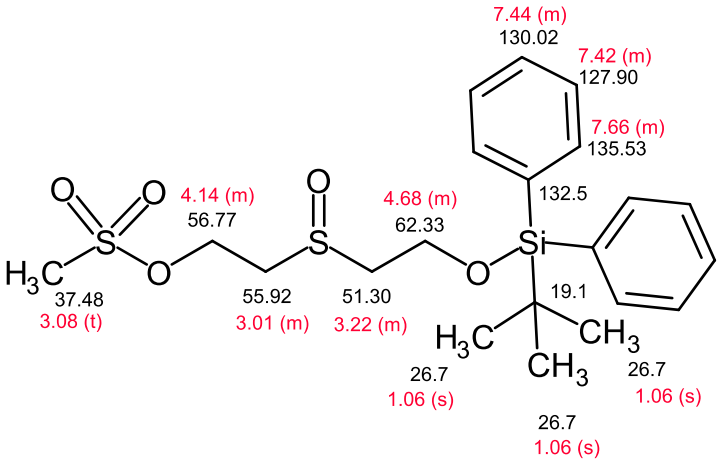

^{1}H-NMR (500 MHz, $CDCl_3$): 1.06(s, 9H, -C(CH_3)$_3$,), 3.01 (m, 2H,-CH_2), 3.08 (t, 3H, -S-CH_3), 3.22 (t, 3H, -S-CH_2), 4.14 (m, 2H, 0-CH_2), 4.68 (m, 2H, 0-CH_2), 7.42 (m, 4H, 2x($C^{3'}$H, $C^{5'}$ H), 7.44 (m, 2H, 2x($C^{4'}$H)), 7.66 (m, 4H, 2x($C^{2'}$H, $C^{6'}$H)).

^{13}C-NMR (125 MHz, $CDCl_3$): 19.1 (-C(CH_3)$_3$), 26.7 (-C(CH_3)$_3$), 37.48 (-S-CH_3), 51.30 (C^3), 55.92 (C^2), 56.0 (C^3), 56.77 (C^1), 62.33 (C^4), 127.90 ($C^{3'}$, $C^{5'}$), 130.02 ($C^{4'}$), 132.5 ($C^{1'}$), 135.53 ($C^{2'}$, $C^{6'}$).

3.3.7. Synthesis of 2-{2-[(tert-butyldiphenylsilyl)oxy]ethanesulfonyl}ethan-1-ol [62]

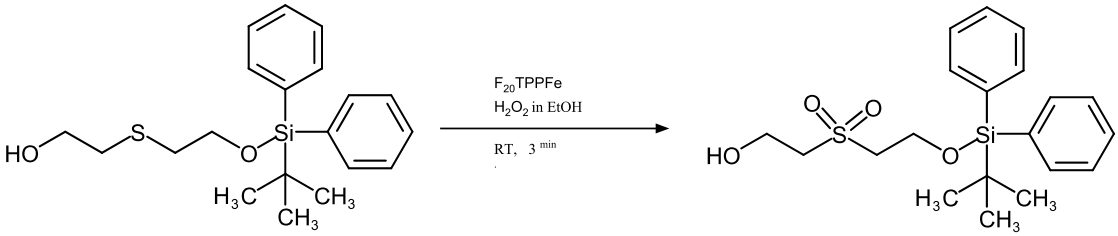

12 **15**

To a solution of the alcohol **(12)** (0.44 mmol, 0.159 g) and $F_{20}TPPFe$ (0.0003 mmol, 0.268mg) in EtOH (1.6 ml), a mixture of H_2O_2 (0.44 mmol, 14.98 mg, 0.05 ml of a 30 % H_2O_2 solution) in EtOH (0.3 ml) was slowly added within 1^{min}, followed by 3^{min} stirring (until the colours of the solution changed from darkgreen to orange-brown). Without adding a tip of a spatula of sodium dithionite, the mixture was diluted with water and extracted with CH_2Cl_2. The organic layer was dried with Na_2SO_4 and concentrated *in vacuo*. According to NMR analysis of the crude product, the oxidation did not lead to the sulfone **(15)**, but to the sulfoxide **(17)** (0.098 g, 75 %)**.** No further attempts were performed.

HRMS: m/z calc. for $C_{20}H_{28}NaO_3SSi$ ($[M+Na]^+$): 399.1421; found: 399.1422.

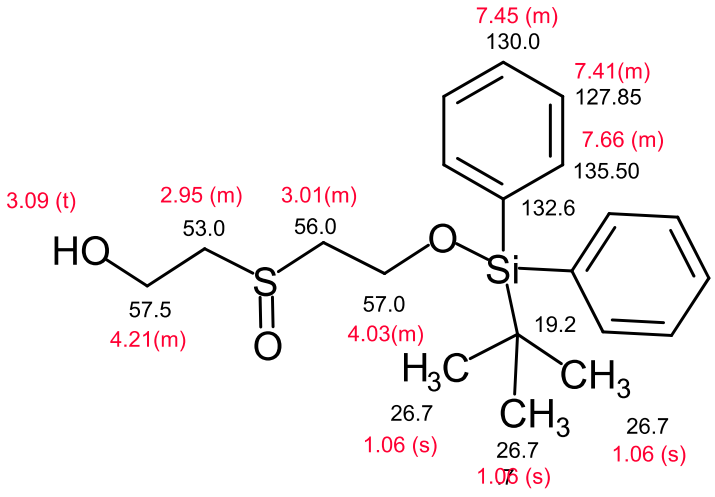

^{1}H-NMR (500 MHz, $CDCl_3$): 1.06(s, 9H,-$(CH_3)_3$,), 2.95(m, 2H, -CH_2), 3.01(m, 2H,-CH_2), 3.09 (t, 1H, (5.7 Hz), -0H), 4.03 (m, 2H, 0-CH_2), 4.21(m, 2H, HO-CH_2), 7.41 (m, 4H, 2x($C^{3'}$H, $C^{5'}$ H), 7.45 (m, 2H, 2x($C^{4'}$H)), 7.66 (m, 4H, 2x($C^{2'}$H, $C^{6'}$H))

^{13}C-NMR (125 MHz, $CDCl_3$): 19.2 (-<u>C</u>$(CH_3)_3$), 26.7 (-C(<u>C</u>$H_3)_3$), 53.0 (C^2), 56.0 (C^3), 57.0 (C^4), 57.5 (C^1), 127.85 ($C^{3'}$, $C^{5'}$), 130.0 ($C^{4'}$), 132.6 ($C^{1'}$), 135.50 ($C^{2'}$, $C^{6'}$).

3.3.8. Synthesis of 2-{2-[(tert-butyldiphenylsilyl)oxy]ethanesulfonyl}ethan-1-ol [62]

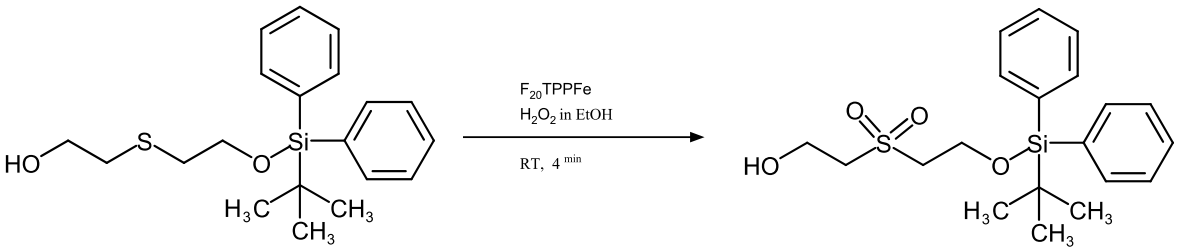

12 **15**

To a solution of the alcohol **(12)** (0.26 mmol, 0.093g) and F_{20}TPPFe (0.00016 mmol, 0.161 mg) in EtOH (0.95 ml), a mixture of H_2O_2 (0.26 mmol, 8.76 mg, 0.03 ml of a 30% H_2O_2 solution) in EtOH (0.23 ml) was slowly added within 1^{min}, followed by 4^{min} stirring (until the colours of the solution changed from darkgreen to orange-brown). Without adding a tip of a spatula of sodium dithionite, the mixture was diluted with water and extracted with CH_2Cl_2. The organic layer was dried with Na_2SO_4 and concentrated *in vacuo*. According to NMR analysis of the crude product, the oxidation did not lead to the sulfone **(15)**, but to the sulfoxide **(17)** (0,078 g, 80 %). No further attempts were performed.

HRMS: m/z calc. for $C_{20}H_{28}NaO_3SSi$ ($[M+Na]^+$): 399.1421; found: 399.1422.

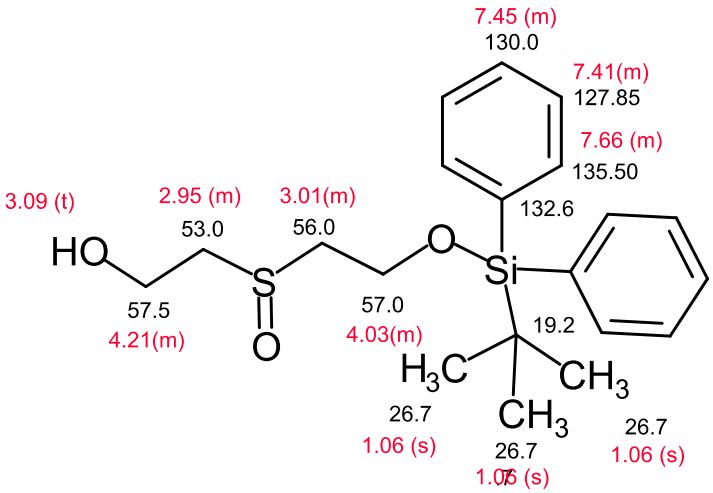

^{1}H-NMR (500 MHz, $CDCl_3$): 1.06 (s, 9H, -C(CH_3)$_3$,), 2.95 (m, 2H, -CH_2), 3.01 (m, 2H,-CH_2), 3.09 (t, 1H, (5.7 Hz), -OH), 4.03 (m, 2H, 0-CH_2), 4.21 (m, 2H, HO-CH_2), 7.41 (m, 4H, 2x ($C^{3'}$H, $C^{5'}$ H), 7.45 (m, 2H, 2x ($C^{4'}$H)), 7.66 (m, 4H, 2x ($C^{2'}$H, $C^{6'}$H)).

^{13}C-NMR (125 MHz, $CDCl_3$): 19.2 (-<u>C</u>(CH_3)$_3$), 26.7 (-C(<u>C</u>H_3)$_3$), 53.0 (C^2), 56.0 (C^3), 57.0 (C^4), 57.5 (C^1), 127.85 ($C^{3'}$, $C^{5'}$), 130.0 ($C^{4'}$), 132.6 ($C^{1'}$), 135.50 ($C^{2'}$, $C^{6'}$).

3.3.9. Synthesis of 2-{2-[(tert-butyldiphenylsilyl)oxy]ethanesulfonyl}ethan-1-ol [62]

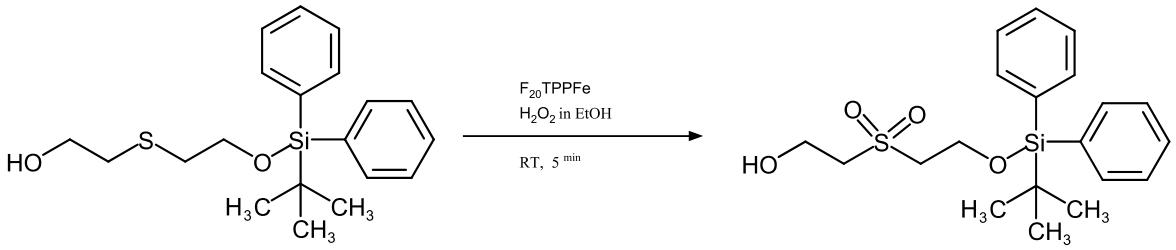

12 **15**

To a solution of the alcohol **(12)** (0.20 mmol, 0.071 g) and F_{20}TPPFe (0.00012 mmol, 0.12 mg) in EtOH (0.73 ml), a mixture of H_2O_2 (0.20 mmol, 6.70 mg, 0.02 ml of a 30 % H_2O_2 solution) in EtOH (0.18 ml) was slowly added within 1^{min}, followed by 5^{min} stirring (until the colours of the solution changed from darkgreen to orange-brown). Without adding a tip of a spatula of sodium dithionite, the mixture was diluted with water and extracted with CH_2Cl_2. The organic layer was dried with Na_2SO_4 and concentrated *in vacuo*. According to NMR analysis of the crude product, the oxidation did not lead to the sulfone **(15)**, but to the sulfoxide **(17)** (0.056 g, 76 %)**.** No further attempts were performed.

HRMS: m/z calc. for $C_{20}H_{28}NaO_3SSi$ ($[M+Na]^+$): 399.1421; found: 399.1422.

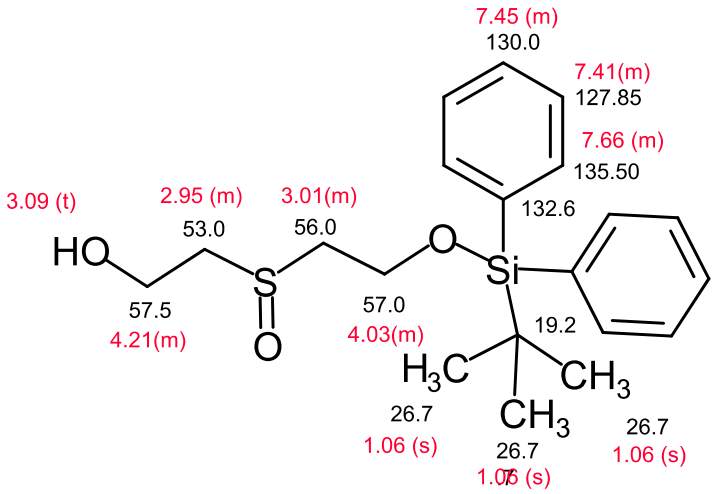

^{1}H-NMR (500 MHz, $CDCl_3$): 1.06 (s, 9H, -C(CH_3)$_3$,), 2.95 (m, 2H, -CH_2), 3.01 (m, 2H,-CH_2), 3.09 (t, 1H, (5.7 Hz), -OH), 4.03 (m, 2H, O-CH_2), 4.21 (m, 2H, HO-CH_2), 7.41 (m, 4H, 2x ($C^{3'}$H, $C^{5'}$ H), 7.45 (m, 2H, 2x ($C^{4'}$H)), 7.66 (m, 4H, 2x ($C^{2'}$H, $C^{6'}$H)).

^{13}C-NMR (125 MHz, $CDCl_3$): 19.2 (-C(CH_3)$_3$), 26.7 (-C(CH_3)$_3$), 53.0 (C^2), 56.0 (C^3), 57.0 (C^4), 57.5 (C^1), 127.85 ($C^{3'}$, $C^{5'}$), 130.0 ($C^{4'}$), 132.6 ($C^{1'}$), 135.50 ($C^{2'}$, $C^{6'}$).

3.3.10. Synthesis of 2-{2-[(tert-butyldiphenylsilyl)oxy]ethanesulfonyl}ethan-1-ol [62]

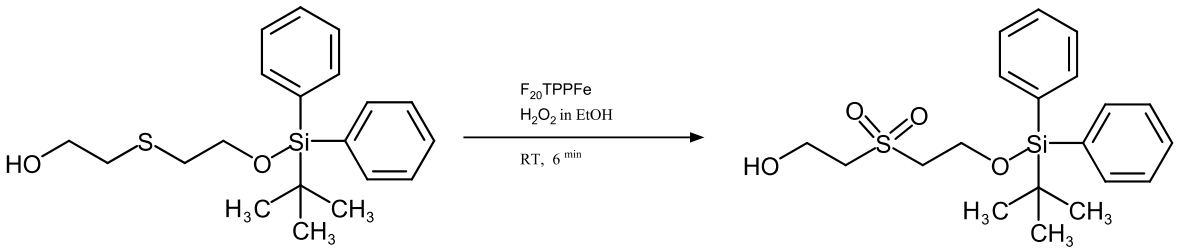

To a solution of the alcohol **(12)** (0.24 mmol, 0.085 g) and F_{20}TPPFe (0.00015 mmol, 0.15 mg) in EtOH (0.87 ml), a mixture of H_2O_2 (0.24 mmol, 8.01 g, 0.03 ml of a 30% H_2O_2 solution) in EtOH (0.21 ml) was slowly added within 1^{min} followed by 6^{min} stirring (until the colours of the solution changed from darkgreen to orange-brown). Without adding a tip of a spatula of sodium dithionite, the mixture was diluted with water and extracted with Ch_2Cl_2. The organic layer was dried with Na_2SO_4 and concentrated in *vacuo*. According to NMR analysis of the crude product, the oxidation did not lead to the sulfone **(15)**, but to the sulfoxide **(17)** (0.070 g, 79 %). No further attempts were performed.

HRMS: m/z calc. for $C_{20}H_{28}NaO_3SSi$ ($[M+Na]^+$): 399.1421; found: 399.1422.

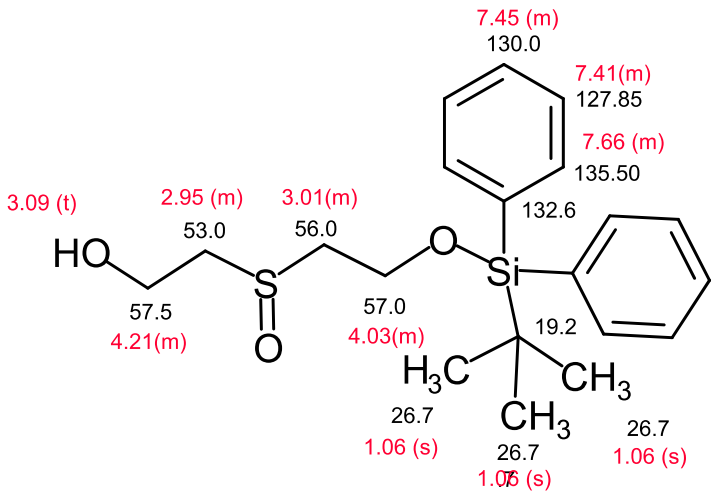

^{1}H-NMR (500 MHz, $CDCl_3$): 1.06 (s, 9H, -$(CH_3)_3$,), 2.95 (m, 2H, -CH_2), 3.01 (m, 2H, -CH_2), 3.09 (t, 1H, (5.7 Hz), -OH), 4.03 (m, 2H, O-CH_2), 4.21 (m, 2H, HO-CH_2), 7.41 (m, 4H, 2x($C^{3'}$H, $C^{5'}$H), 7.45 (m, 2H, 2x($C^{4'}$H)), 7.66 (m, 4H, 2x ($C^{2'}$H, $C^{6'}$H)).

^{13}C-NMR (125 MHz, $CDCl_3$): 19.2 (-C(CH_3)$_3$), 26.7 (-C(CH_3)$_3$), 53.0 (C^2), 56.0 (C^3), 57.0 (C^4), 57.5 (C^1), 127.85 ($C^{3'}$, $C^{5'}$), 130.0 ($C^{4'}$), 132.6 ($C^{1'}$), 135.50 ($C^{2'}$, $C^{6'}$).

3.4. Synthesis of the Core Structure

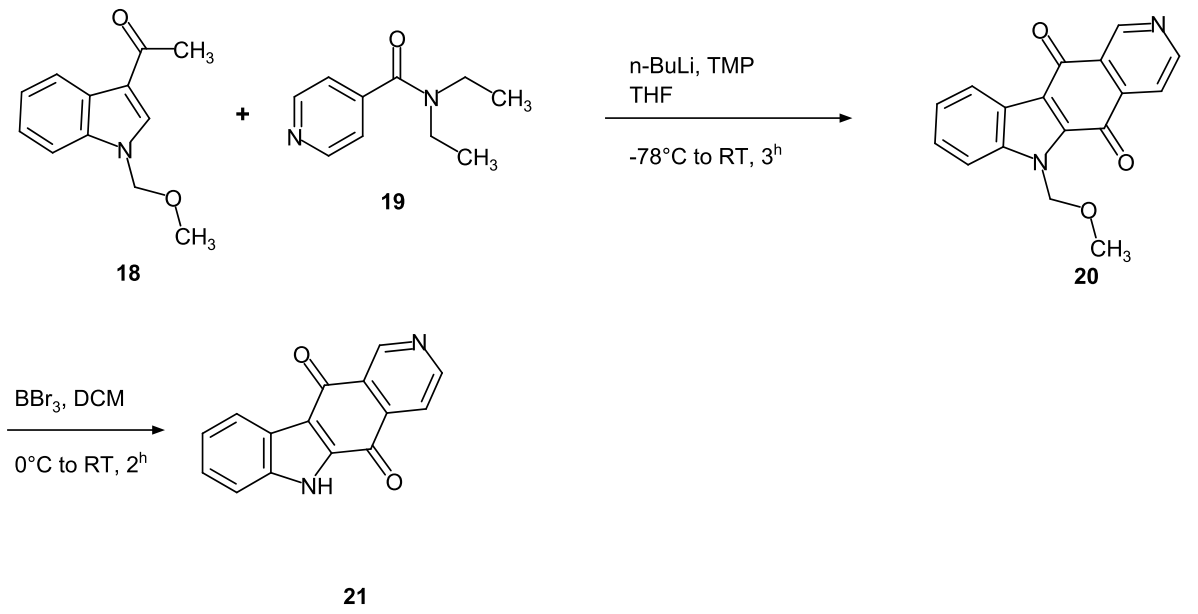

Figure 11: Reaction scheme of the synthesis of the core structure

3.4.1 Synthesis of 6-(Methoxymethyl)-5H,6H,11H-pyrido[4,3-b]carbazole-5,11-dione[61]

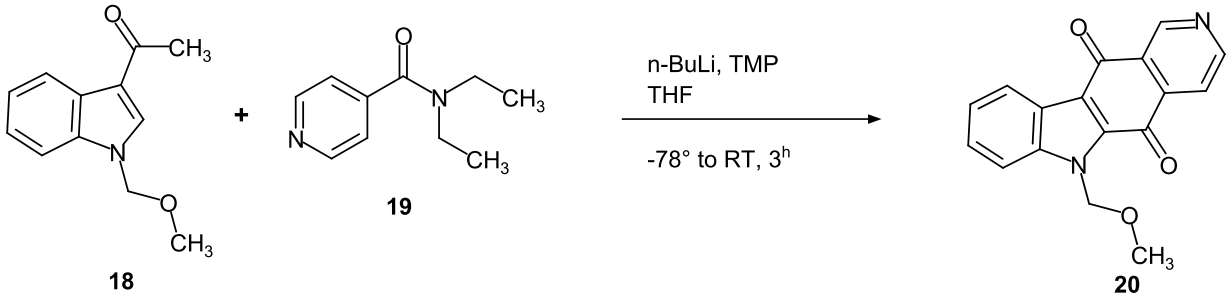

By adding TMP (45.04 mmol, 7.60 ml) dropwise to a solution of n-BuLi (4 equiv. 45.04 mmol, 18 ml of the 2.5M solution in hexanes) in abs. THF (160 ml) under an argon atmosphere at -70° C a Li-TMP solution was prepared. Then, the reaction was allowed to warm up to -5° C to 0° C within 30^{min} and was stirred at the same temperature for further 30^{min}, following cooling down to -78° C. At this temperature, a solution of **(19)** (1 equiv. 11.26 mmol, 2.0 g) and **(18)** (1 equiv. 11.26 mmol, 2.12 g) in abs. THF (160 ml) was added dropwise in order to keep the internal temperature not higher than -65° C. After this, the flask was allowed to gradually reach the room temperature within 2^{h}. The mixture was quenched with water (100 ml) and the aqueous layer was extracted with EtOAc, dried with Na_2SO_4 and concentrated *in vacuo*. The dark orange residue was purified by flash column chromatography

(silica gel, petroleum ether/EtOAc, 5/5), and recrystallized from EtOAc, giving the desired product **(20)** (0.754 g, 22 %) as orange needles.

HRMS: m/z calc. for $C_{17}H_{13}N_2O_3$ ($[M+Na]^+$): 293.0921; found: 293.0922.

3.4.2 Synthesis of 5H,6H,11H-Pyrido[4,3-b]carbazole-5,11-dione[61]

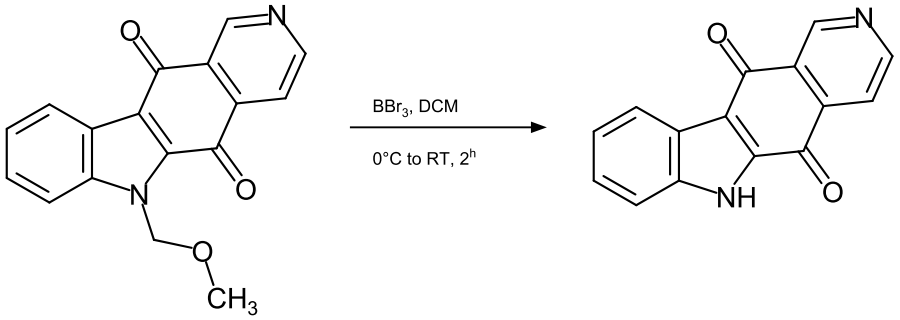

20 **21**

To an ice-cold mixture of the product prepared above **(20)** (1.278 g) in abs. CH_2Cl_2 (285 ml), a solution of BBr_3 (5.30 ml of 1M solution in CH_2Cl_2) was slowly added. After reaching room temperature and stirring for 1^h at the same temperature, a saturated $NaHCO_3$ solution (285 ml) was added to the reaction. The mixture was stirred vigorously at 60°C for further $1^{h.}$ The flask was cooled down to room temperature, and the crude product was filtrated. The filter cake was washed with cold water and CH_2Cl_2, and recrystallized from EtOAc, giving the desired product **(21)** (0.918 g, 85 %) as orange crystals.

HRMS: m/z calc. for $C_{15}H_9N_2O_2$ ($[M+Na]^+$): 249.0659; found: 249.0657.

3.4.3 Synthesis of 6-[(3E)-6-[(tert-Butyldiphenylsilyl)oxy] hex-3-en-1-yl]-5H,6H,11H-pyrido[4,3-b]carbazole-5,11-dione[61]

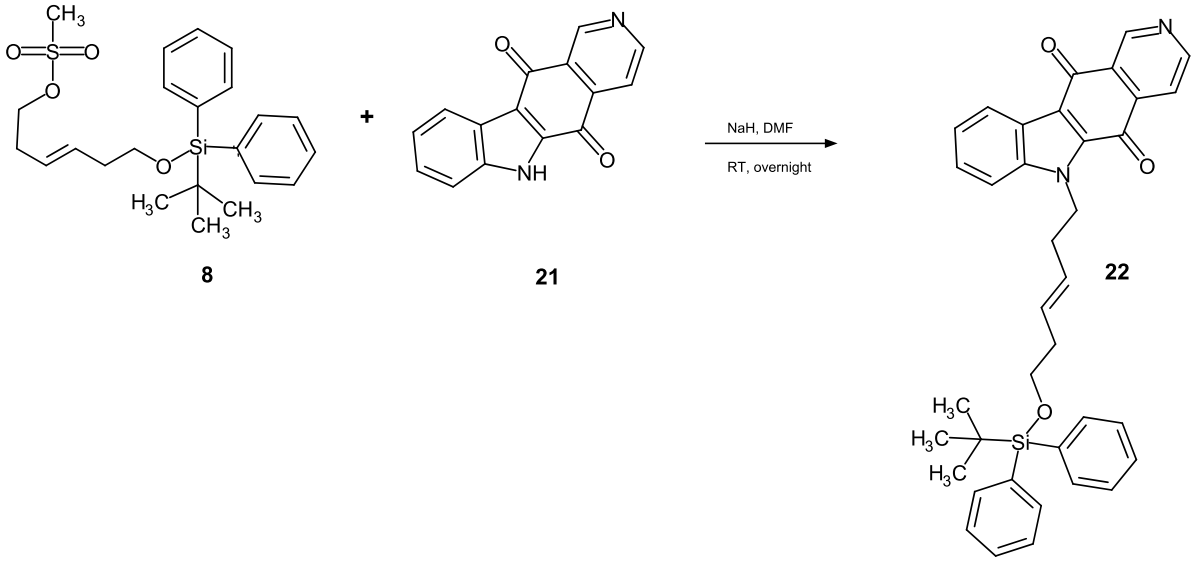

8 21 22

NaH (2 equiv. 4.03 mmol, 0,161g) was suspended in abs. DMF (25 ml) and cooled down to -10° C. A solution of **(21)** (1 equiv. 2.01 mmol, 0.5 g) in abs. DMF (50 ml) was prepared and dropwise added to the cold suspension. The cooling bath was removed and the mixture was stirred for further 30^{min}. Then, the side chain **(6)** (2 equiv. 4.03 mmol, 1.742 g) in abs. DMF (50 ml) was slowly added and the reaction was running overnight at 75° C. After controlling the reaction with TLCs and the spot of the side chain completely disappeared, the reaction was cooled down and stopped by quenching it with water. After extraction with EtOAc. the combined organic layers were dried with Na_2SO_4 and concentrated *in vacuo.* The crude product was purified by flash chromatography (silica gel, petroleum ether/EtOAc, 7/3), giving the desired product **(22) (**0.175 g, 70 %) as orange crystals.

HRMS: m/z calc. for $C_{37}H_{37}N_2O_3Si([M+Na]^+)$: 585.2568; found: 585.2552

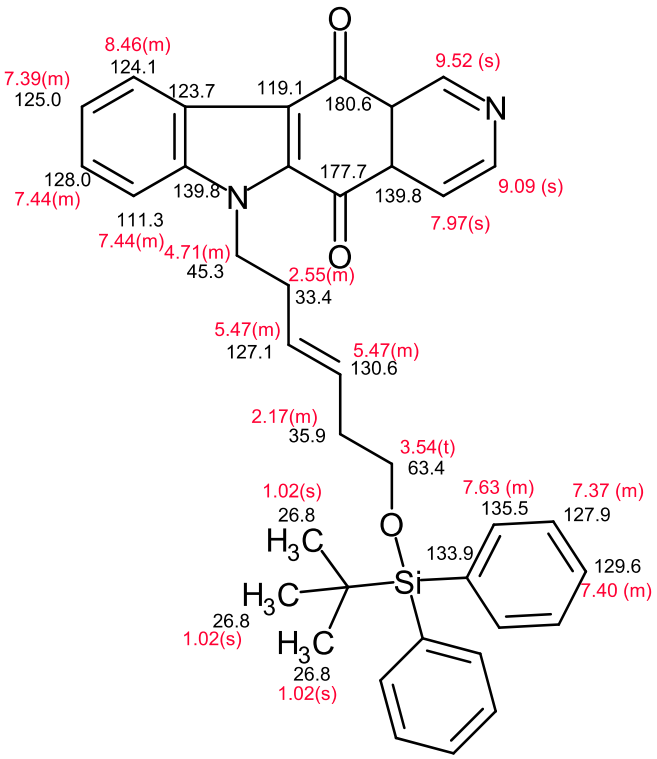

^{1}H-NMR (500 MHz, $CDCl_3$): 1.02 (s, 9H, -C(CH_3)$_3$,), 2.17(m, 2H, -CH_2), 2.55 (m, 2H, -CH_2), 3.54 (t, 2H, (6.8Hz), -O-(CH_2)), 4.71 (m, 2H, -N-(CH_2)), 5.47 (m, 2H, -(CH)$_2$), 7.37 (m, 4H, 2x ($C^{3''}$H, $C^{5''}$H)), 7.39 (m, 1H, C^{9}H), 7.40 (m, 2H, ($C^{4''}$H), 7.44 (m, 2H, C^{8}H), 7.63 (m, 2H, 2x($C^{2'}$H, $C^{6'}$H)), 7.97 (s, 1H, C^{4}H), 9.09 (s, 1H, C^{3}H), 9.52 (s, 1H, C^{1}H).

^{13}C-NMR (125 MHz, $CDCl_3$): 19.2(-<u>C</u>(CH_3)$_3$), 26.8 (-C(<u>C</u>H_3)$_3$), 33.4 ($C^{2'}$,), 35.9($C^{5'}$) 45.3 ($C^{1'}$), 63.4 ($C^{6'}$), 111.3 (C^{7}), 119.1 (C^{10b}), 123.7(C^{10a}), 124.1(C^{10a}), 125.0 (C^{9}), 127.1($C^{3'}$), 127.6 ($C^{3''}$, $C^{5''}$), 128.0(C^{8}), 129.6 ($C^{4''}$), 130.6 ($C^{4'}$), 133.9 ($C^{1'}$), 134.1 (C^{5a}), 135.5 ($C^{2'}$, $C^{6'}$), 138.9 (C^{4a}), 139.8 (C^{6a}), 177.7 (C^{5}), 180.6 (C^{11}).

4. Conclusion

4. Conclusion

The structures of the cytostatic drugs Mitoxantrone and Pixantrone form the basis of the present topic. The latter was the result of the search for a structure analogue to Mitoxantrone, which finally should show no or at least a reduced cardiotoxicity. Based on these studies, a modification with electron deficient aromatic rings led to a significant reduction or to a complete loss of the myocardial damaging effect. Further developments in this context were based on these findings that amino groups have an additional high affinity to DNA and topoisomerase II due to their basicity and the ability to form hydrogen bonds. In this thesis, a series of side chains such as trans-alkenes and chains with S-insertion are synthesized and one of them has been linked to the core structure in order to ensure that the alkylation can be successfully performed. Further steps, including synthesis of the final compound and the investigation of the cytotoxic activities were not part of this work.

4. Zusammenfassung

Die Strukturen der Zytostatika Mitoxantron und Pixantron bilden die Grundlage des vorliegenden Themas. Letzteres war das Ergebnis der Suche nach einer Struktur analog zu Mitoxantron, die keine oder zumindest eine reduzierte Kardiotoxizität aufweisen sollte. Laut Studien führt eine Modifikation mit elektronendefizitären Aromaten statt des Dihydroxyphenylrings des Mitoxantrons zu einer signifikanten Reduktion oder zu einem vollständigen Verlust der myokardialen Schädigung. Weitere Entwicklungen in diesem Zusammenhang basierten auf seinen Erkenntnissen, dass Aminogruppen aufgrund ihres basischen Charakters und der Fähigkeit, Wasserstoffbrücken zu bilden, eine zusätzliche hohe Affinität zu DNA und Topoisomerase II aufweisen. In dieser Arbeit wurde eine Reihe von Seitenketten wie trans-Alkene und Ketten mit S-Insertionen synthetisiert und eine davon mit dem Grundbaustein verknüpft, um sicherzustellen, dass die Alkylierung erfolgreich durchgeführt werden kann. Weitere Schritte, einschließlich der Synthese der endgültigen Verbindung und der Untersuchung der zytotoxischen Aktivitäten waren nicht Teil dieser Arbeit.

5. Bibliography

5. Bibliography

1. (US) NI of H, Study BSC. Understanding Cancer. 2007.

2. Sudhakar A. History of Cancer, Ancient and Modern Treatment Methods. *J Cancer Sci Ther*. 2009;1(2):1-4. doi:10.4172/1948-5956.100000e2.

3. Early History of Cancer | American Cancer Society. https://www.cancer.org/cancer/cancer-basics/history-of-cancer/what-is-cancer.html. Accessed March 26, 2018.

4. SEER Training:Cancer: A Historic Perspective. https://training.seer.cancer.gov/disease/history/. Accessed April 1, 2018.

5. Ma X, Yu H. Global burden of cancer. *Yale J Biol Med*. 2006;79(3-4):85-94.

6. WORLD HEALTH STATISTICS 2007 Part 1 Ten statistical highlights in global public health.

7. Fact Sheets by Cancer. http://globocan.iarc.fr/Pages/fact_sheets_cancer.aspx. Accessed March 26, 2018.

8. Jemal A, Bray F, Center MM, Ferlay J, Ward E, Forman D. Global cancer statistics. *CA Cancer J Clin*. 2011;61(2):69-90. doi:10.3322/caac.20107.

9. Fact Sheets by Population. http://globocan.iarc.fr/Pages/fact_sheets_population.aspx. Accessed March 26, 2018.

10. Estimated Number of New Cancer Cases by World Area, 2008*.

11. Cooper GM. The Development and Causes of Cancer. 2000.

12. Insel PM, Ross D, McMahon K, Bernstein M. *Nutrition*.

13. SEER Training:Cancer Classification. https://training.seer.cancer.gov/disease/categories/classification.html. Accessed March 26, 2018.

14. DeLong L, Burkhart NW. *General and Oral Pathology for the Dental Hygienist*.

Lippincott Williams & Wilkins; 2008. https://books.google.at/books/about/General_and_Oral_Pathology_for_the_Denta.html?id=pkxrRi16ZfcC&redir_esc=y. Accessed March 26, 2018.

15. Brierley J, National Cancer Institute of Canada Committee on Cancer Staging. The evolving TNM cancer staging system: an essential component of cancer care. *CMAJ*. 2006;174(2):155-156. doi:10.1503/cmaj.045113.

16. TNM | UICC. https://www.uicc.org/resources/tnm/. Accessed March 26, 2018.

17. Cancer Staging. https://www.cancer.org/treatment/understanding-your-diagnosis/staging.html. Accessed March 26, 2018.

18. Cowherd SM. Tumor Staging and Grading: A Primer. In: *Methods in Molecular Biology (Clifton, N.J.)*. Vol 823. ; 2012:1-18. doi:10.1007/978-1-60327-216-2_1.

19. AJCC - What is Cancer Staging? https://cancerstaging.org/references-tools/Pages/What-is-Cancer-Staging.aspx. Accessed March 26, 2018.

20. Williams GH, Stoeber K. The cell cycle and cancer. *J Pathol*. 2012;226(2):352-364. doi:10.1002/path.3022.

21. Schafer KA. The Cell Cycle: A Review. *Vet Pathol*. 1998;35(6):461-478. doi:10.1177/030098589803500601.

22. Daignan-Fornier B, Sagot I. Proliferation/Quiescence: When to start? Where to stop? What to stock? *Cell Div*. 2011;6(1):20. doi:10.1186/1747-1028-6-20.

23. Pospelova T V, Demidenko ZN, Bukreeva EI, Pospelov VA, Gudkov A V, Blagosklonny M V. Pseudo-DNA damage response in senescent cells. *Cell Cycle*. 2009;8(24):4112-4118. doi:10.4161/cc.8.24.10215.

24. Jones PA, Baylin SB. The Epigenomics of Cancer. *Cell*. 2007;128(4):683-692. doi:10.1016/j.cell.2007.01.029.

25. Sharma S, Kelly TK, Jones PA. Epigenetics in cancer. *Carcinogenesis*. 2010;31(1):27-36. doi:10.1093/carcin/bgp220.

26. Hanahan D, Weinberg RA. The hallmarks of cancer. *Cell*. 2000;100(1):57-70.

doi:10.1007/s00262-010-0968-0.

27. Hanahan D, Weinberg RA. Hallmarks of Cancer: The Next Generation. *Cell*. 2011;144(5):646-674. doi:10.1016/j.cell.2011.02.013.

28. Fouad YA, Aanei C. Revisiting the hallmarks of cancer. *Am J Cancer Res*. 2017;7(5):1016-1036.

29. Hickman ES, Moroni MC, Helin K. The role of p53 and pRB in apoptosis and cancer. *Curr Opin Genet Dev*. 2002;12(1):60-66.

30. Wang E. *Cancer Systems Biology*. CRC Press; 2010.

31. Anand P, Kunnumakara AB, Sundaram C, et al. Cancer is a Preventable Disease that Requires Major Lifestyle Changes. 2008. doi:10.1007/s11095-008-9661-9.

32. Masrour-Roudsari J, Ebrahimpour S. Causal role of infectious agents in cancer: An overview. *Casp J Intern Med*. 2017;8(3):153-158. doi:10.22088/cjim.8.3.153.

33. How Cancer is Treated | Cancer.Net. https://www.cancer.net/navigating-cancer-care/how-cancer-treated. Accessed April 2, 2018.

34. Mutschler E. *Mutschler Arzneimittelwirkungen Lehrbuch Der Pharmakologie Und Toxikologie ; Mit Einführenden Kapiteln in Die Anatomie, Physiologie Und Pathophysiologie ; 264 Tabellen*. Wiss. Verl.-Ges; 2013.

35. Urruticoechea A, Alemany R, Balart J, Villanueva A, Vinals F, Capella G. Recent Advances in Cancer Therapy: An Overview. *Curr Pharm Des*. 2010;16(1):3-10. doi:10.2174/138161210789941847.

36. Pollock RE, Morton DL. Principles of Surgical Oncology. 2003.

37. Baudino TA. Targeted Cancer Therapy: The Next Generation of Cancer Treatment. *Curr Drug Discov Technol*. 2015;12(1):3-20.

38. Research Areas: Treatment - National Cancer Institute. https://www.cancer.gov/research/areas/treatment. Accessed April 2, 2018.

39. Chabner BA, Roberts TG. Timeline: Chemotherapy and the war on cancer. *Nat Rev Cancer*. 2005;5(1):65-72. doi:10.1038/nrc1529.

40. Pérez-Herrero E, Fernández-Medarde A. Advanced targeted therapies in cancer: Drug nanocarriers, the future of chemotherapy. *Eur J Pharm Biopharm*. 2015;93:52-79. doi:10.1016/j.ejpb.2015.03.018.

41. Liang X-J, Chen C, Zhao Y, Wang PC. Circumventing tumor resistance to chemotherapy by nanotechnology. *Methods Mol Biol*. 2010;596:467-488. doi:10.1007/978-1-60761-416-6_21.

42. Partridge AH, Burstein HJ, Winer EP. Side effects of chemotherapy and combined chemohormonal therapy in women with early-stage breast cancer. *J Natl Cancer Inst Monogr*. 2001;(30):135-142. http://www.ncbi.nlm.nih.gov/pubmed/11773307. Accessed April 2, 2018.

43. Chemotherapy | Cancer.Net. https://www.cancer.net/navigating-cancer-care/how-cancer-treated/chemotherapy/side-effects-chemotherapy - Side Effects of Chemotherapy. Accessed March 18, 2018.

44. Koedoot CG, de Haan RJ, Stiggelbout AM, et al. Palliative chemotherapy or best supportive care? A prospective study explaining patients' treatment preference and choice. *Br J Cancer*. 2003;89(12):2219-2226. doi:10.1038/sj.bjc.6601445.

45. Gottesman MM. Mechanisms of Cancer Drug Resistance. *Annu Rev Med*. 2002;53(1):615-627. doi:10.1146/annurev.med.53.082901.103929.

46. Housman G, Byler S, Heerboth S, et al. Drug resistance in cancer: an overview. *Cancers (Basel)*. 2014;6(3):1769-1792. doi:10.3390/cancers6031769.

47. Li J, Chen F, Cona MM, et al. A review on various targeted anticancer therapies. *Target Oncol*. 2012;7(1):69-85. doi:10.1007/s11523-012-0212-2.

48. American Academy of Family Physicians. DE. *American Family Physician.* Vol 77. American Academy of Family Physicians; 1970. https://www.aafp.org/afp/2008/0201/p311.html. Accessed March 18, 2018.

49. Kufe DW, Holland JF, Frei E, American Cancer Society. *Cancer Medicine 6*. BC Decker; 2003. https://books.google.at/books/about/Cancer_Medicine_6.html?id=UmxzRQAACAAJ&redir_esc=y. Accessed April 2, 2018.

50. Noll DM, Mason TM, Miller PS. Formation and repair of interstrand cross-links in DNA. *Chem Rev*. 2006;106(2):277-301. doi:10.1021/cr040478b.

51. Minotti G, Menna P, Salvatorelli E, Cairo G, Gianni L. Anthracyclines: molecular advances and pharmacologic developments in antitumor activity and cardiotoxicity. *Pharmacol Rev*. 2004;56(2):185-229. doi:10.1124/pr.56.2.6.

52. Strekowski L, Wilson B. Noncovalent interactions with DNA: An overview. *Mutat Res Mol Mech Mutagen*. 2007;623(1-2):3-13. doi:10.1016/j.mrfmmm.2007.03.008.

53. Lerman LS. Structural considerations in the interaction of DNA and acridines. *J Mol Biol*. 1961;3(1):18-IN14. doi:10.1016/S0022-2836(61)80004-1.

54. Karimi Goftar M, Moradi Kor N, Moradi Kor Z. DNA Intercalators and Using Them as Anticancer Drugs. *CASRP Publ Co*. 2014;2(3):811-822. http://ijabbr.com/article_7245.html. Accessed April 2, 2018.

55. Marosi C. Complications of chemotherapy in neuro-oncology. *Handb Clin Neurol*. 2012;105:873-885. doi:10.1016/B978-0-444-53502-3.00029-X.

56. Rahman AM, Yusuf SW, Ewer MS. Anthracycline-induced cardiotoxicity and the cardiac-sparing effect of liposomal formulation. *Int J Nanomedicine*. 2007;2(4):567-583. http://www.ncbi.nlm.nih.gov/pubmed/18203425. Accessed April 2, 2018.

57. Edwardson DW, Narendrula R, Chewchuk S, Mispel-Beyer K, Mapletoft JPJ, Parissenti AM. Role of Drug Metabolism in the Cytotoxicity and Clinical Efficacy of Anthracyclines. *Curr Drug Metab*. 2015;16(6):412-426. doi:10.2174/1389200216888150915112039.

58. Pratt WB, Pratt WB. *The Anticancer Drugs*. Oxford University Press; 1994. https://books.google.at/books?id=nPR1L4K5HuEC&dq=mitoxantrone+intercalation&hl=hr&source=gbs_navlinks_s. Accessed April 2, 2018.

59. Allegra JC, Woodcock T, Woolf S, et al. A randomized trial comparing mitoxantrone with doxorubicin in patients with stage IV breast cancer. *Invest New Drugs*. 1985;3(2):153-161. http://www.ncbi.nlm.nih.gov/pubmed/3894278. Accessed April 2, 2018.

60. Krapcho AP, Gallagher CE, Hammach A, et al. Synthesis of hydroxy-substituted aza-analogues of antitumor anthrapyrazoles. *J Heterocycl Chem*. 1998;35(4):895-906. doi:10.1002/jhet.5570350419.

61. Nagel T. DNA intercalating compounds with a Tetra- or Pentacyclic Nucleus. 2015. http://othes.univie.ac.at/38910/. Accessed May 9, 2018.

62. Shahabi Mohammad Shahi M. Synthese und biologische Evaluierung neuer tetracyclischer Isochinolinone mit zytotoxischer Wirkung. 2016. http://othes.univie.ac.at/45243/. Accessed May 9, 2018.

63. Triantafyllakis M, Tofi M, Montagnon T, Kouridaki A, Vassilikogiannakis G. Singlet Oxygen-Mediated Synthesis of *Bis* -spiroketals Found in Azaspiracids. *Org Lett*. 2014;16(11):3150-3153. doi:10.1021/ol501301w.

64. Fischer E. CHEM360 Lab Manual Experiment 10 Fischer Esterification: An ester from a carboxylic acid and an alcohol. 2002. http://fs.huntingdon.edu/jberch/classes/OrgIIlab/3Fischer Esterification.pdf. Accessed April 29, 2018.

65. Whelton BD, Huitric AC. 3-Nitromethylphthalide and 2-phenyl-3-nitromethylphthalimidine. *J Org Chem*. 1970;35(9):3143-3144. doi:10.1021/jo00834a063.

Image Index

Ich habe mich bemüht, sämtliche Inhaber der Bildrechte ausfindig zu machen und ihre Zustimmung zur Verwendung der Bilder in dieser Arbeit eingeholt. Sollte dennoch eine Urheberrechtsverletzung bekannt werden, ersuche ich um Meldung bei mir.

6. Appendix

6.Appendix

6.1 Abbreviations and Acronyms

Å	Ångström
abs.	absolute
anh.	anhydrous
aqu.	aqueous
°C	degree Celsius
^{13}C-NMR	carbon nuclear magnetic resonance
CH_2CH_2	dichlormethane
COSY	Correlated Spectroscopy
D	duplett
DCM	dichlormethane
DMA	dimethylamine
4-DMAP	4-(dimethylamino)-pyridine
DMF	N.N-dimethylformamide
DMSO	dimethylformamide
DNA	deoxyribonucleic acid
equiv.	equivalent(s)
Et	ethyl
EtOH	ethanol
EtOAc	ethylacetate

F_{20} TPPFe	(5, 10, 15, 20- tetrakis-(pentafluorophenyl) porphynatoiron(III) chloride
G	gram
h	hour(s)
^{1}H-NMR	proton nuclear magnetic resonance
H_2O	water
H_2O_2	hydrogen peroxide
H_2SO_4	sulfuric acid
HCl	hydrochloric acid
HIV	human immunodeficiency virus
HPV	human papillomavirus
HRMS	high resolution MS
HSQC	heteronuclear single quantum coherence
Hz	hertz
IR	Infrared radiation
J	coupling constant
$LiAlH_4$	Lithium aluminium hydride (LAH)
M	molar
m	multiplet
MeOH	methanol
MHz	megahertz
min	minute(s)
mol	mole(s)

MOM	Methoxymethyl
mmol	millimole(s)
MS	molecular sieves or mass spectrometry
Ms-Cl	methynesulfonyl chloride
NMR	nuclear magnetic resonance
R_f	retention factor
RT	room temperature
$SOCl_2$	thionylchloride
TBAF--	tetra-n-butylammonium fluoride
TBDMS-Cl	tert.-Butyldimethylsilyl chloride
TBDPS-Cl	tert.- Butyldiphenylsilyl chloride
TLC	thin layer chromatography
TMP	2,2,6,6-Tetramethylpiperidine
TMS	tetramethylsilane

6.2 Spectra

Structure 2

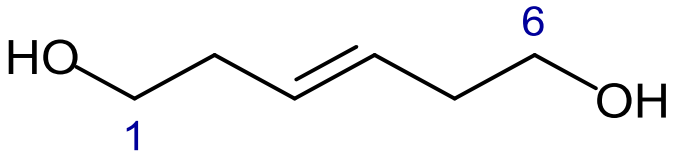

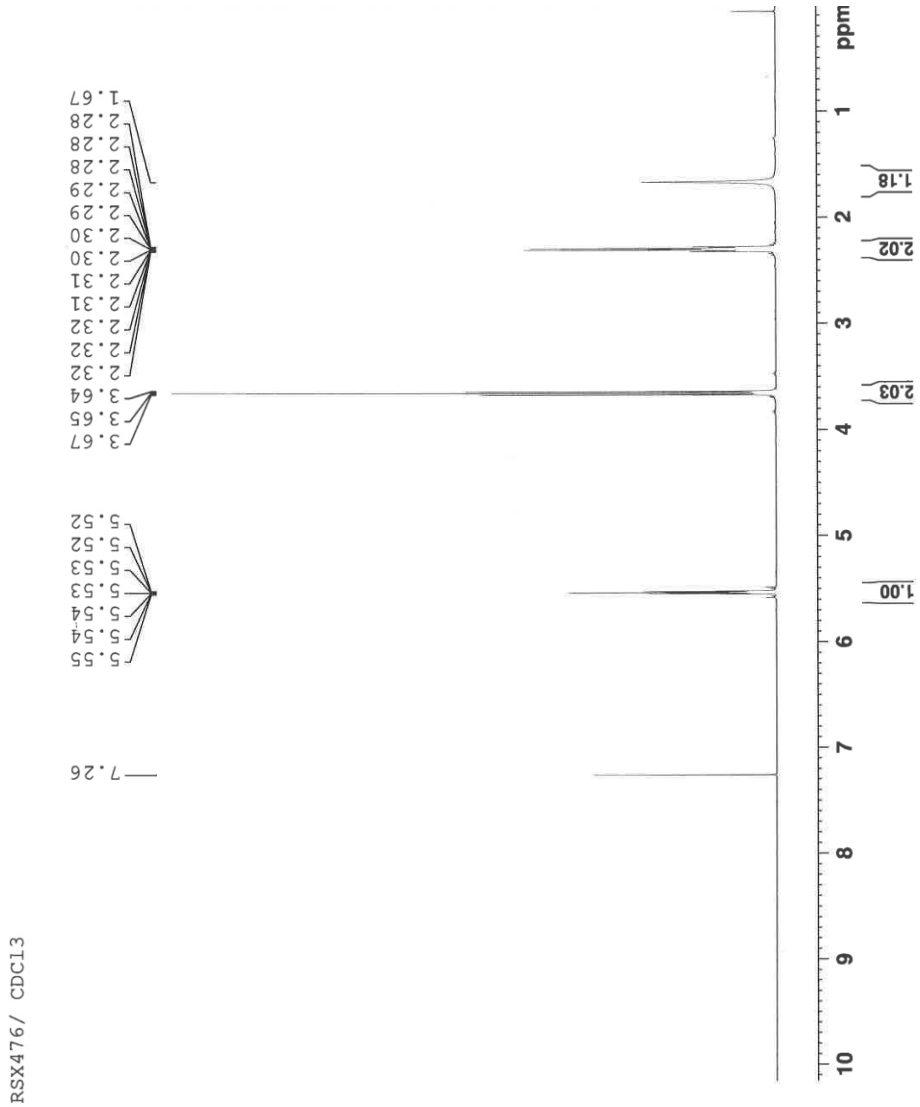

Structure 2

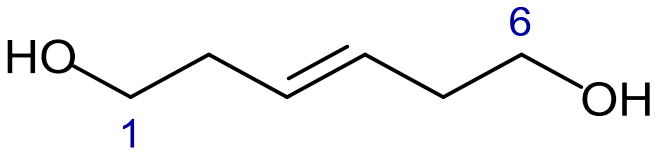
HO
1
6
OH

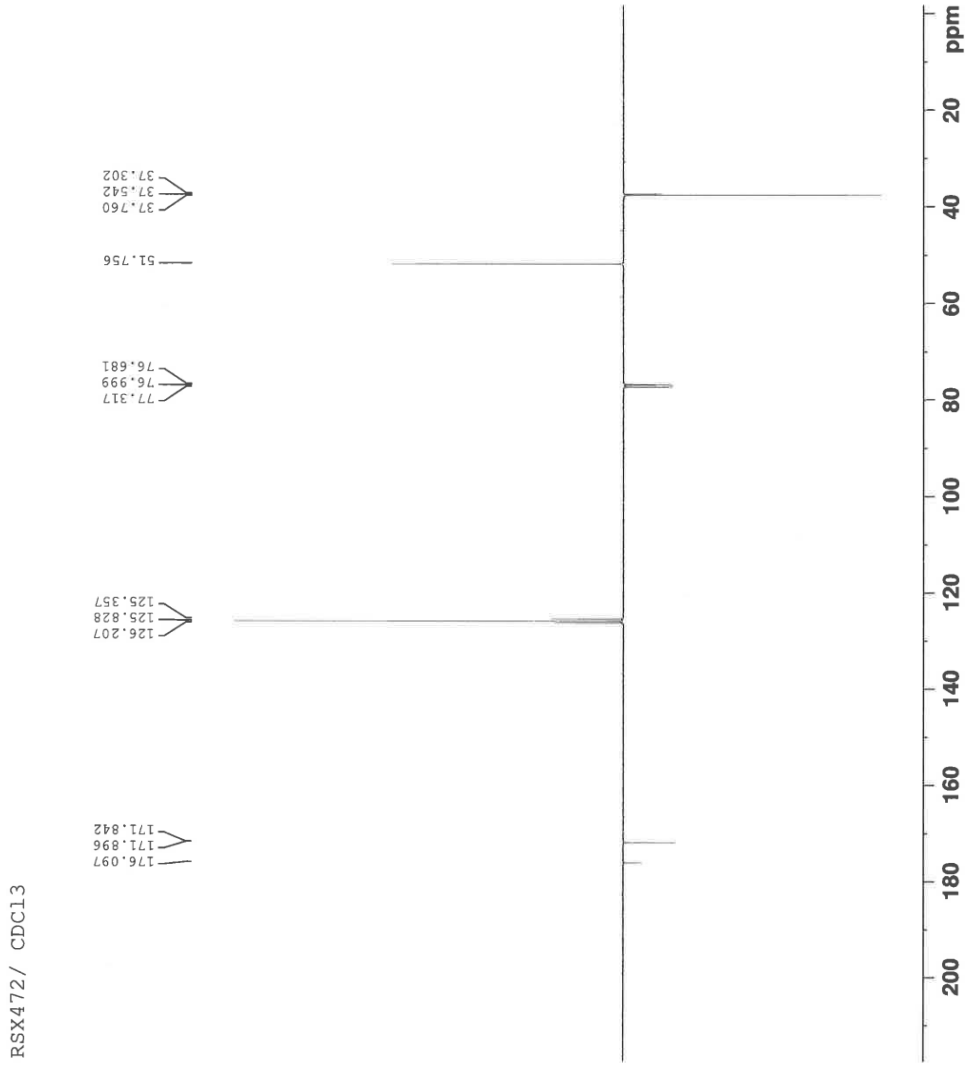
37.302
37.542
37.760
51.756
76.681
76.999
77.317
125.357
125.828
126.207
171.842
171.896
176.097
ppm
20
40
60
80
100
120
140
160
180
200
RSX472/ CDC13

Structure 2

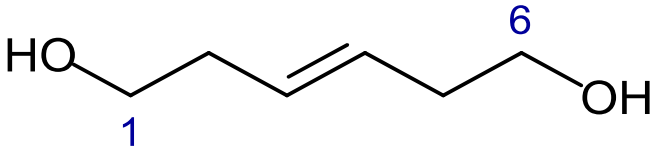
HO
OH
1
6

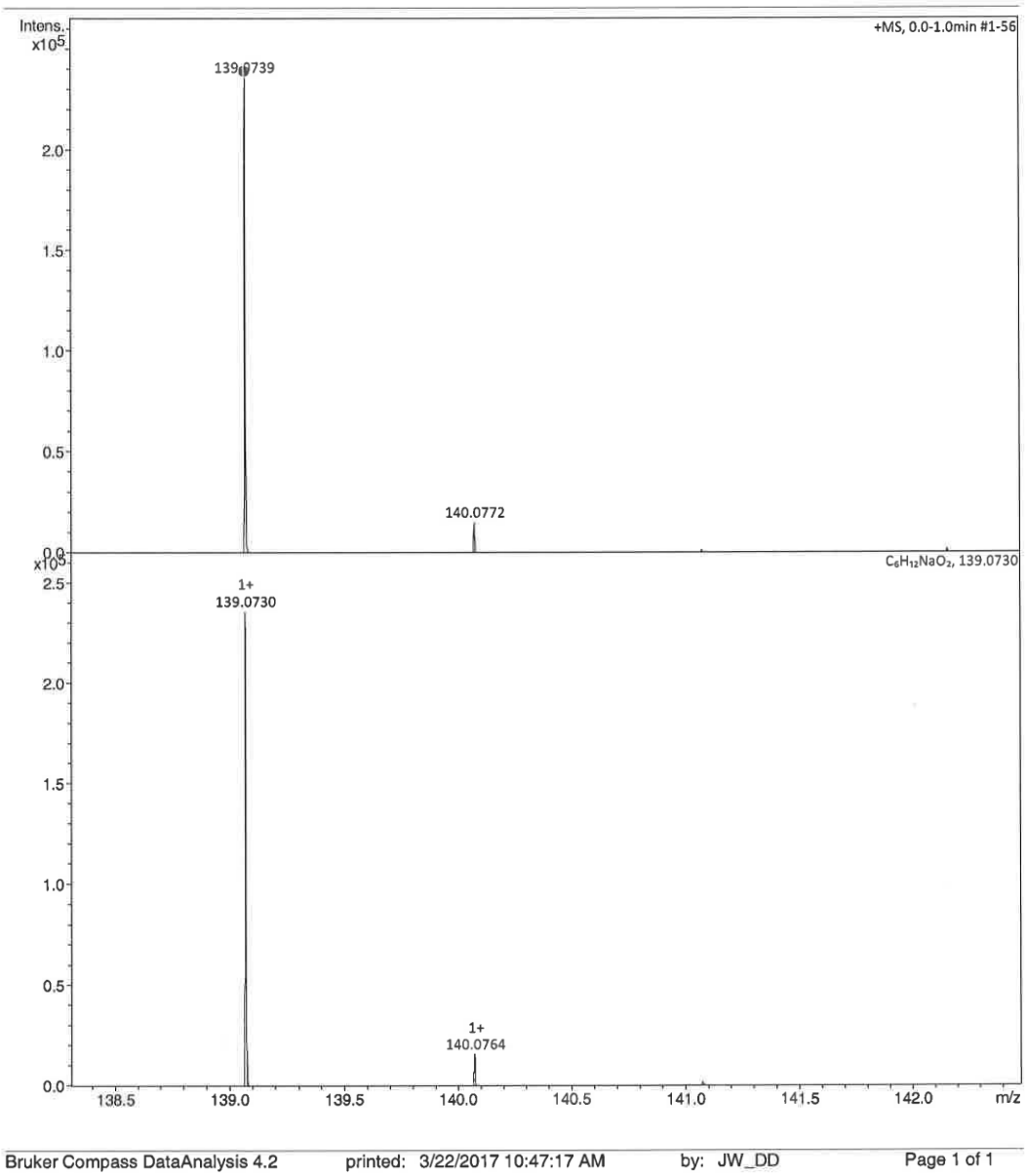
Intens.
x10^5
+MS, 0.0-1.0min #1-56
139.0739
140.0772
2.0
1.5
1.0
0.5
0.0
x10^5
C6H12NaO2, 139.0730
1+
139.0730
1+
140.0764
2.5
2.0
1.5
1.0
0.5
0.0
138.5
139.0
139.5
140.0
140.5
141.0
141.5
142.0
m/z
Bruker Compass DataAnalysis 4.2
printed: 3/22/2017 10:47:17 AM
by: JW_DD
Page 1 of 1

Structure 3

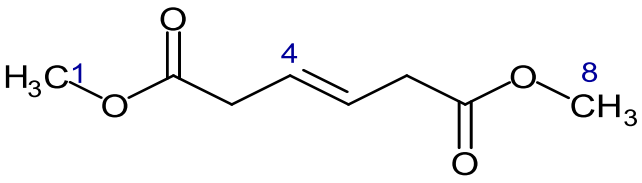
H3C
1
O
O
4
O
O
8
CH3

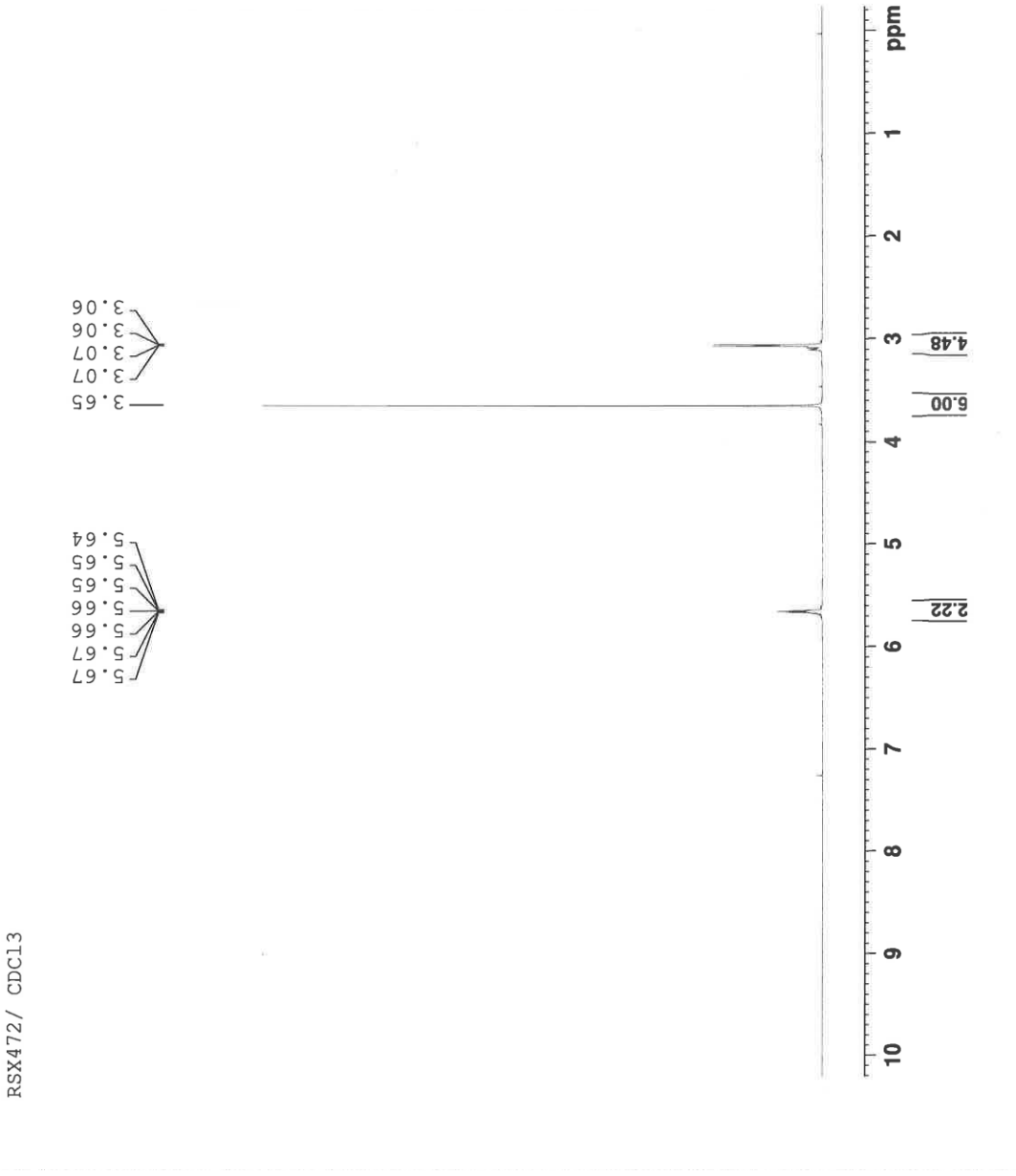
ppm
1
2
3
4
5
6
7
8
9
10
4.48
6.00
2.22
3.65
3.07
3.07
3.06
3.06
5.67
5.66
5.66
5.65
5.65
5.64
RSX472/ CDC13

Structure 3

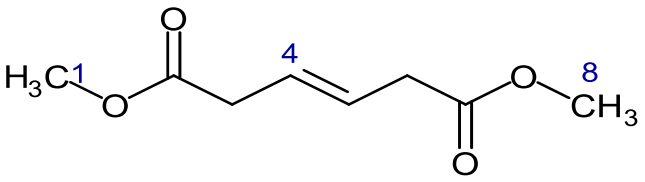
H3C
1
O
O
4
O
8
CH3
O

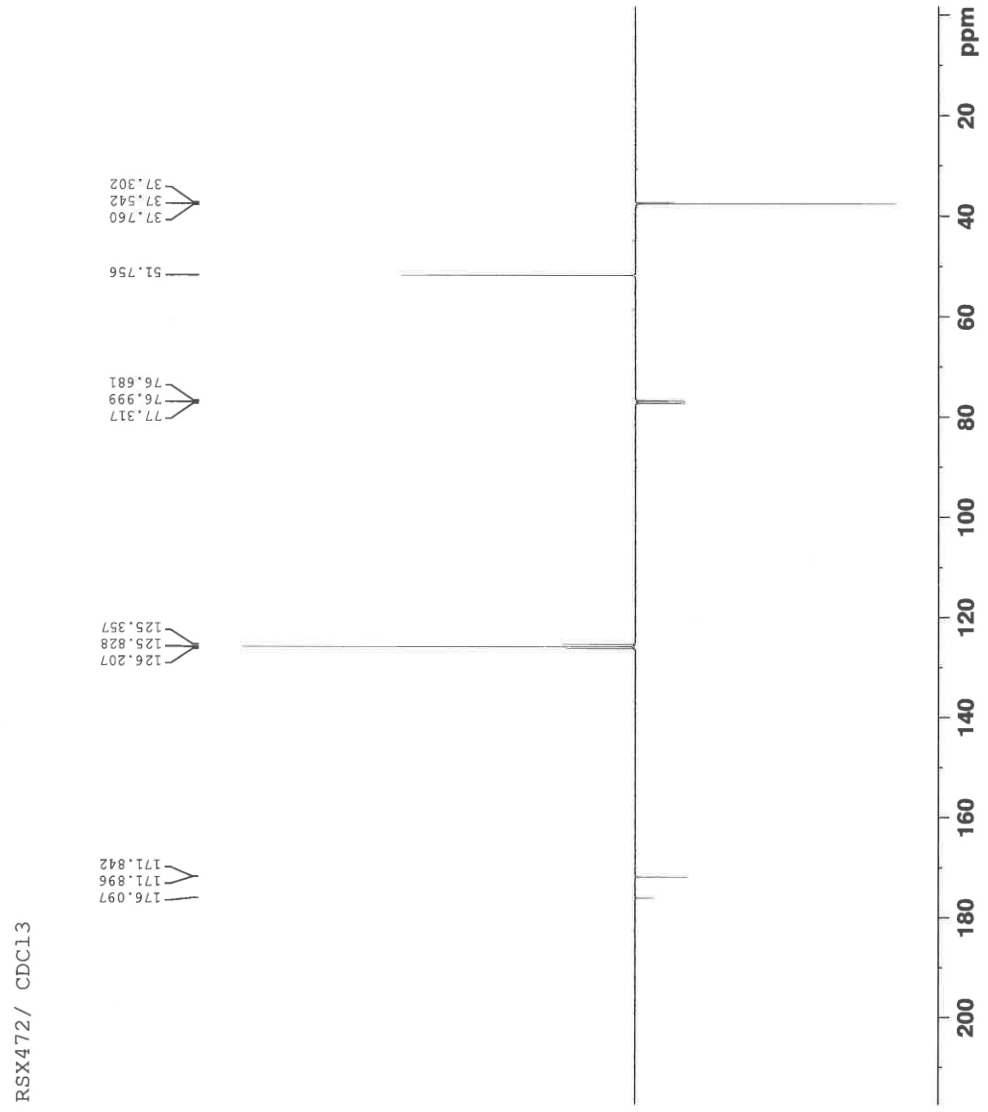
RSX472/ CDC13
ppm
20
40
60
80
100
120
140
160
180
200
37.302
37.542
37.760
51.756
76.681
76.999
77.317
125.357
125.828
126.207
171.842
171.896
176.097

Structure 3

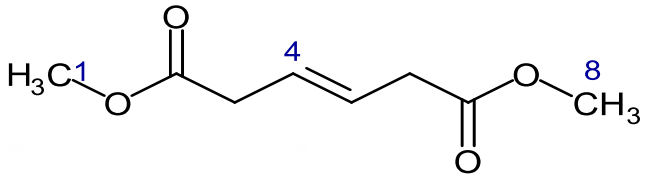
H3C
1
O
O
4
O
8
CH3
O

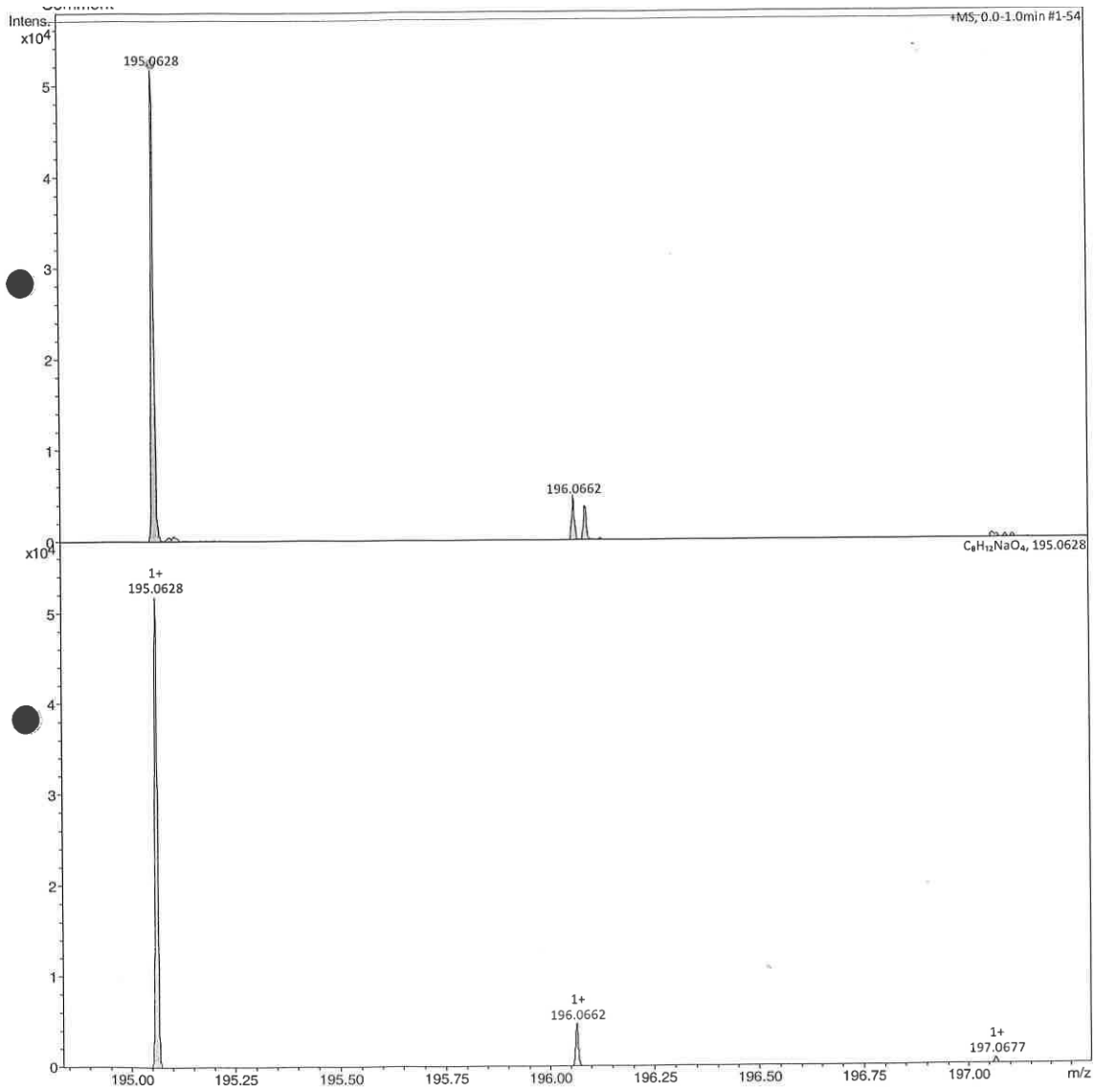
Intens.
x10^4
+MS, 0.0-1.0min #1-54
195.0628
196.0662
C8H12NaO4, 195.0628
1+
195.0628
1+
196.0662
1+
197.0677
195.00
195.25
195.50
195.75
196.00
196.25
196.50
196.75
197.00
m/z

Structure 5

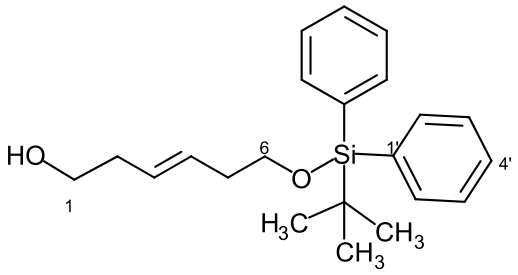
HO
1
6
O
Si
1'
4'
H3C
CH3
CH3

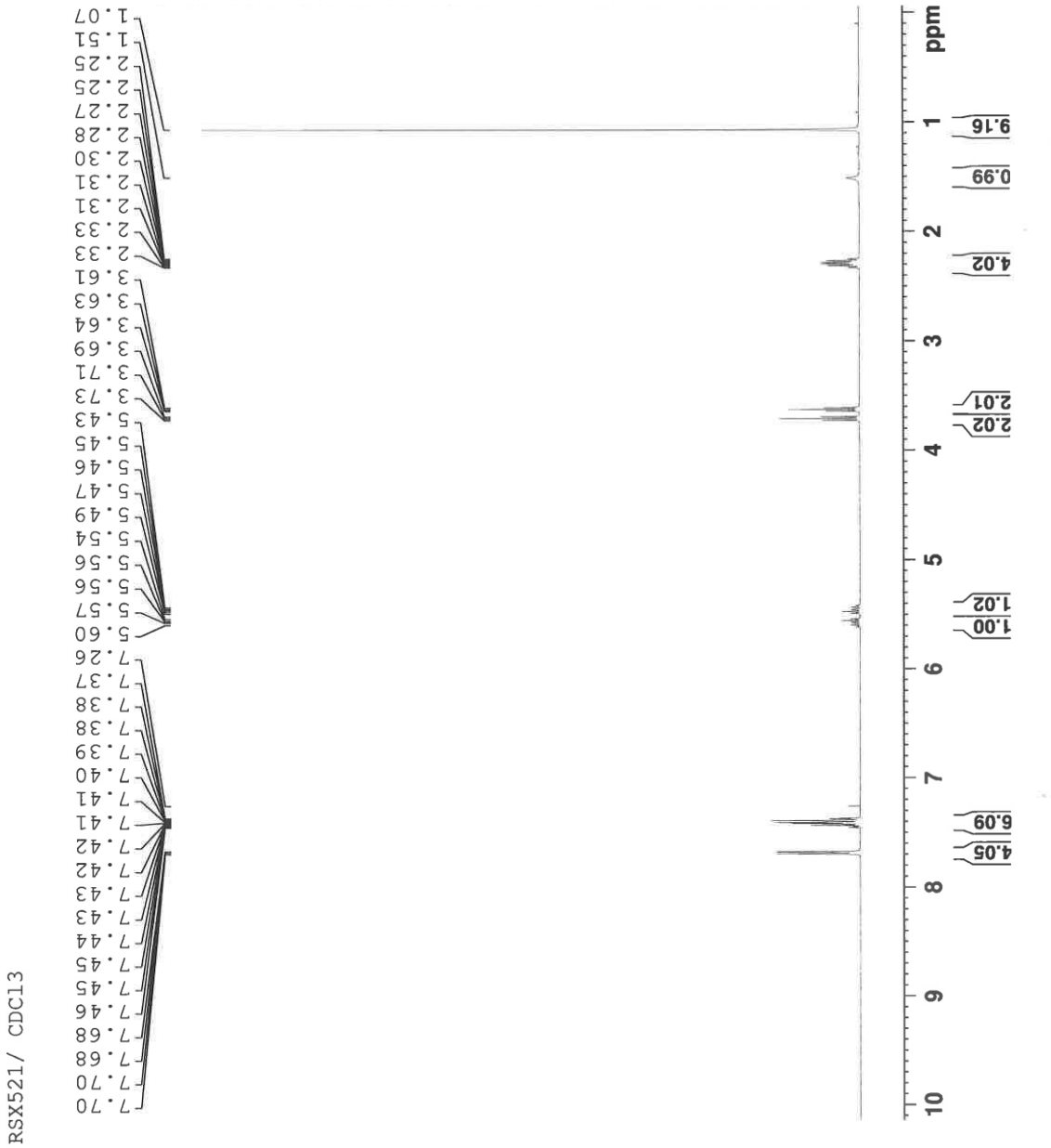
RSX521/ CDC13
ppm
9.16
0.99
4.02
2.01
2.02
1.00
1.02
6.09
4.05

Structure 5

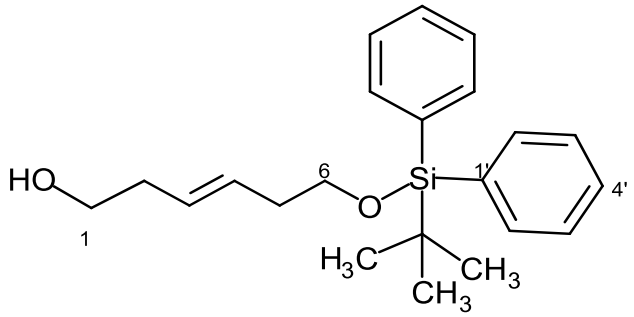
HO
1
6
O
Si
1'
4'
H3C
CH3
CH3

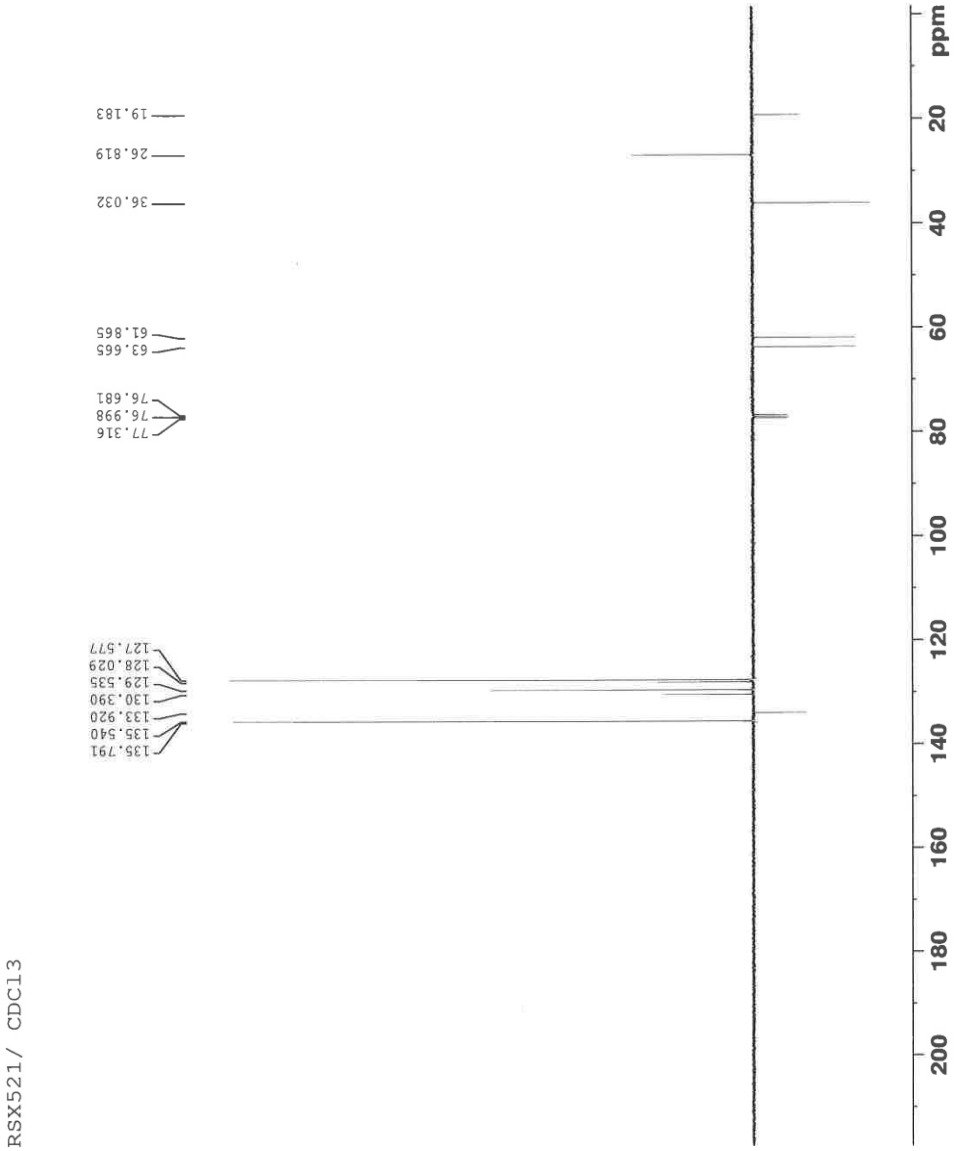
19.183
26.819
36.032
61.865
63.665
76.681
76.998
77.316
127.577
128.029
129.535
130.390
133.920
135.540
135.791
ppm
20
40
60
80
100
120
140
160
180
200
RSX521/ CDC13

Structure 5

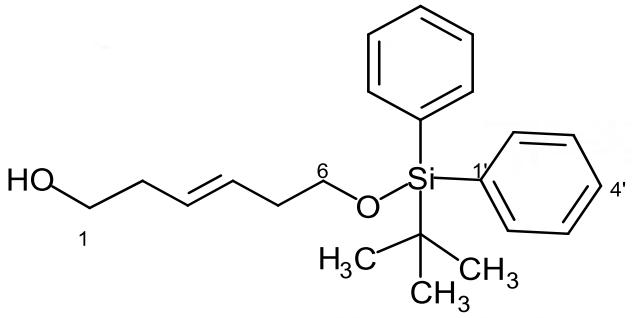
HO
1
6
O
Si
1'
4'
H3C
CH3
CH3

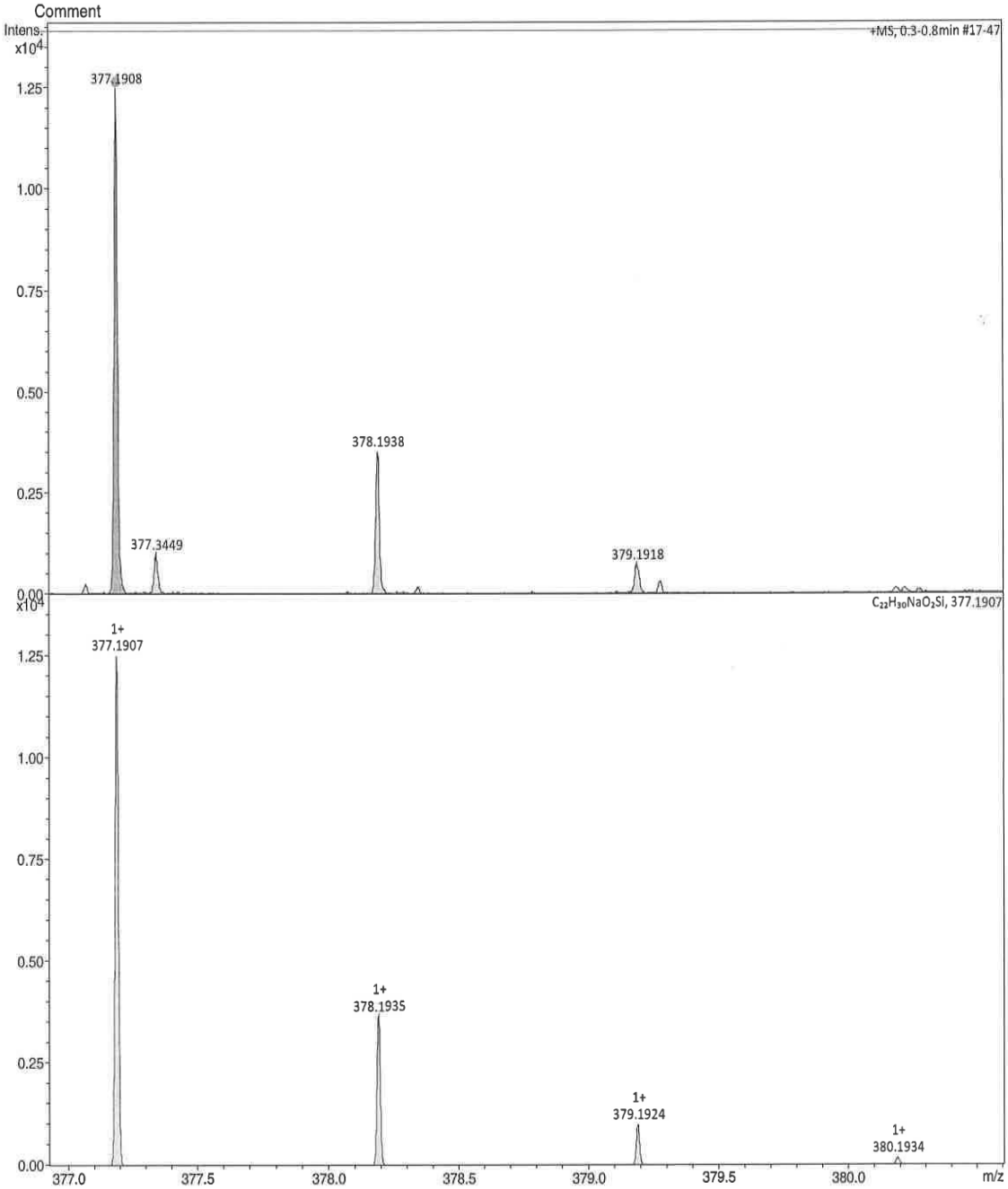
Comment
Intens.
x10^4
+MS, 0.3-0.8min #17-47
377.1908
377.3449
378.1938
379.1918
1.25
1.00
0.75
0.50
0.25
0.00
C22H30NaO2Si, 377.1907
1+
377.1907
1+
378.1935
1+
379.1924
1+
380.1934
377.0
377.5
378.0
378.5
379.0
379.5
380.0
m/z

Structure 6

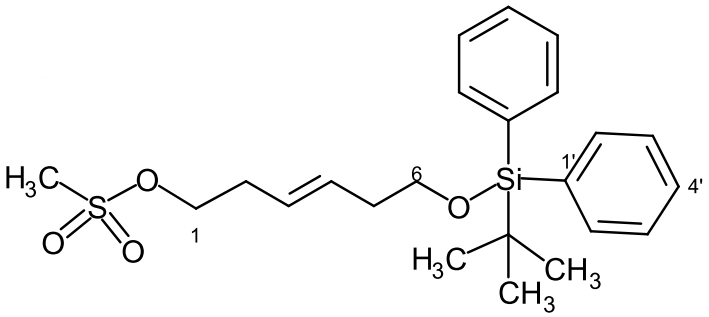
H3C
S
O
O
O
1
6
O
Si
1'
4'
H3C
CH3
CH3

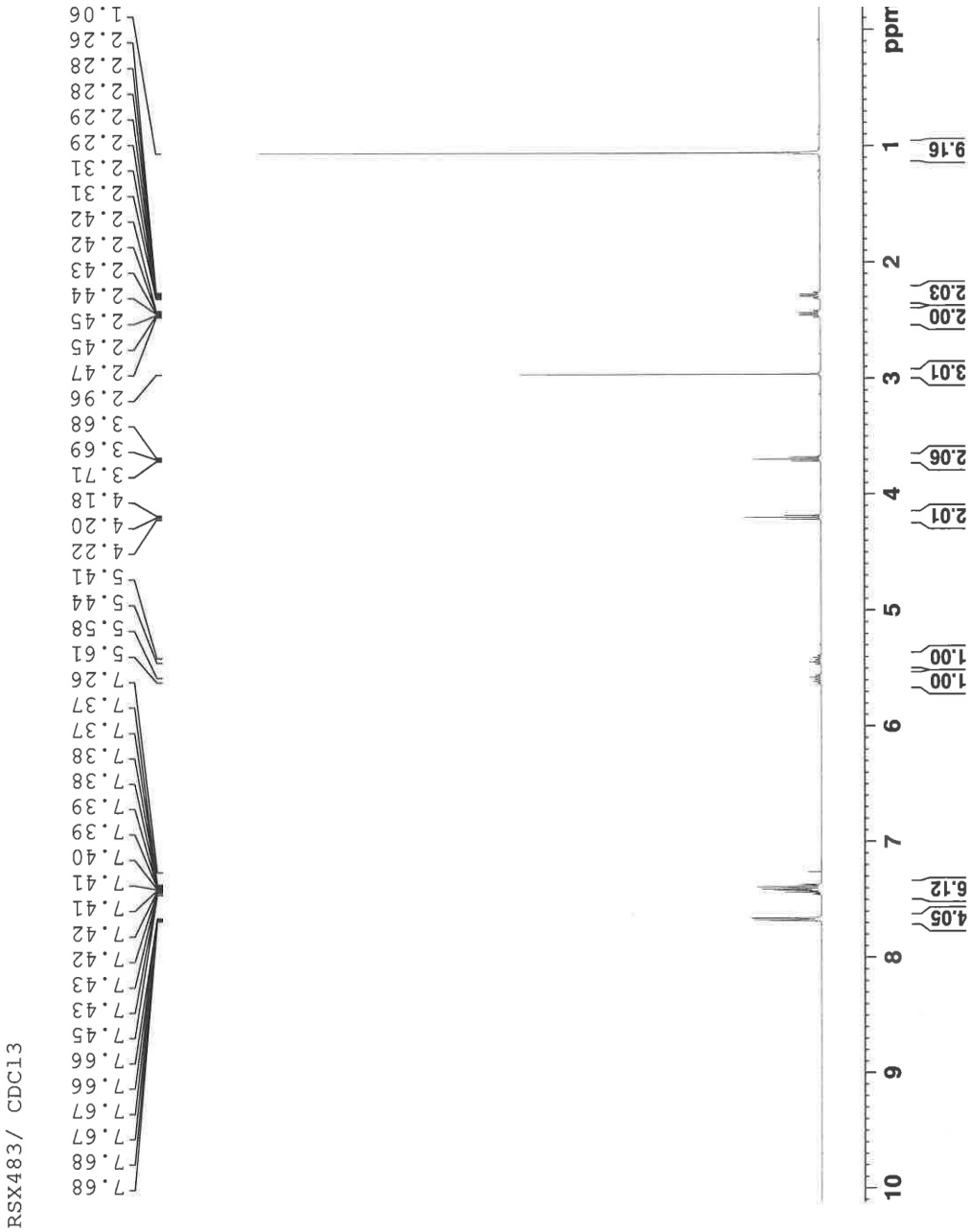
RSX483/ CDC13
ppm
9.16
2.03
2.00
3.01
2.06
2.01
1.00
1.00
6.12
4.05

Structure 6

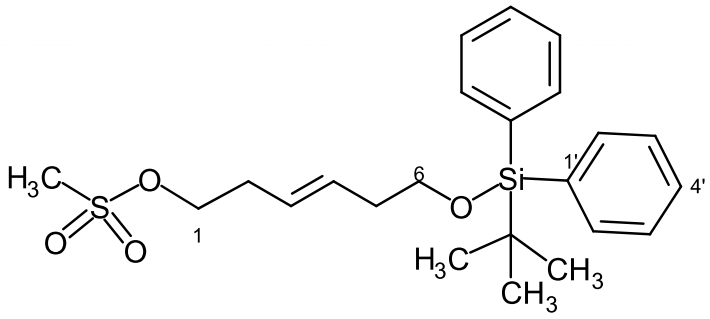
H3C
O
S
O
O
1
6
O
Si
1'
4'
H3C
CH3
CH3

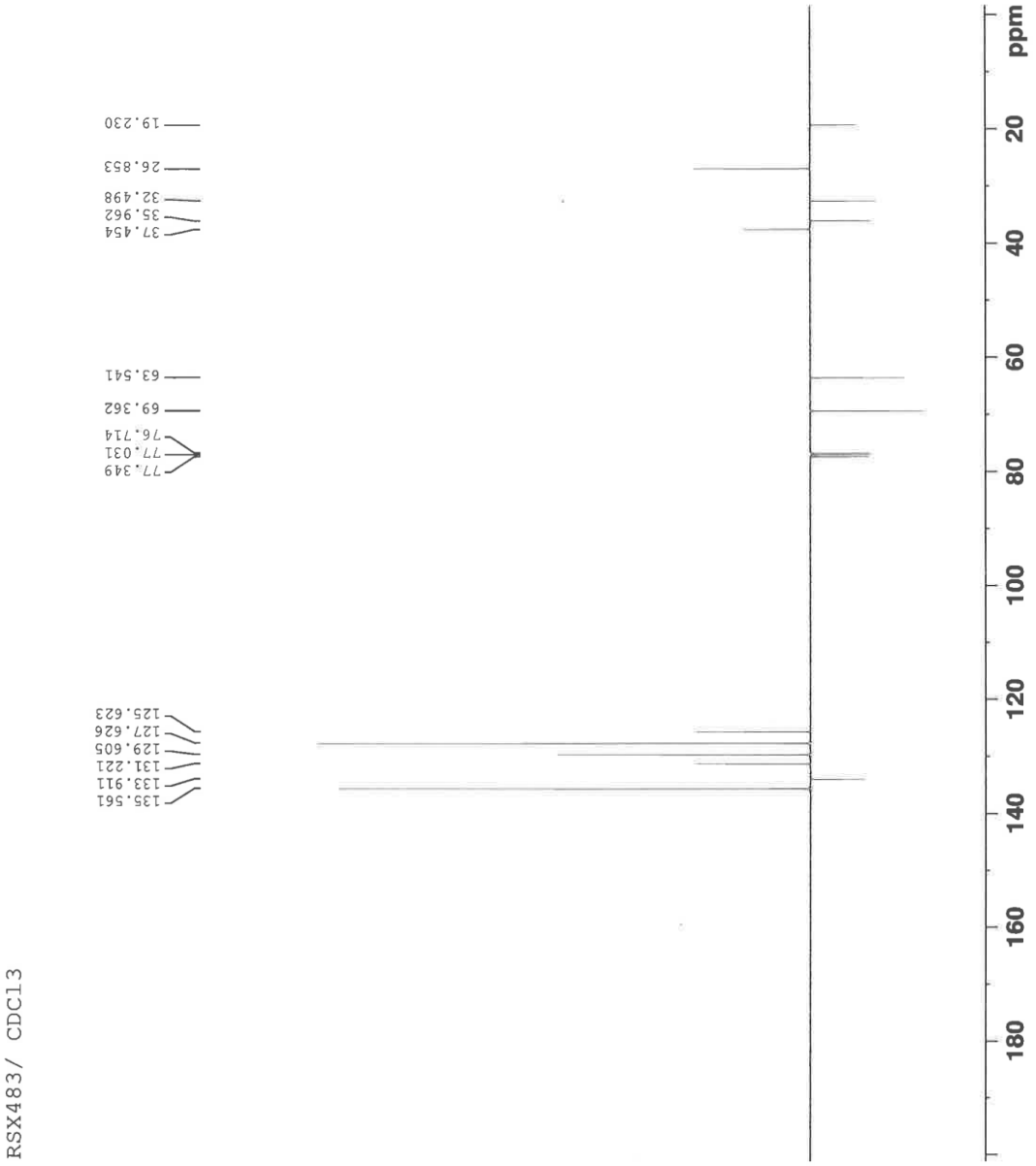
19.230
26.853
32.498
35.962
37.454
63.541
69.362
76.714
77.031
77.349
125.623
127.626
129.605
131.221
133.911
135.561
ppm
20
40
60
80
100
120
140
160
180
RSX483/ CDC13

Structure 7

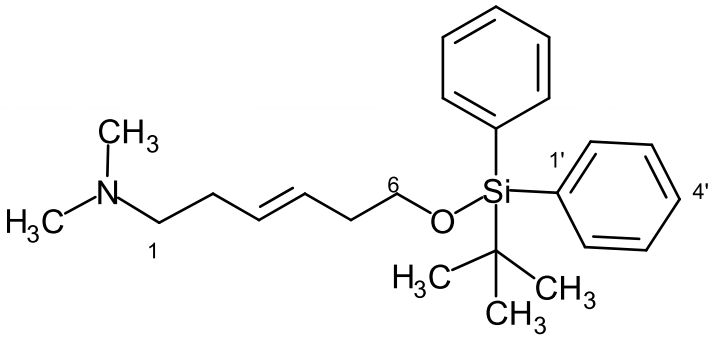
CH3
N
H3C
1
6
O
Si
1'
4'
H3C
CH3
CH3

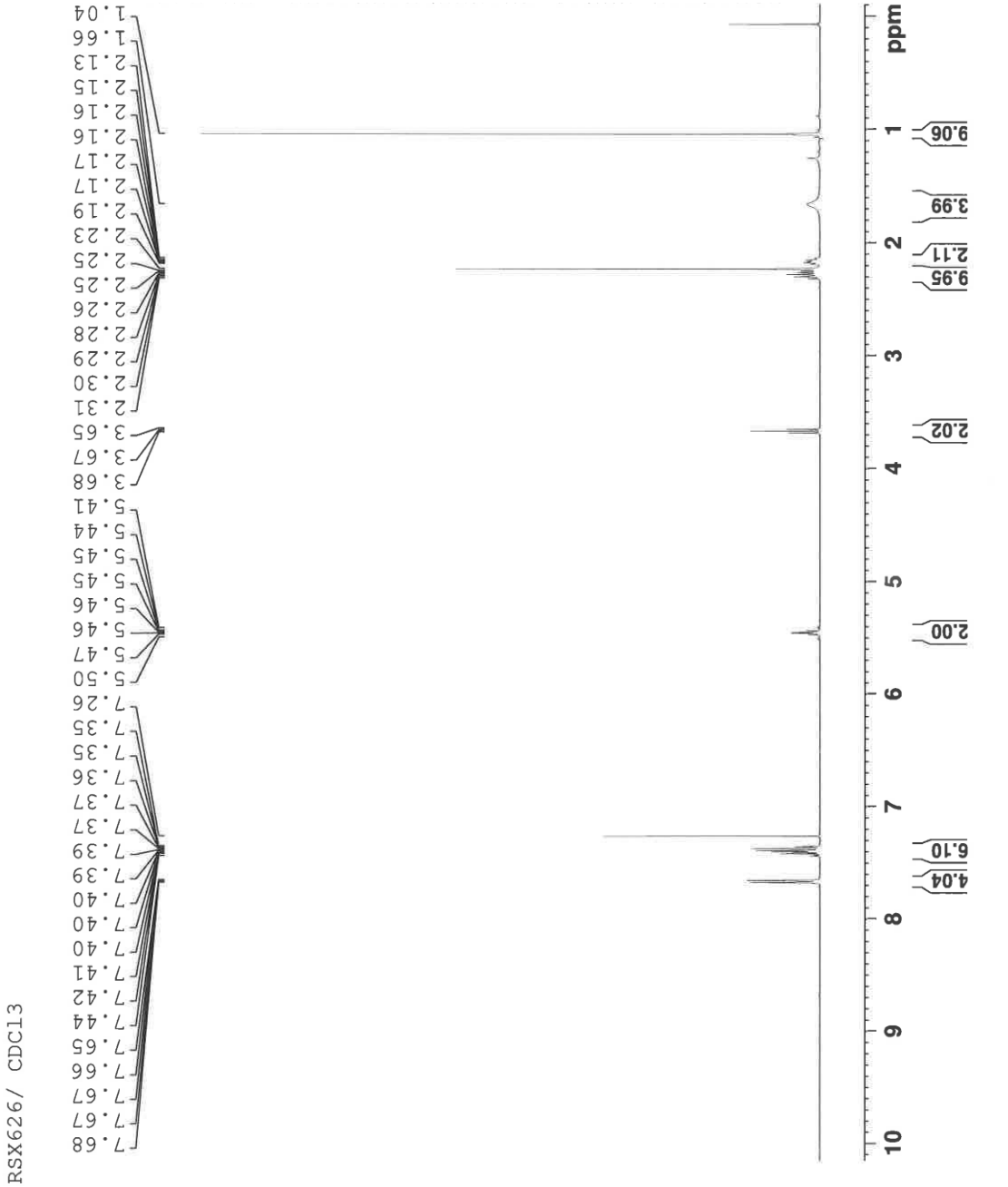
RSX626/ CDC13
ppm
9.06
3.99
2.11
9.95
2.02
2.00
6.10
4.04

Structure 7

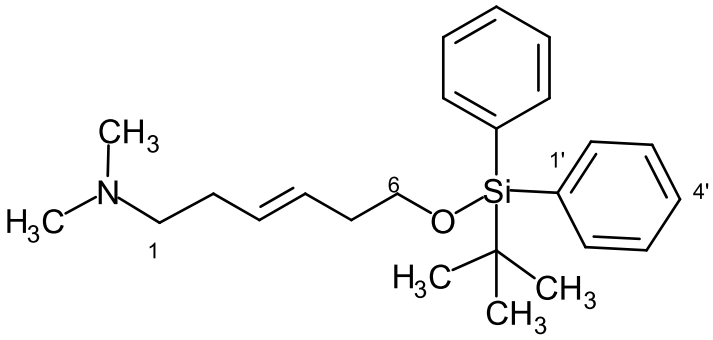
CH3
N
H3C
1
6
O
Si
1'
4'
H3C
CH3
CH3

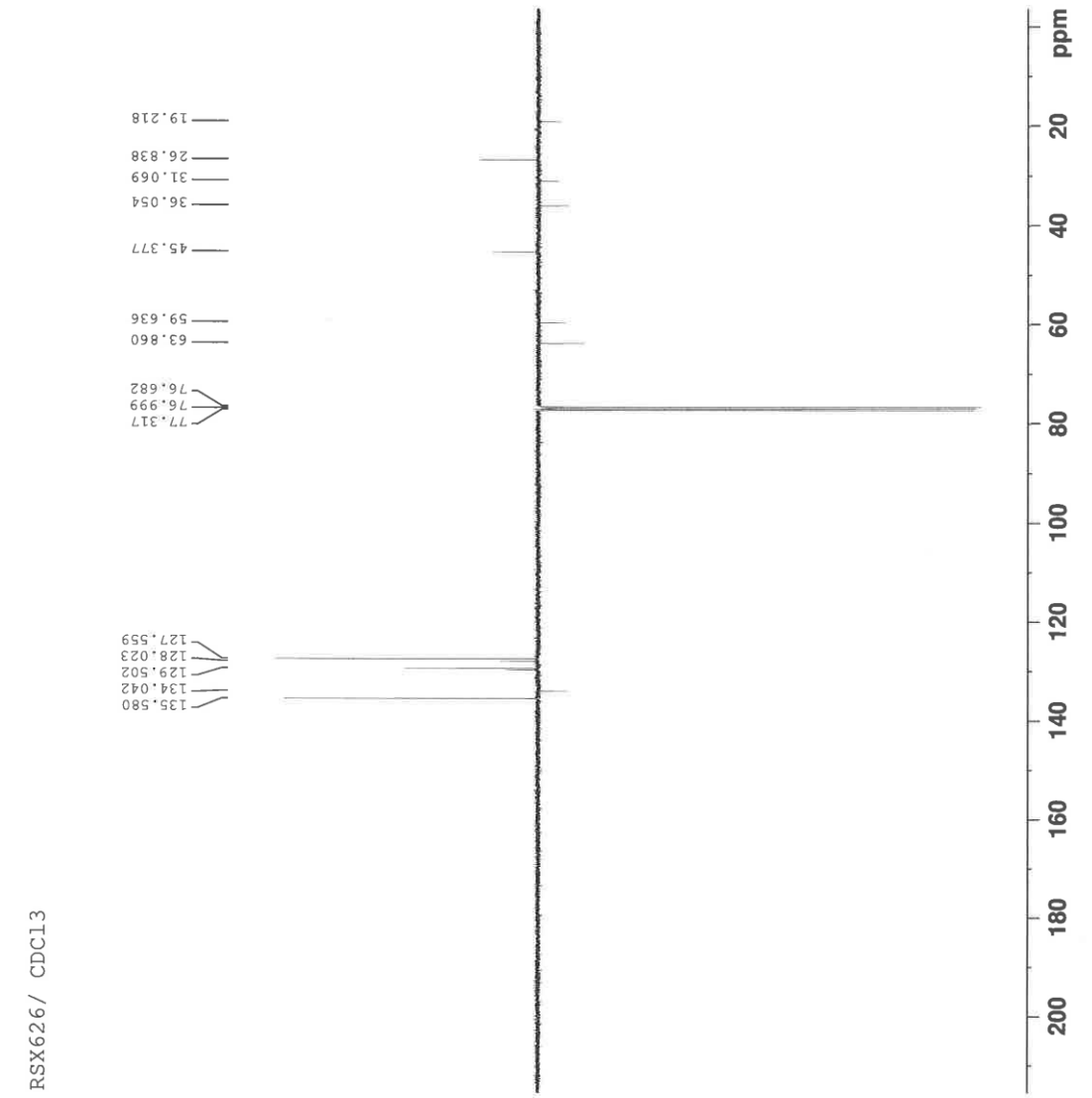
19.218
26.838
31.069
36.054
45.377
59.636
63.860
76.682
76.999
77.317
127.559
128.023
129.502
134.042
135.580
ppm
20
40
60
80
100
120
140
160
180
200
RSX626/ CDC13

Structure 7

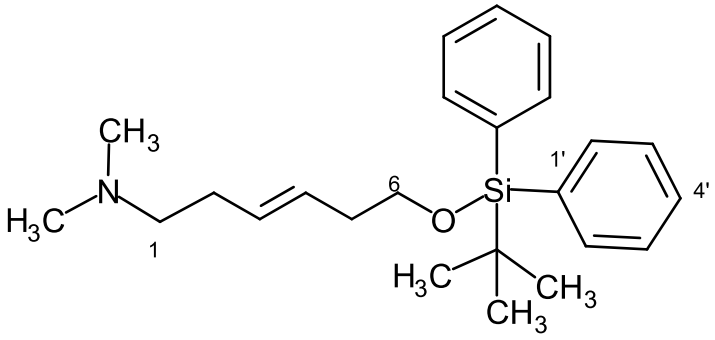
CH3
N
H3C
1
6
O
Si
1'
4'
H3C
CH3
CH3

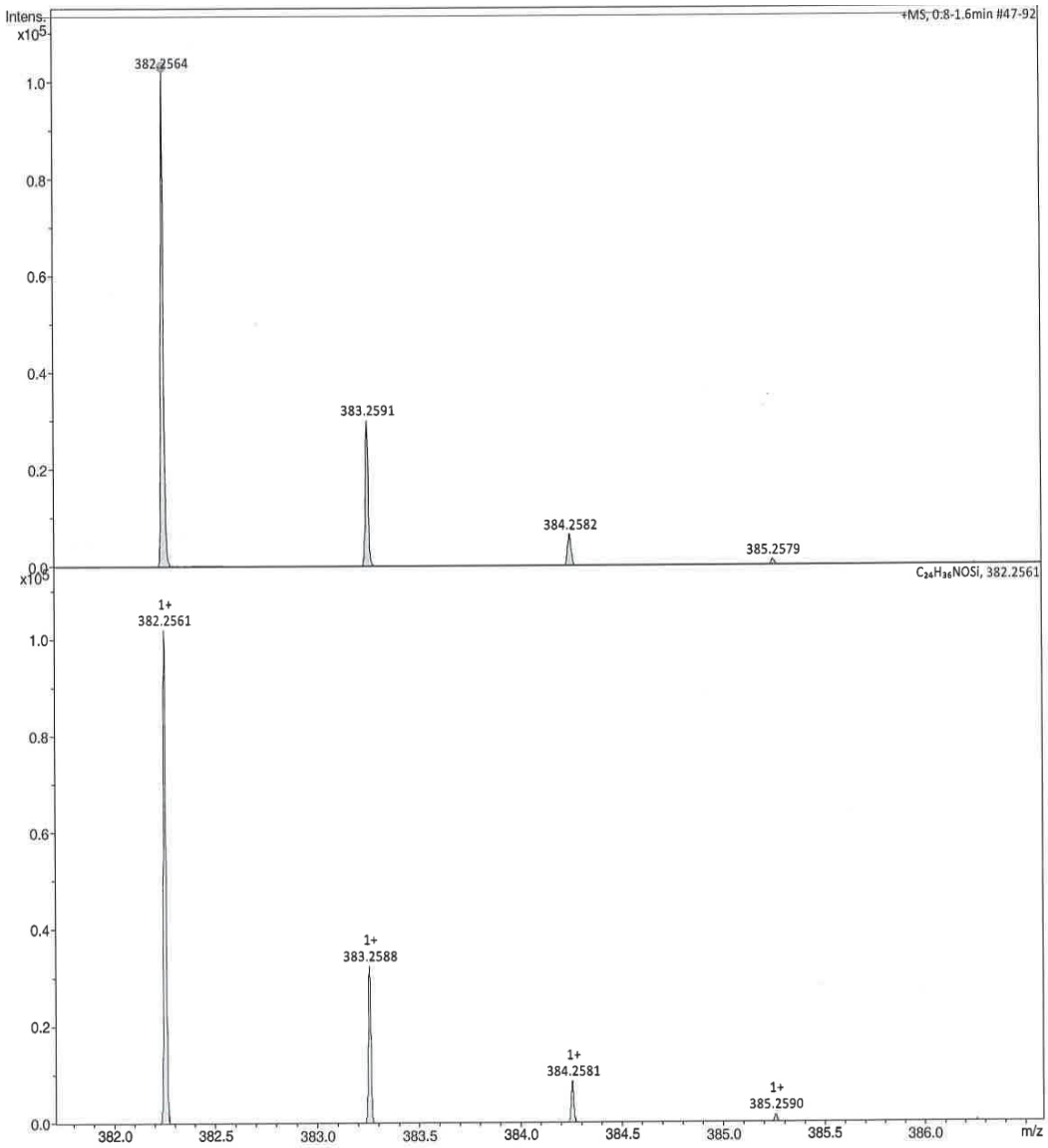
Intens.
x10^5
+MS, 0.8-1.6min #47-92
382.2564
383.2591
384.2582
385.2579
C24H36NOSi, 382.2561
1+
382.2561
1+
383.2588
1+
384.2581
1+
385.2590
382.0
382.5
383.0
383.5
384.0
384.5
385.0
385.5
386.0
m/z

Structure 8

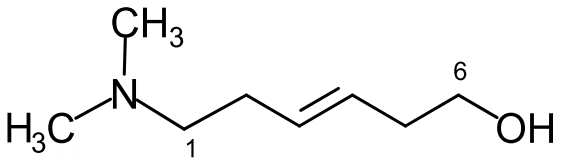
CH3
N
H3C
1
6
OH

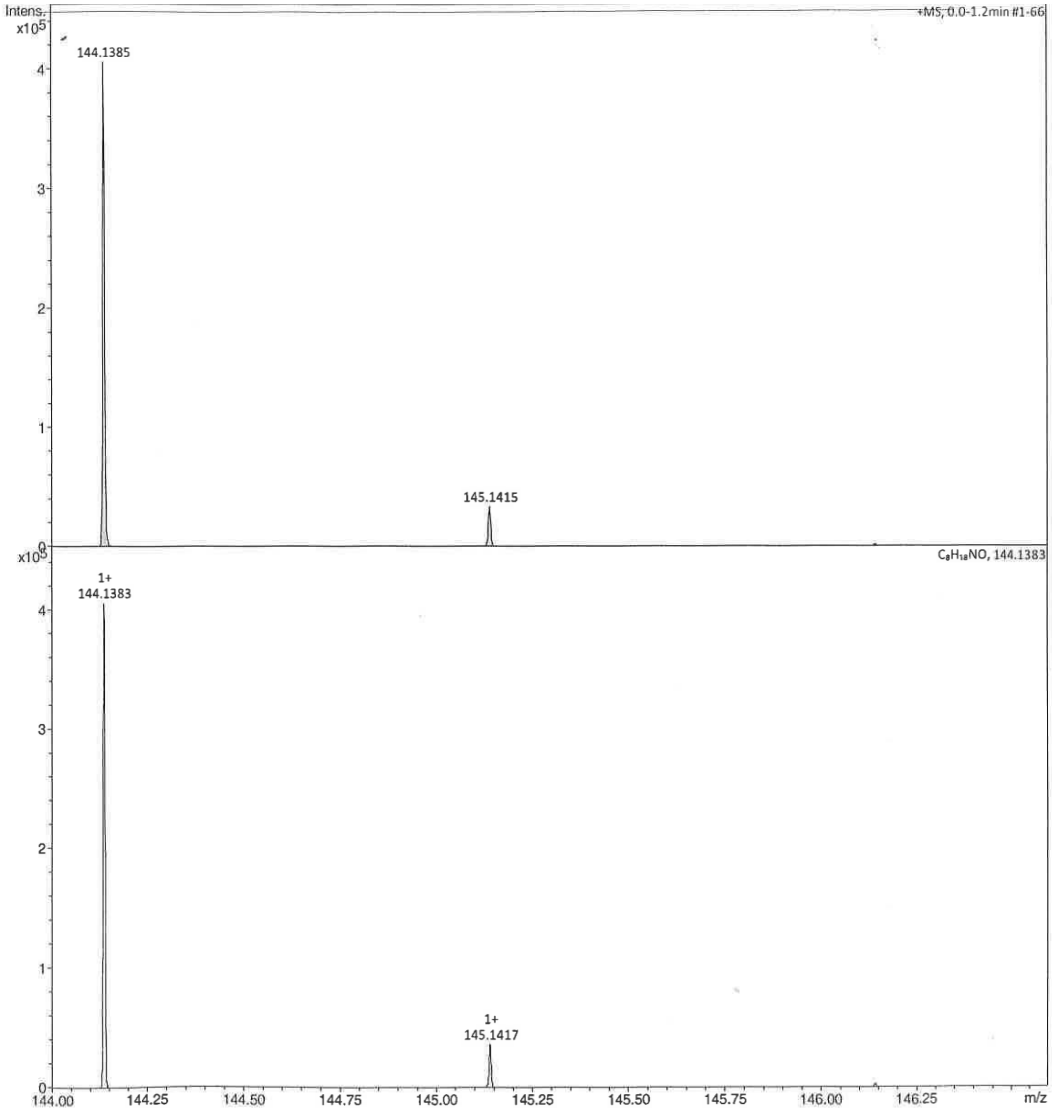
Intens.
x10^5
+MS, 0.0-1.2min #1-66
144.1385
145.1415
C8H18NO, 144.1383
1+
144.1383
1+
145.1417
144.00
144.25
144.50
144.75
145.00
145.25
145.50
145.75
146.00
146.25
m/z

Structure 10

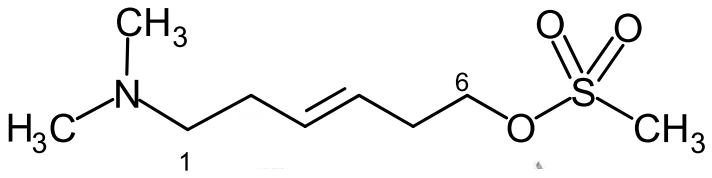

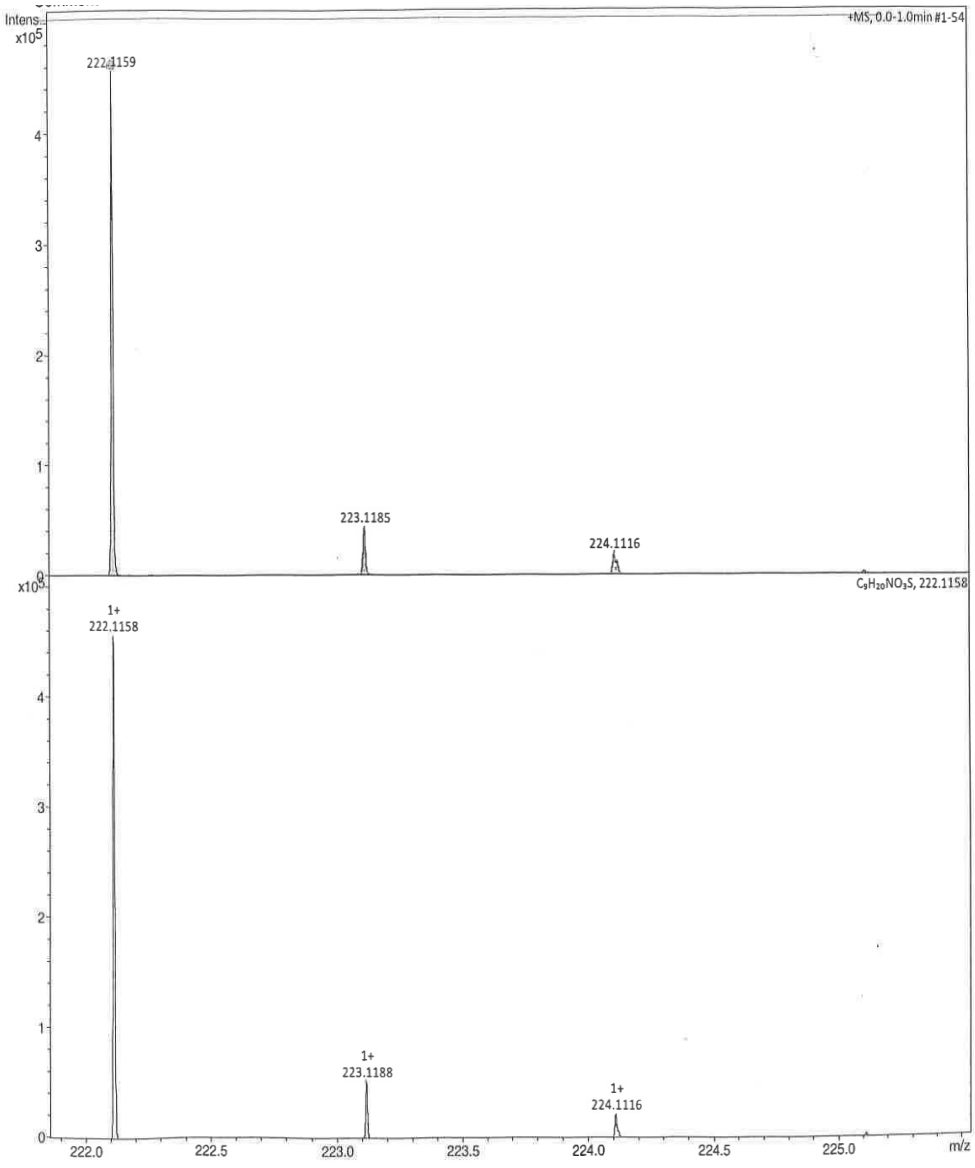

Structure 12

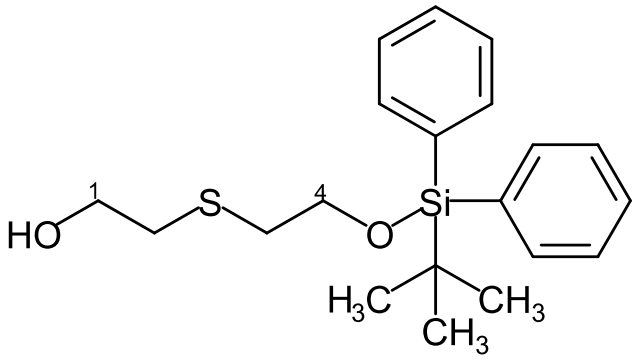

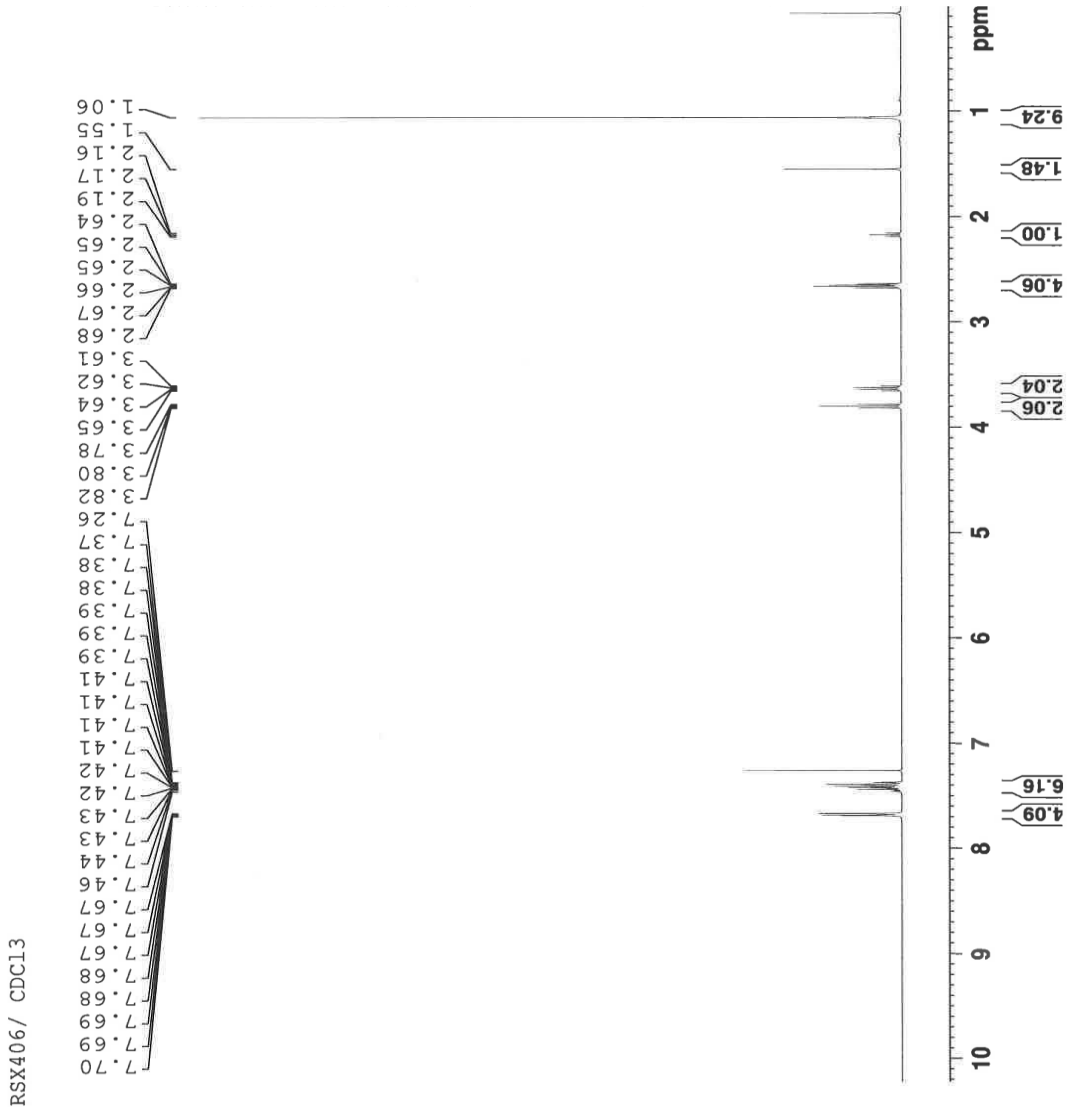

Structure 12

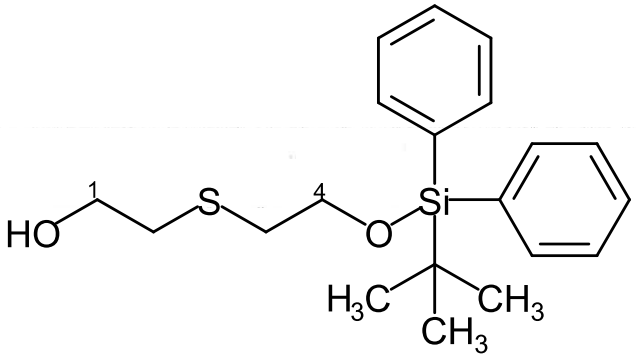

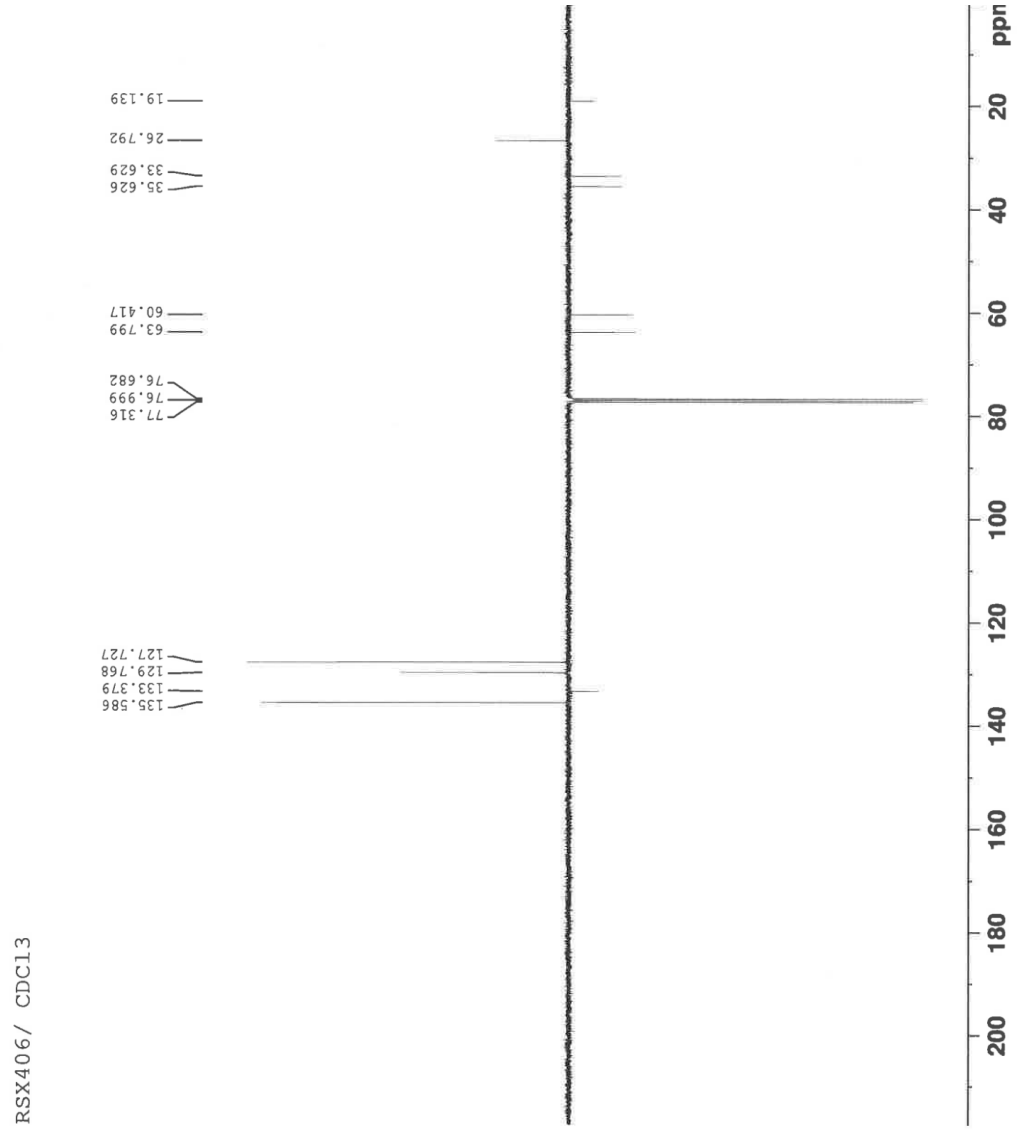

Structure 12

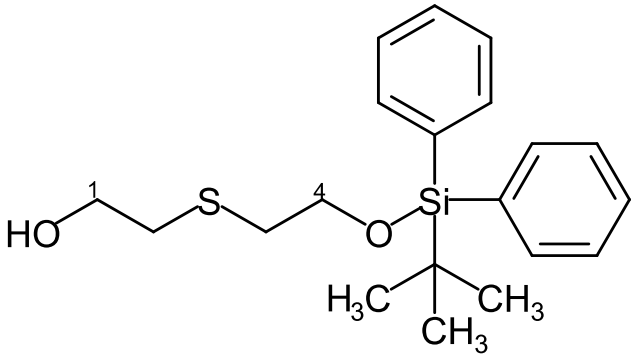

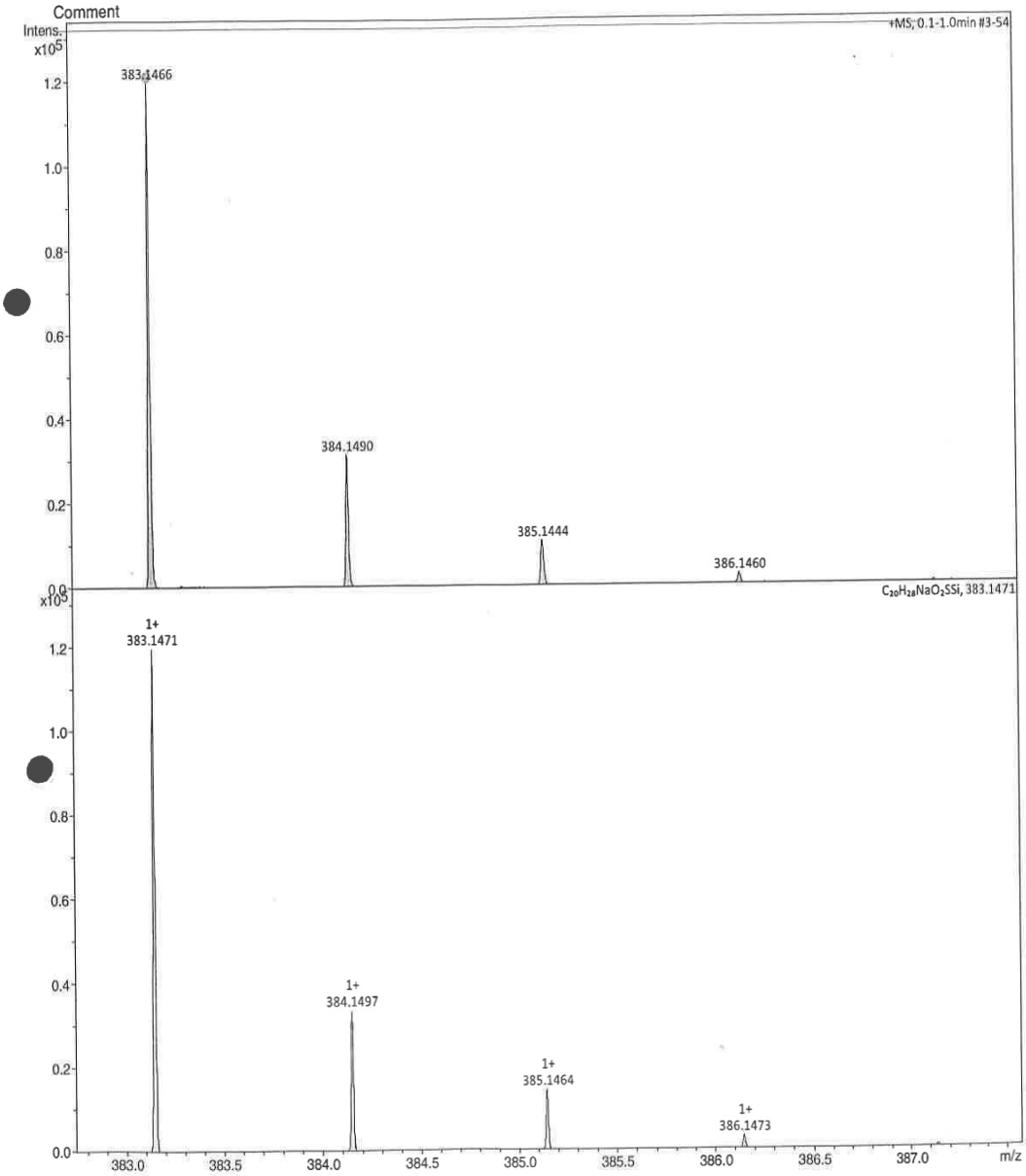

Structure 13

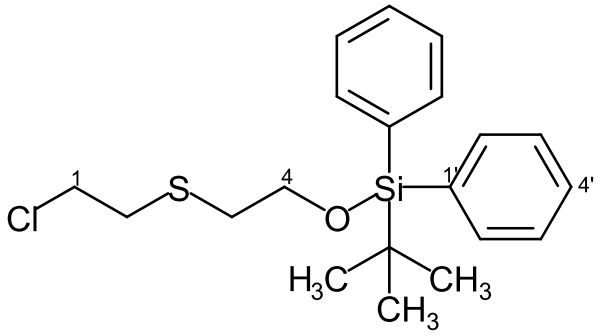

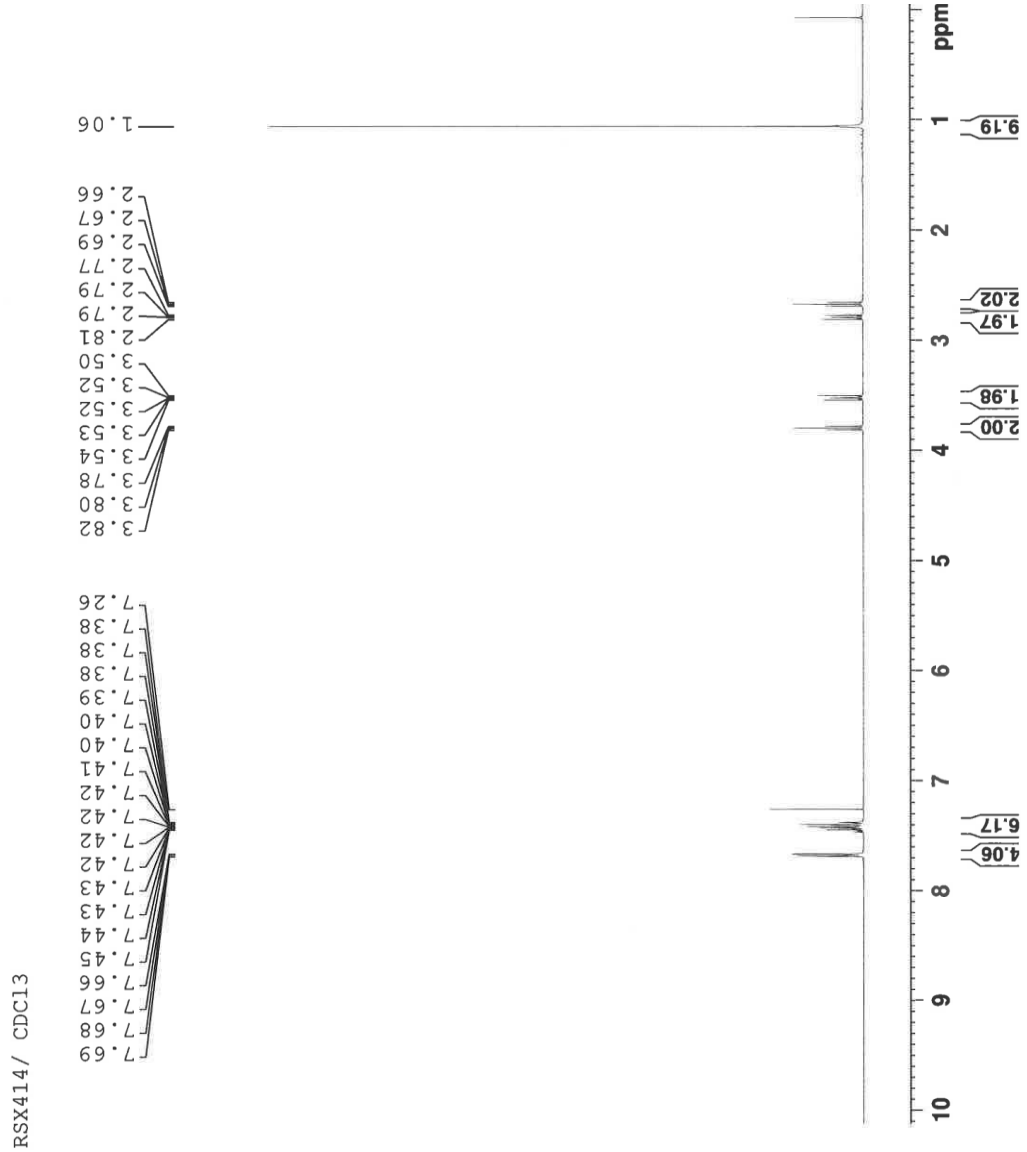

Structure 13

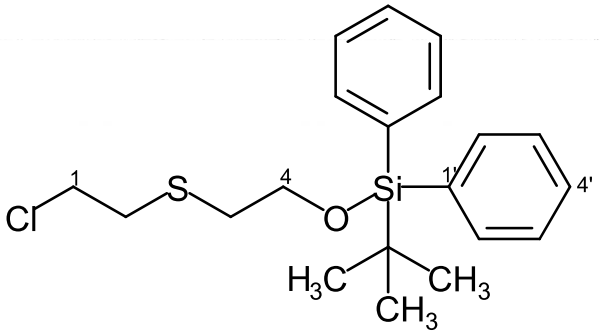

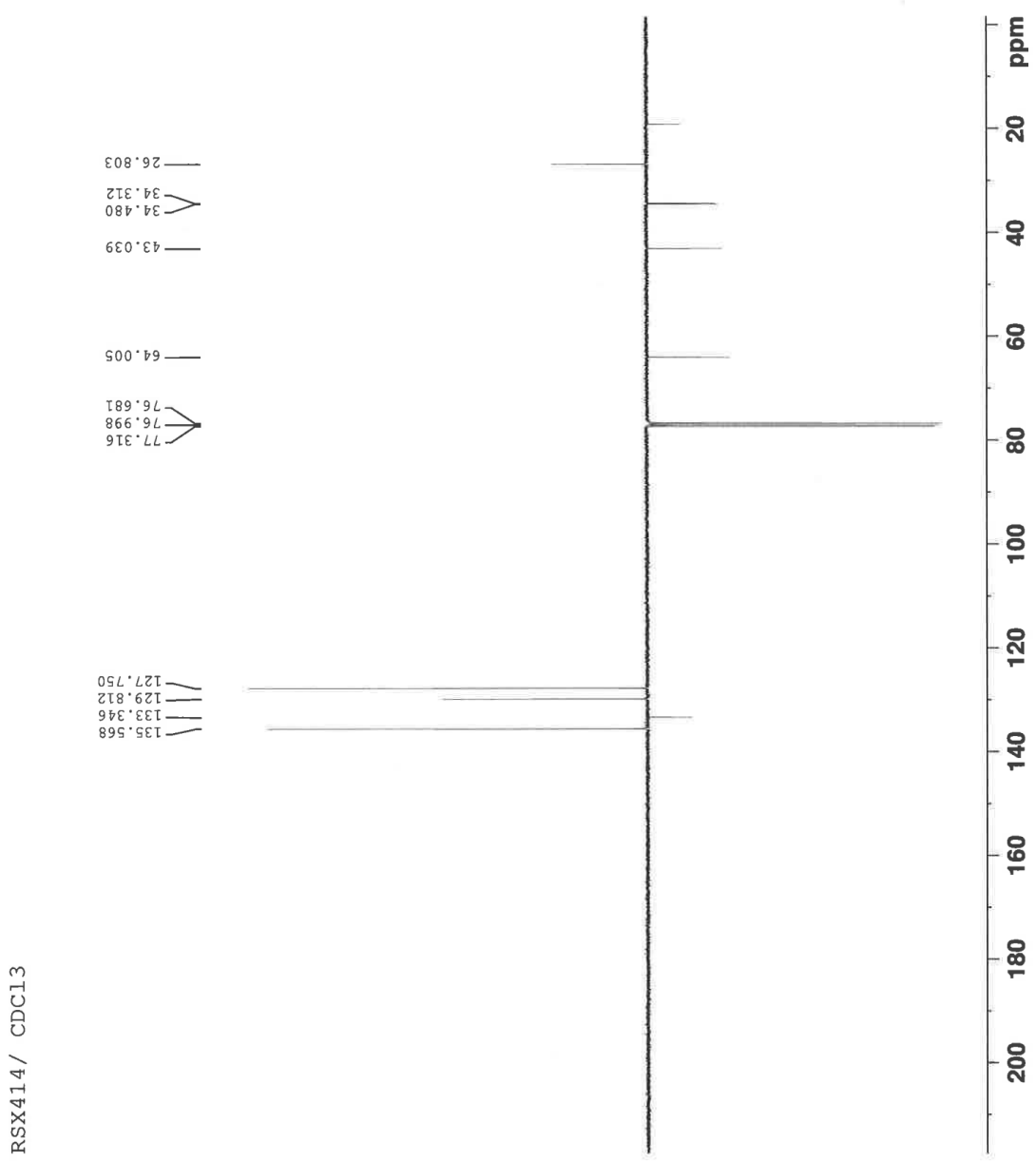

Structure 13

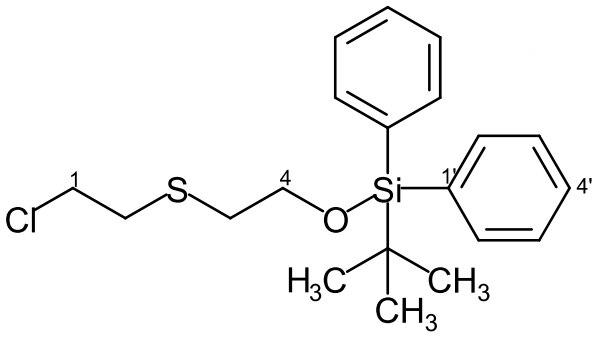

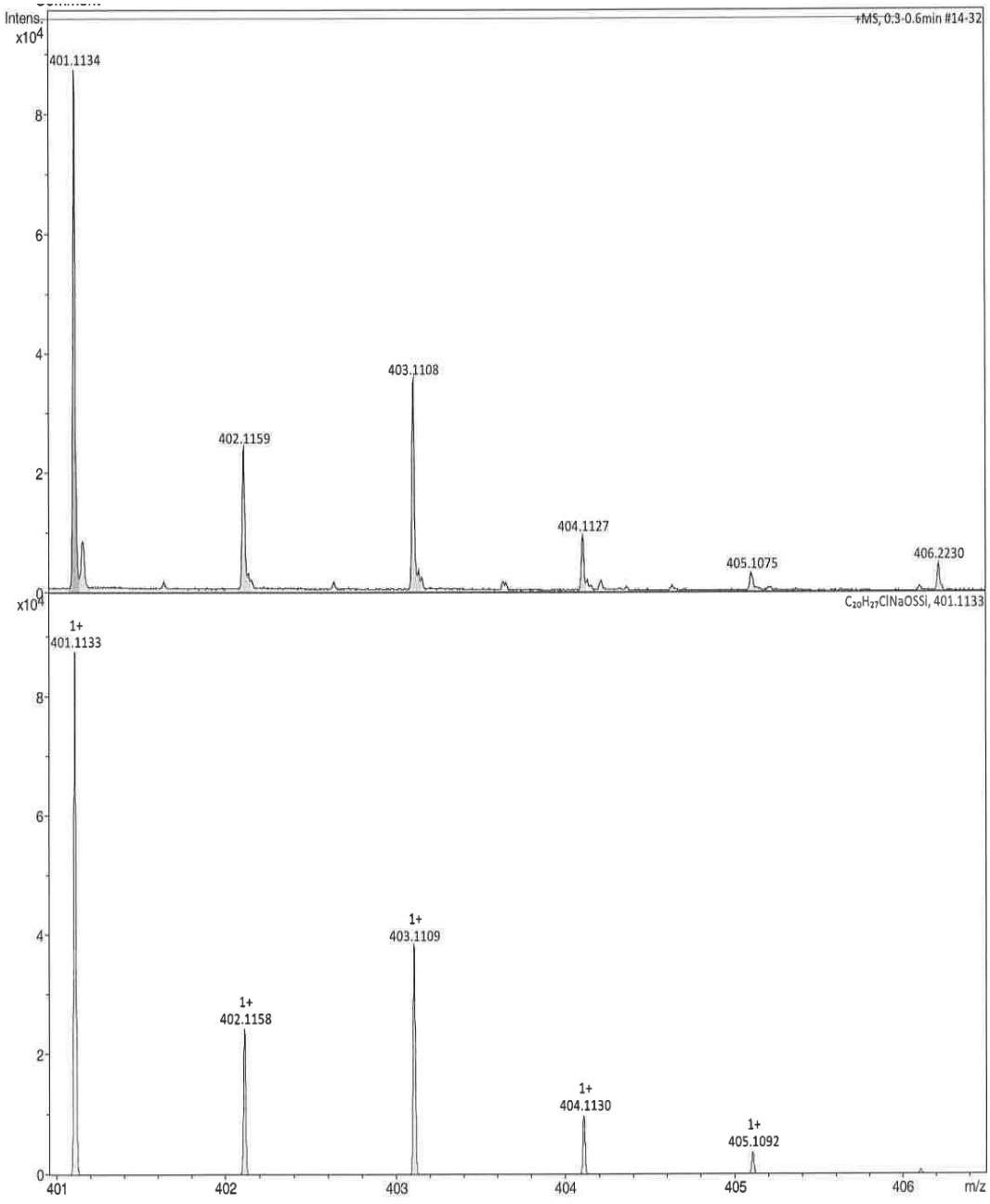

Structure 14

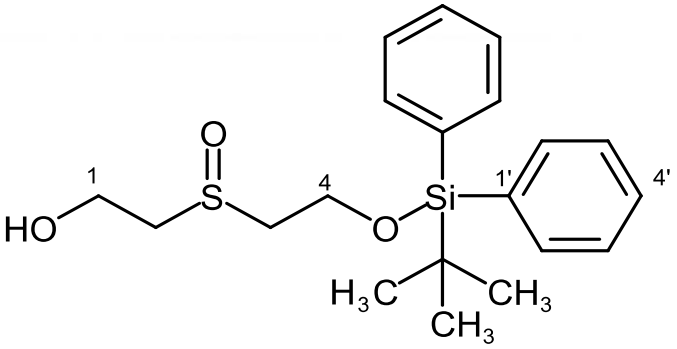

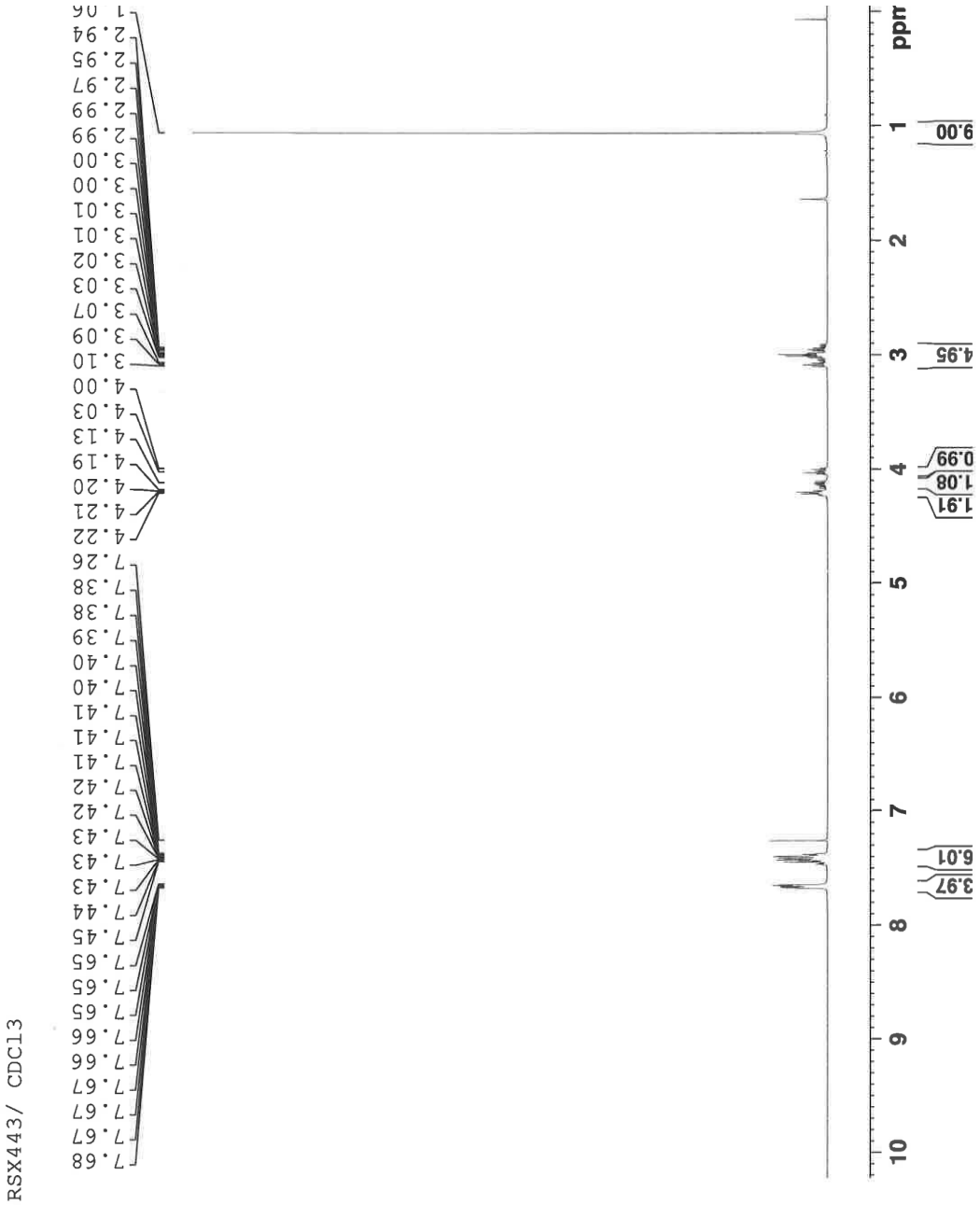

Structure 14

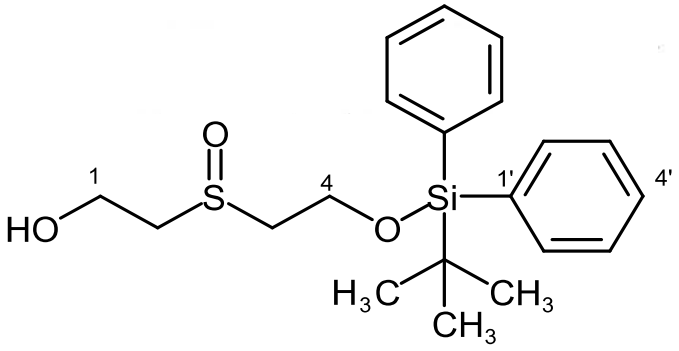

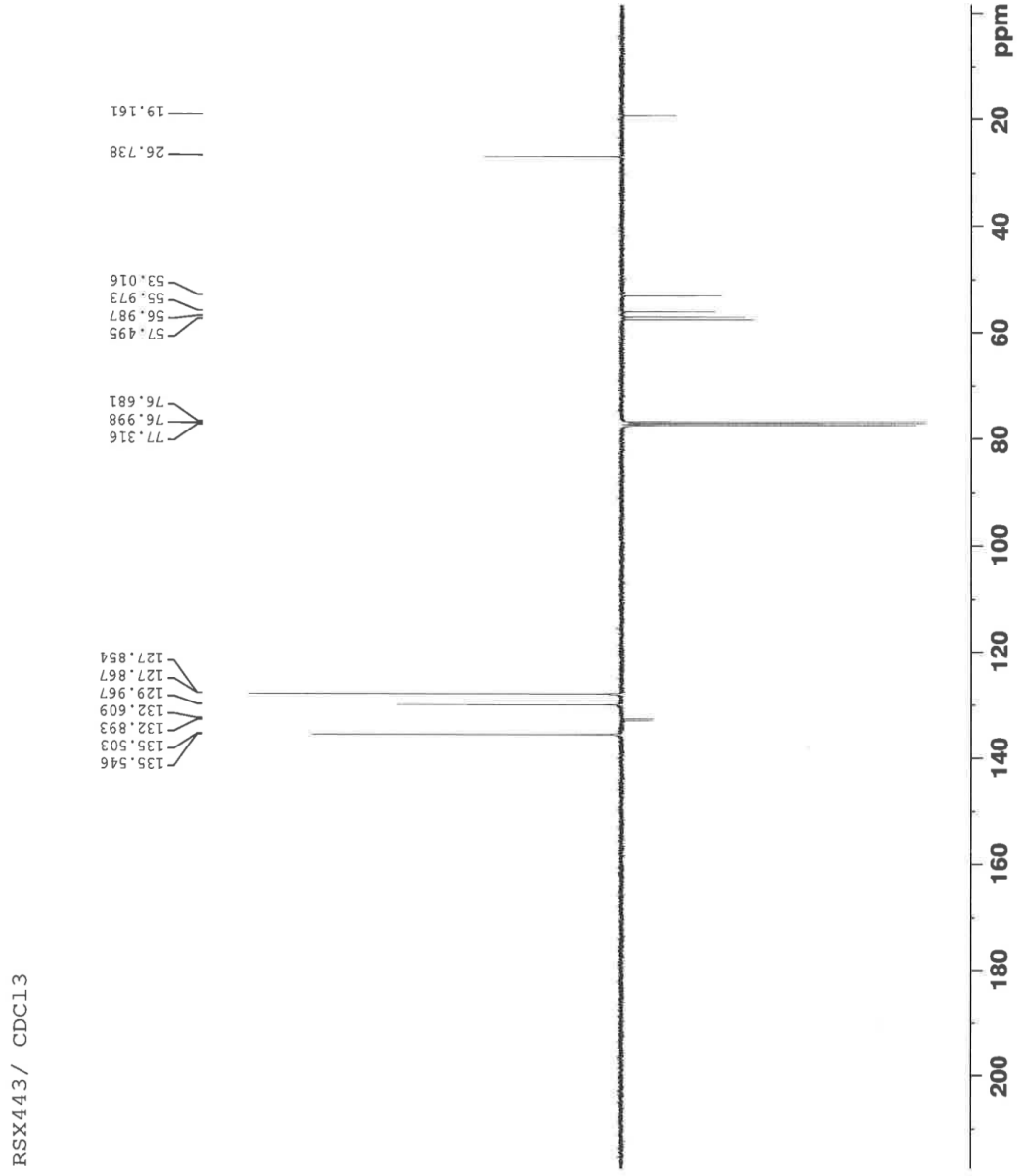

Structure 14

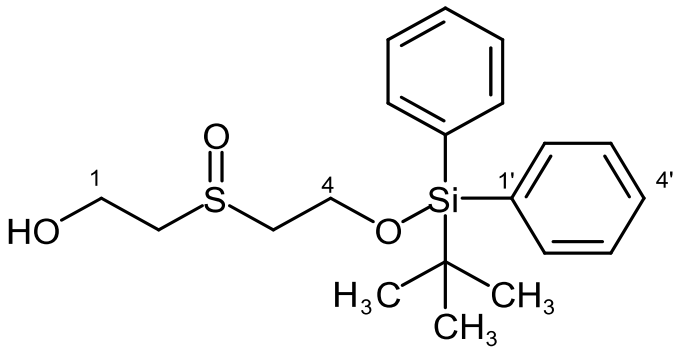

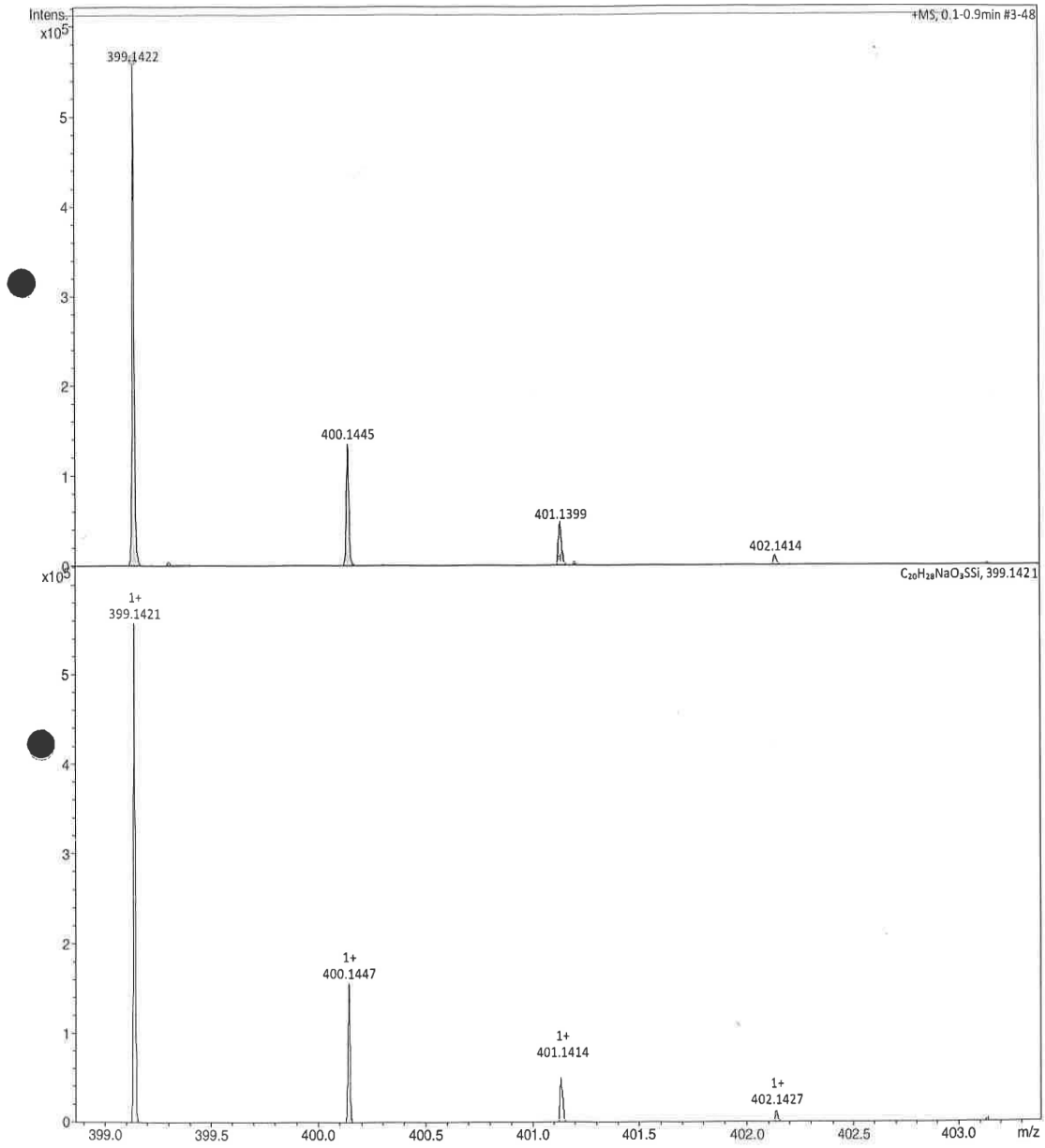

Structure 15

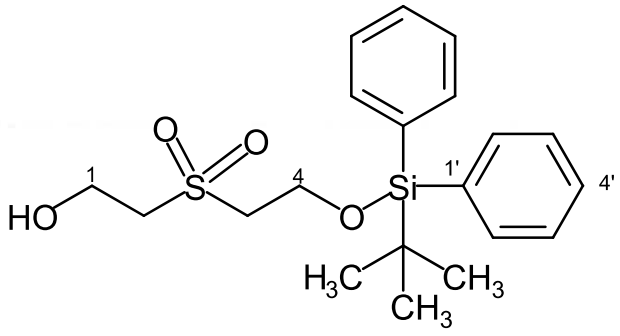

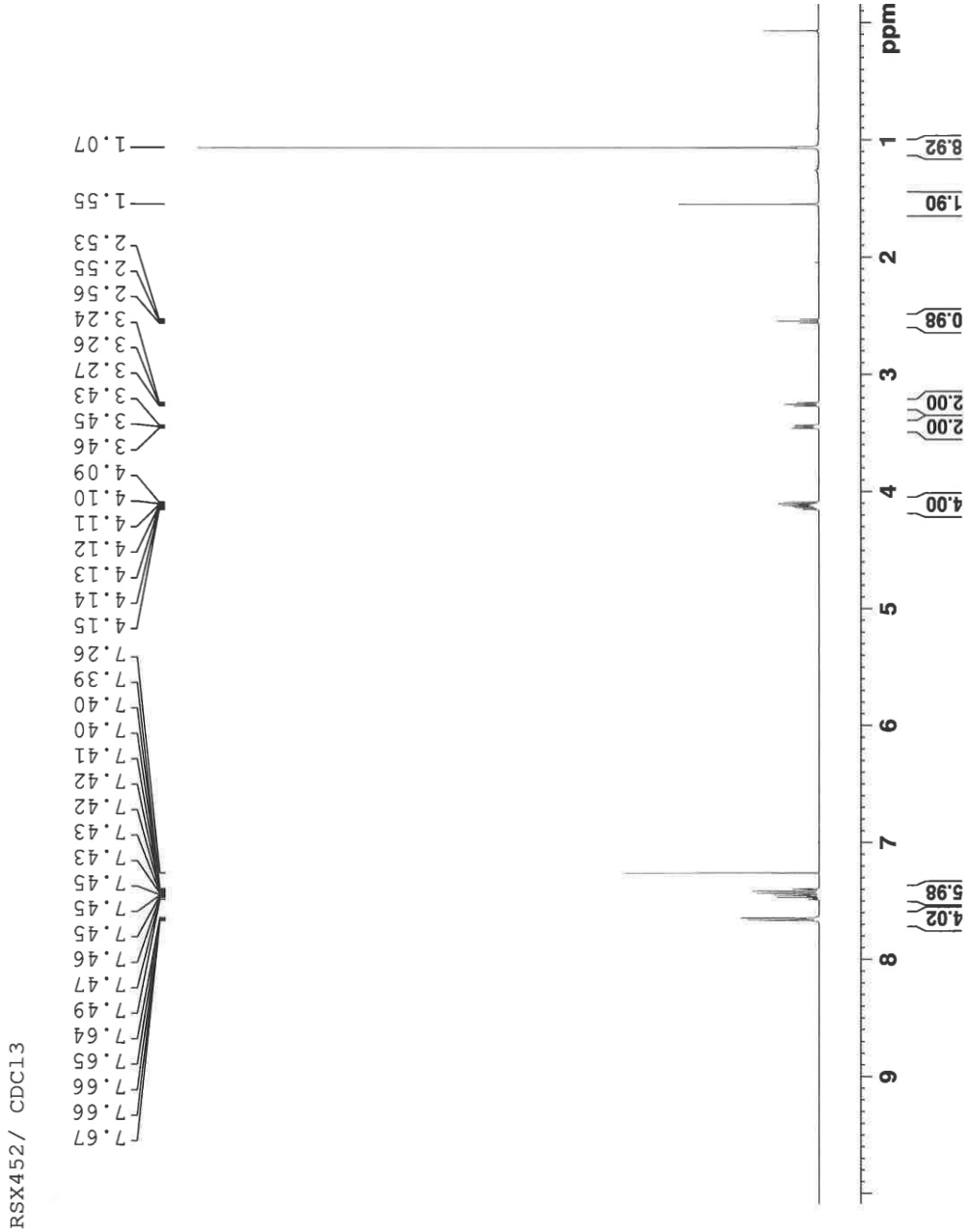

Structure 15

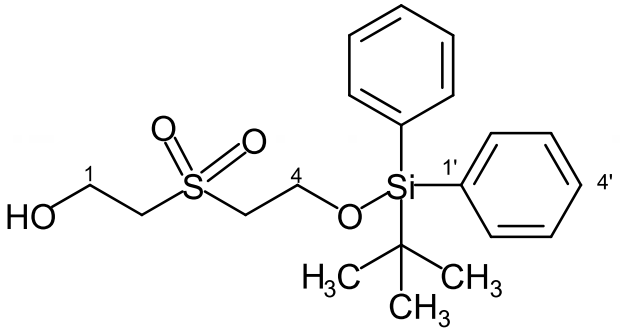

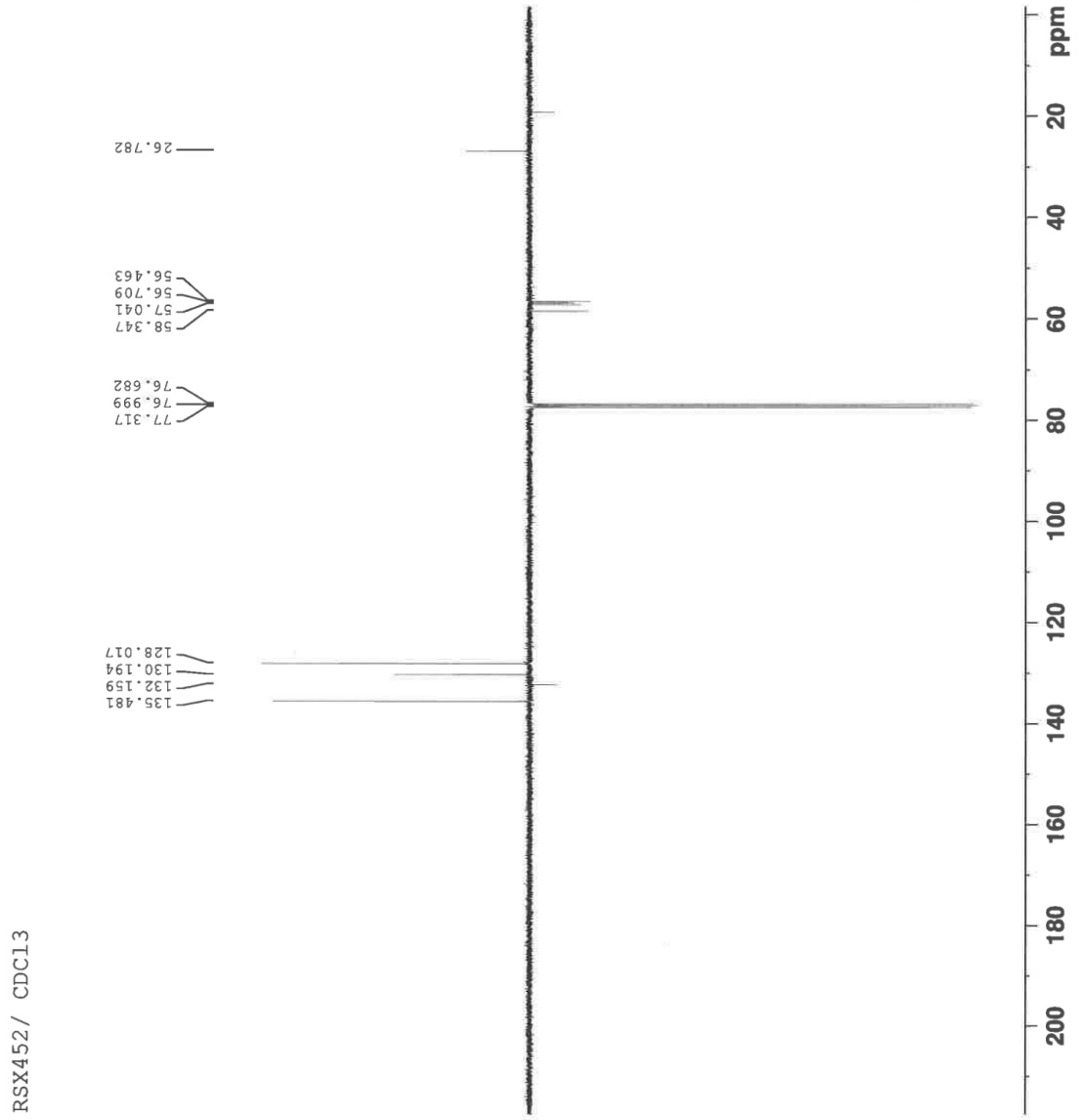

Structure 15

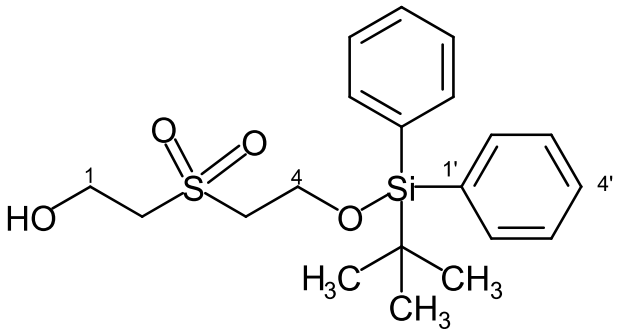

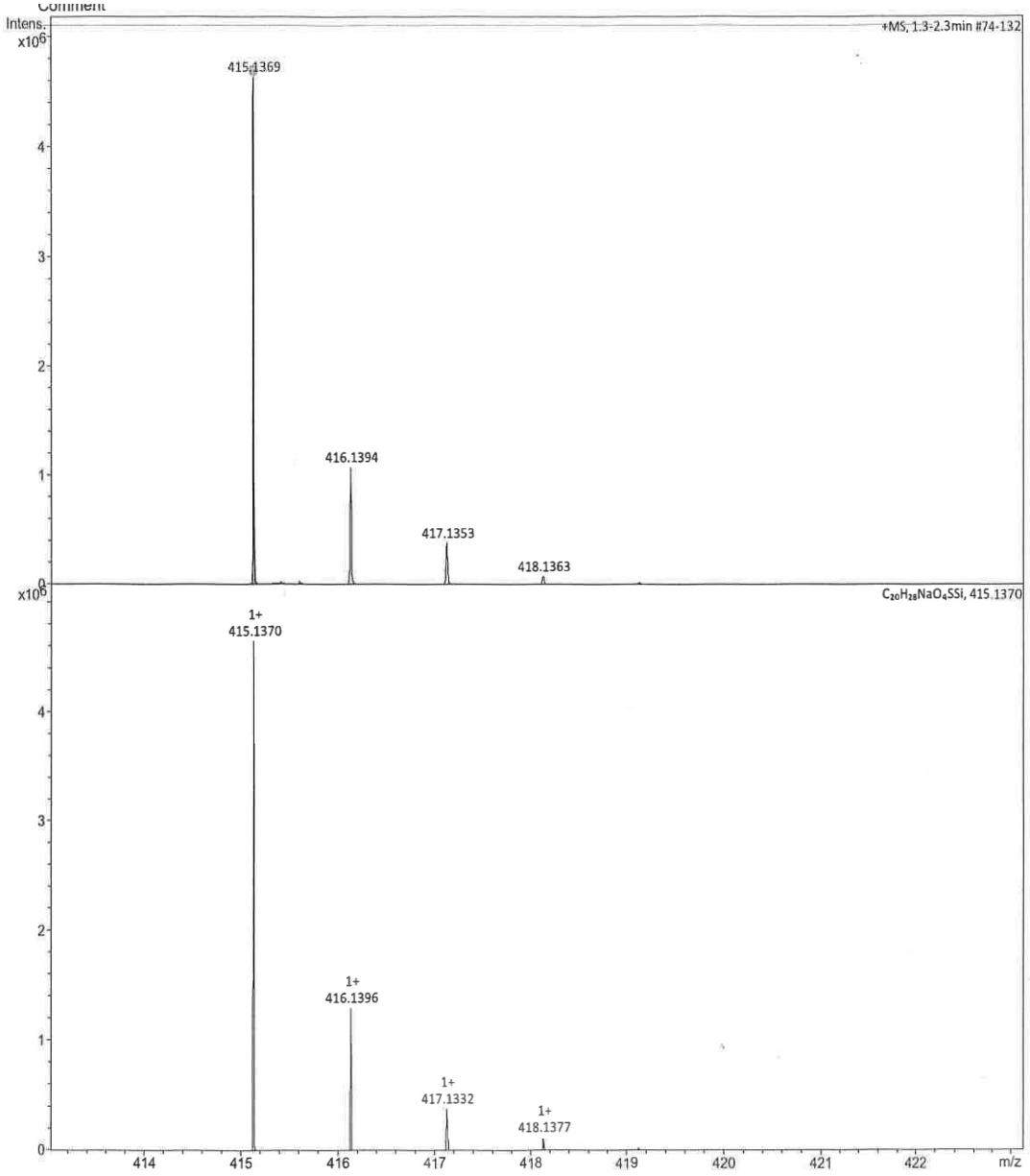

Structure 17

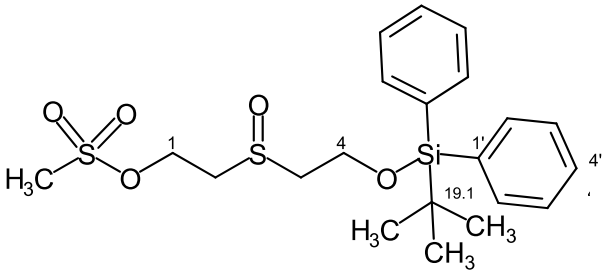

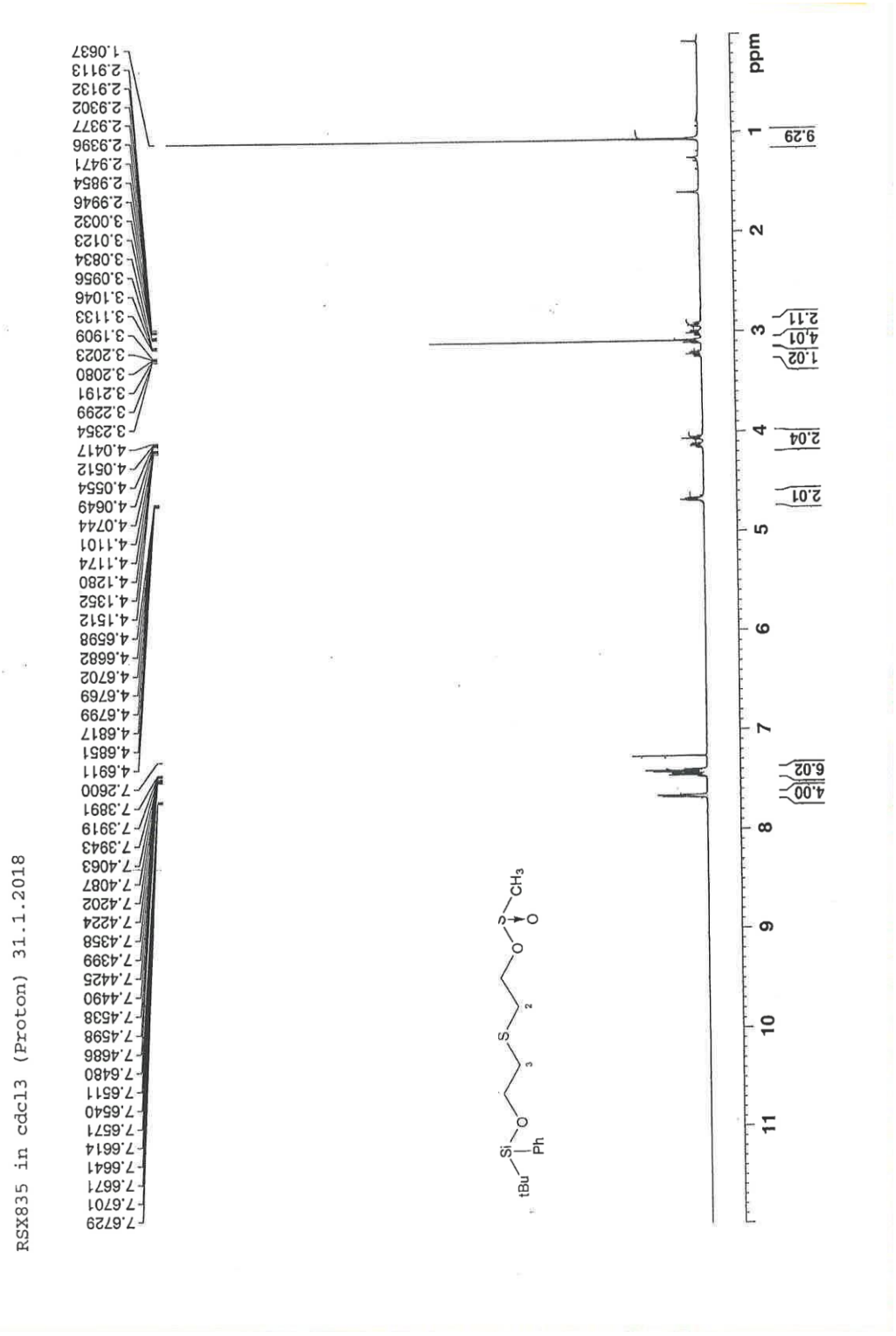

Structure 17

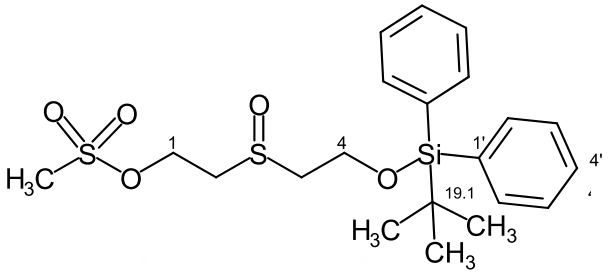

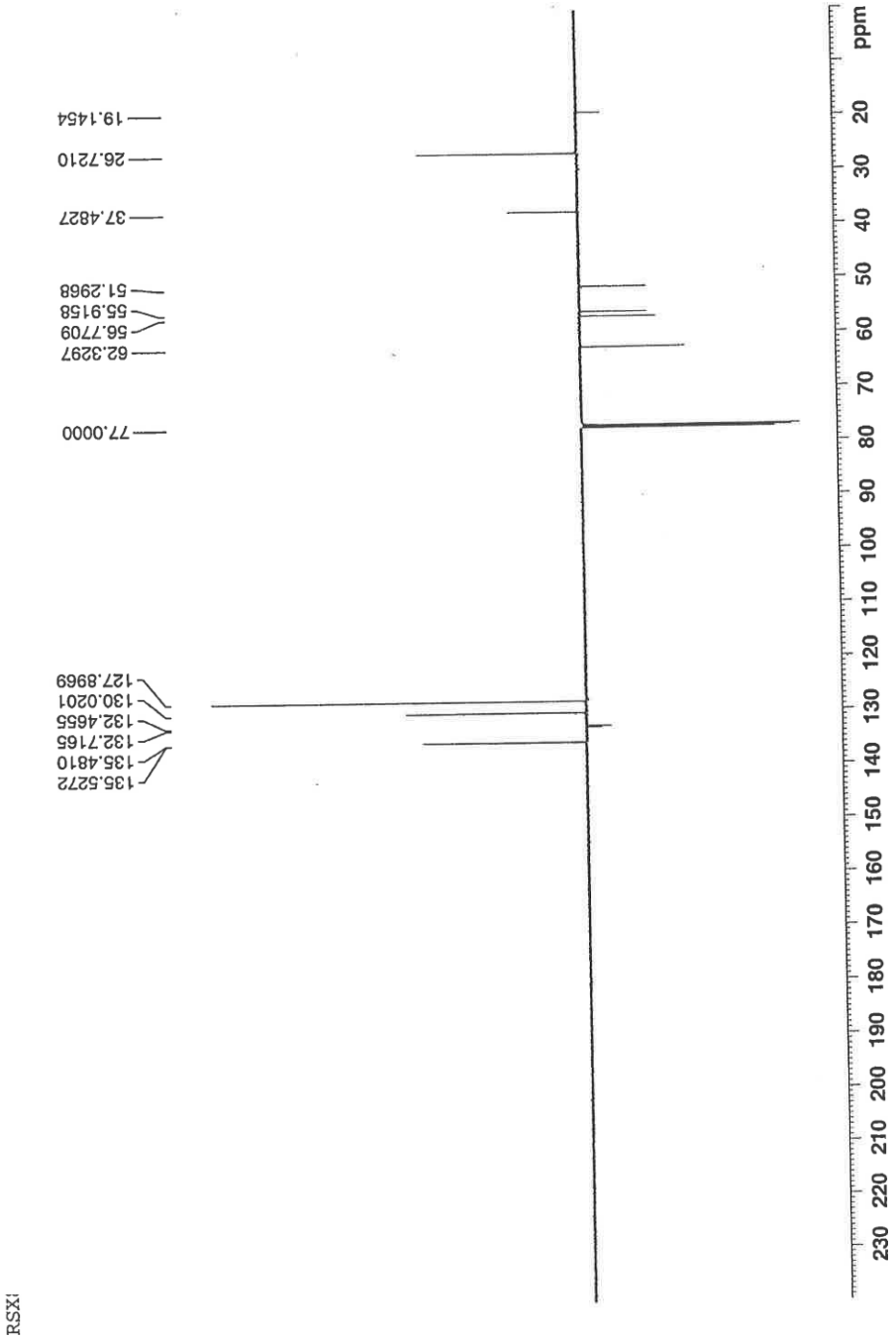

Structure 17

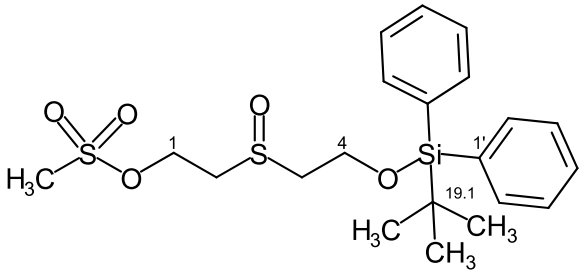

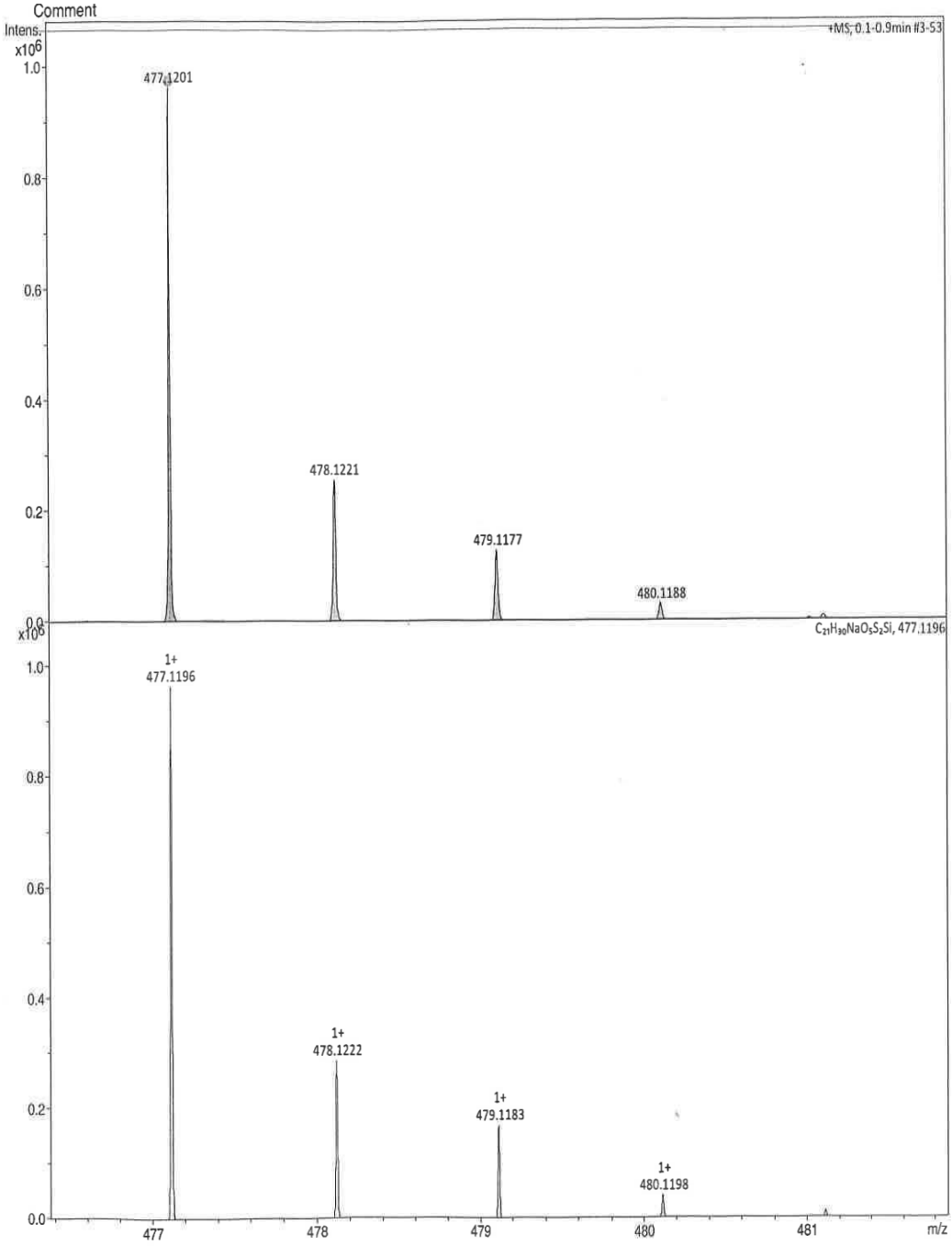

Structure 20

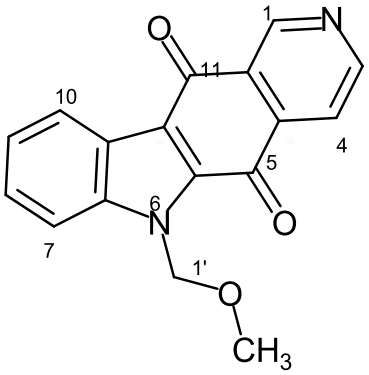

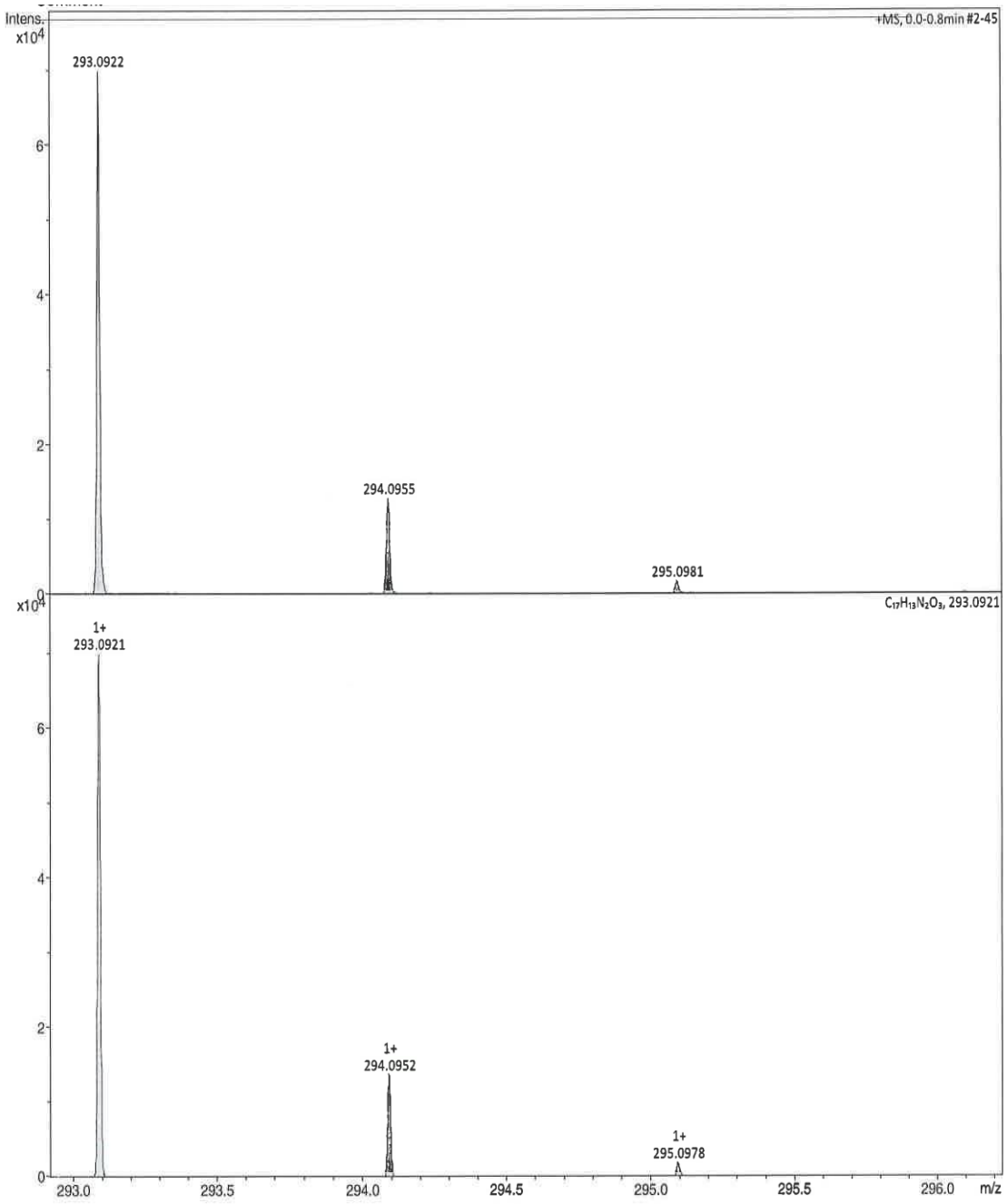

Structure 21

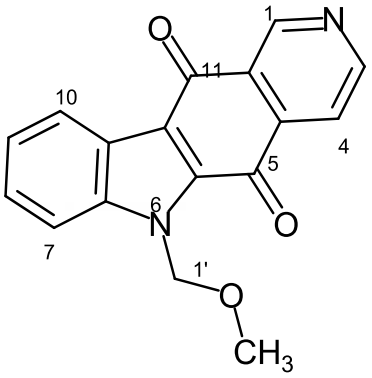

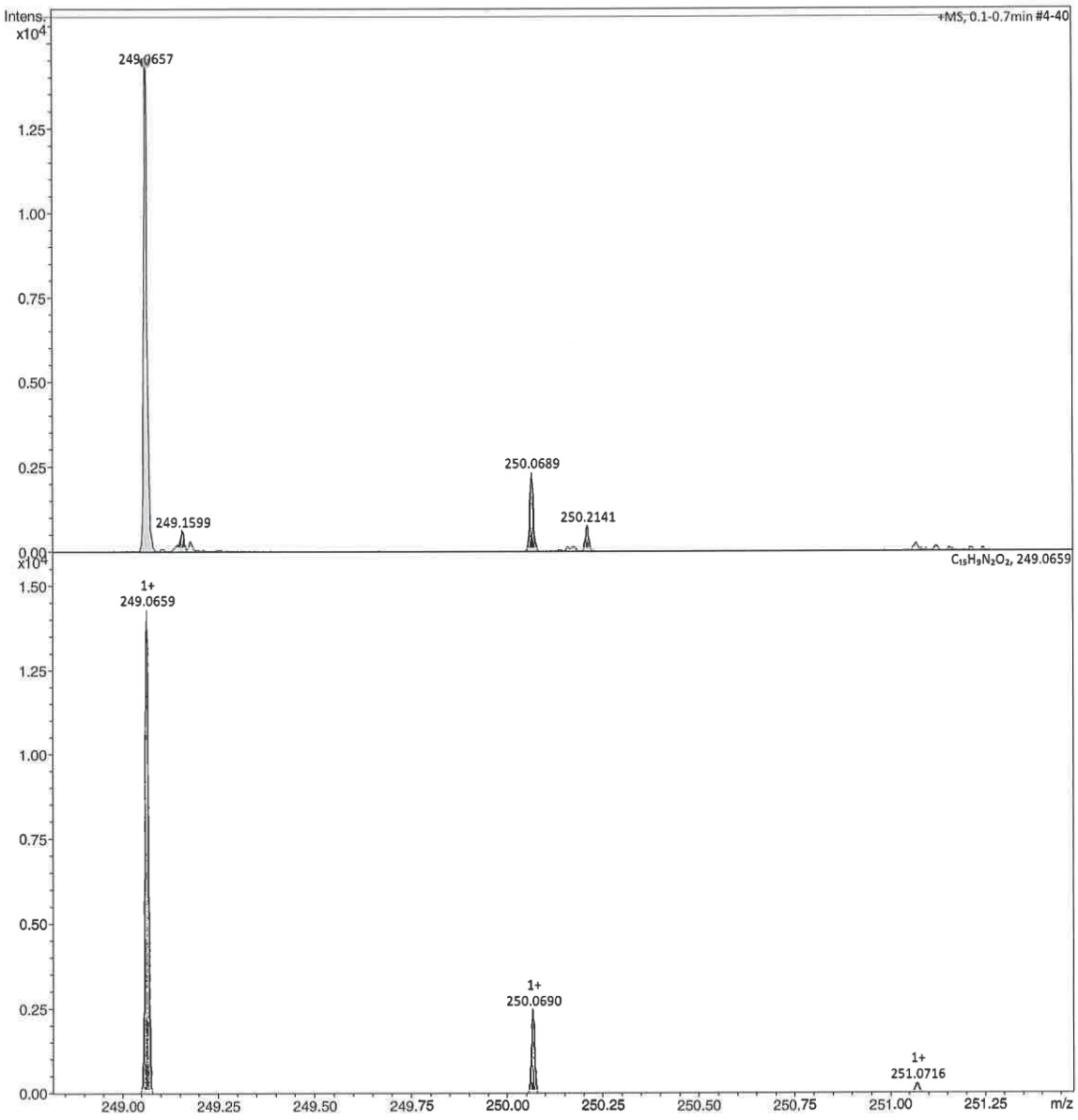

Structure 22

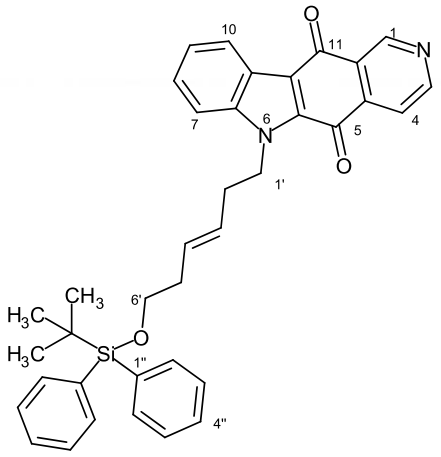

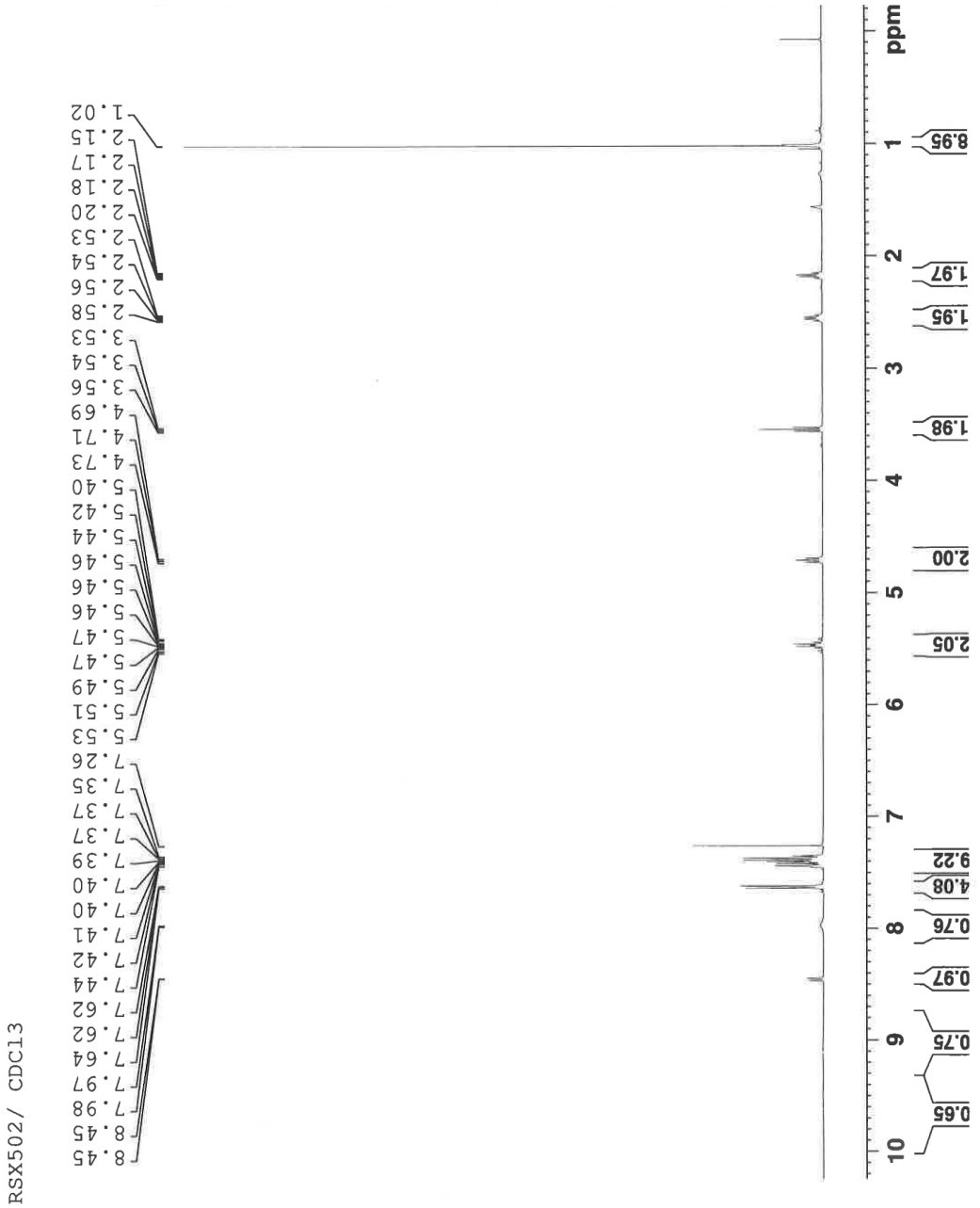

Structure 22

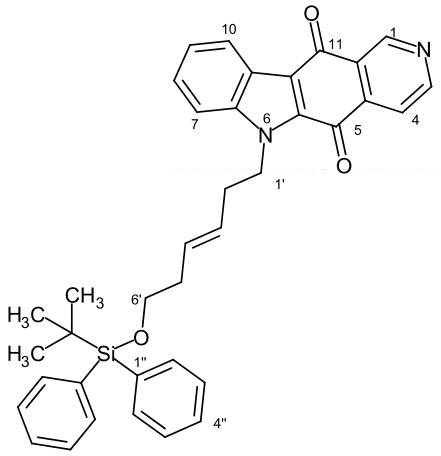

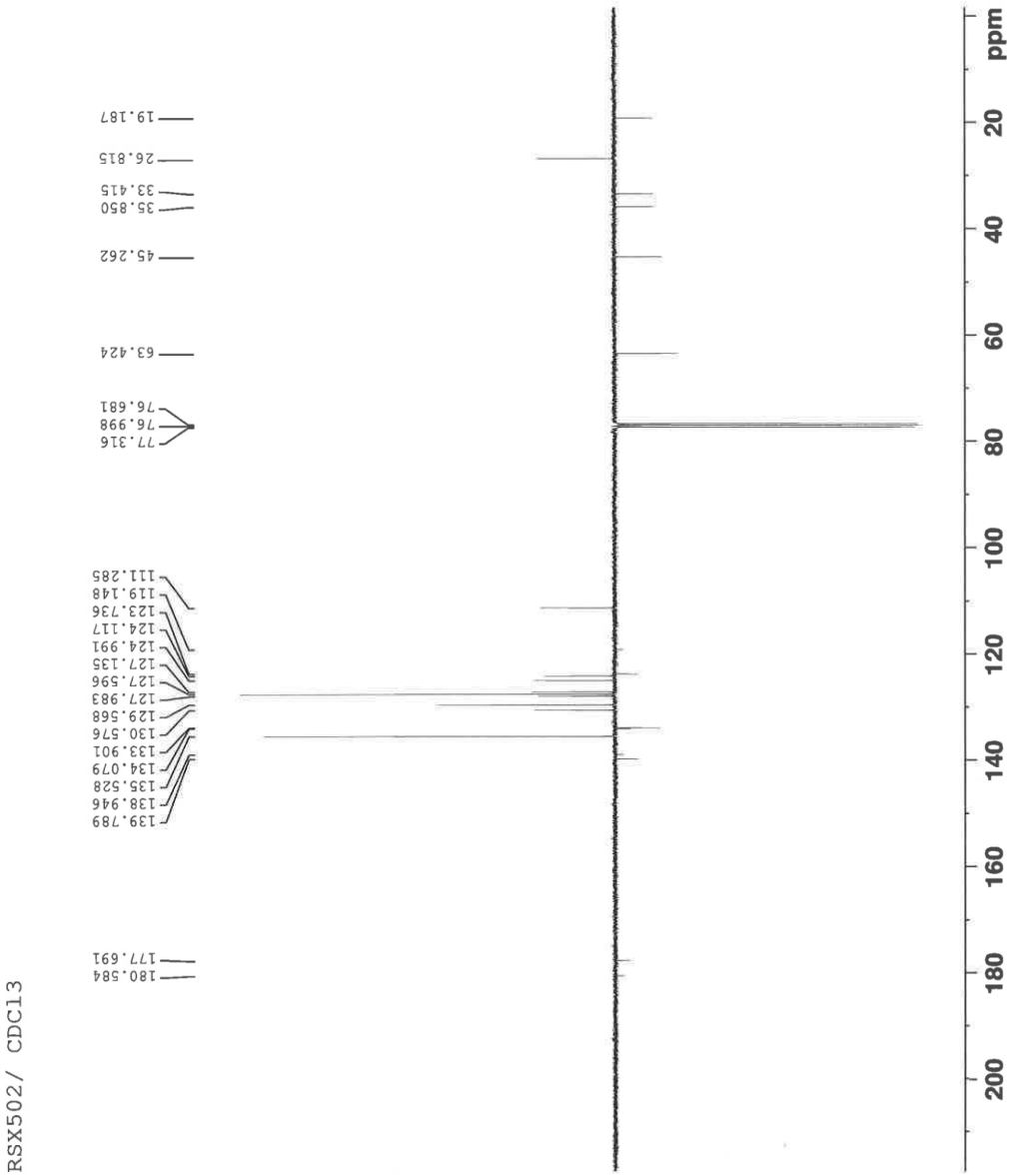

Structure 22

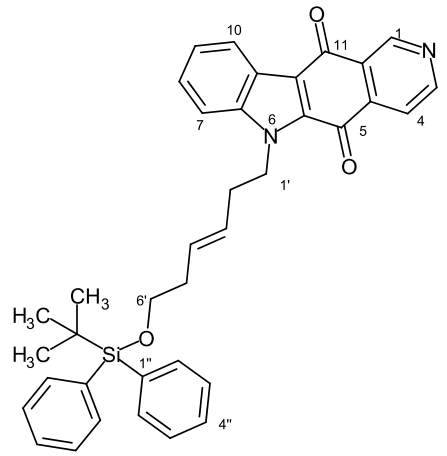

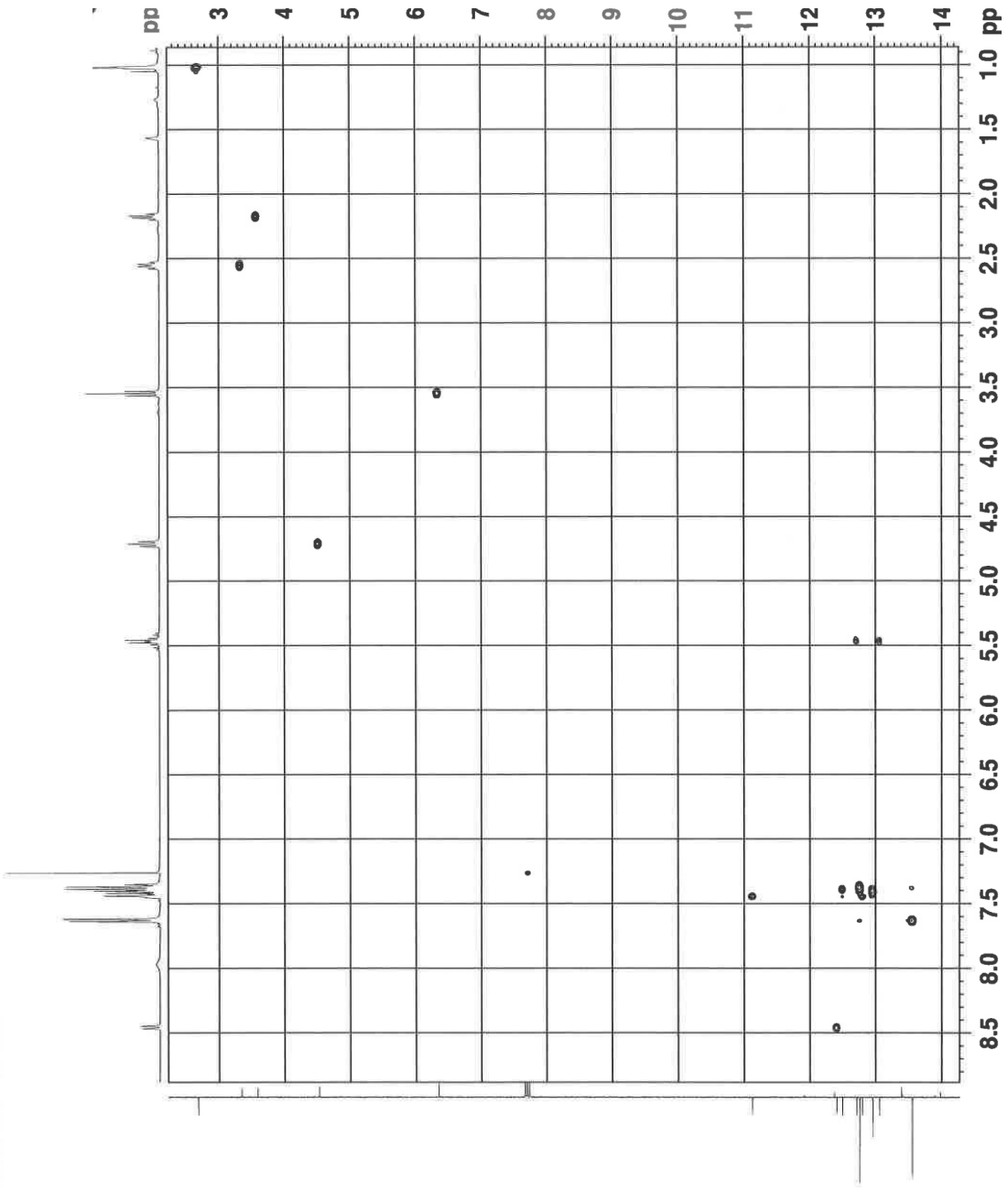

RSX502/ CDC13

Structure 22